ICISE Web Seminar
October 7th, 2021

Diffuse Supernova Neutrino Background Search at Super-Kamiokande

arXiv:2109.11174

Yosuke ASHIDA (WIPAC, University of Wisconsin-Madison)
in corporation with S. El Hedri & A. Giampaolo (Ecole Polytechnique)

2015

2016

2017

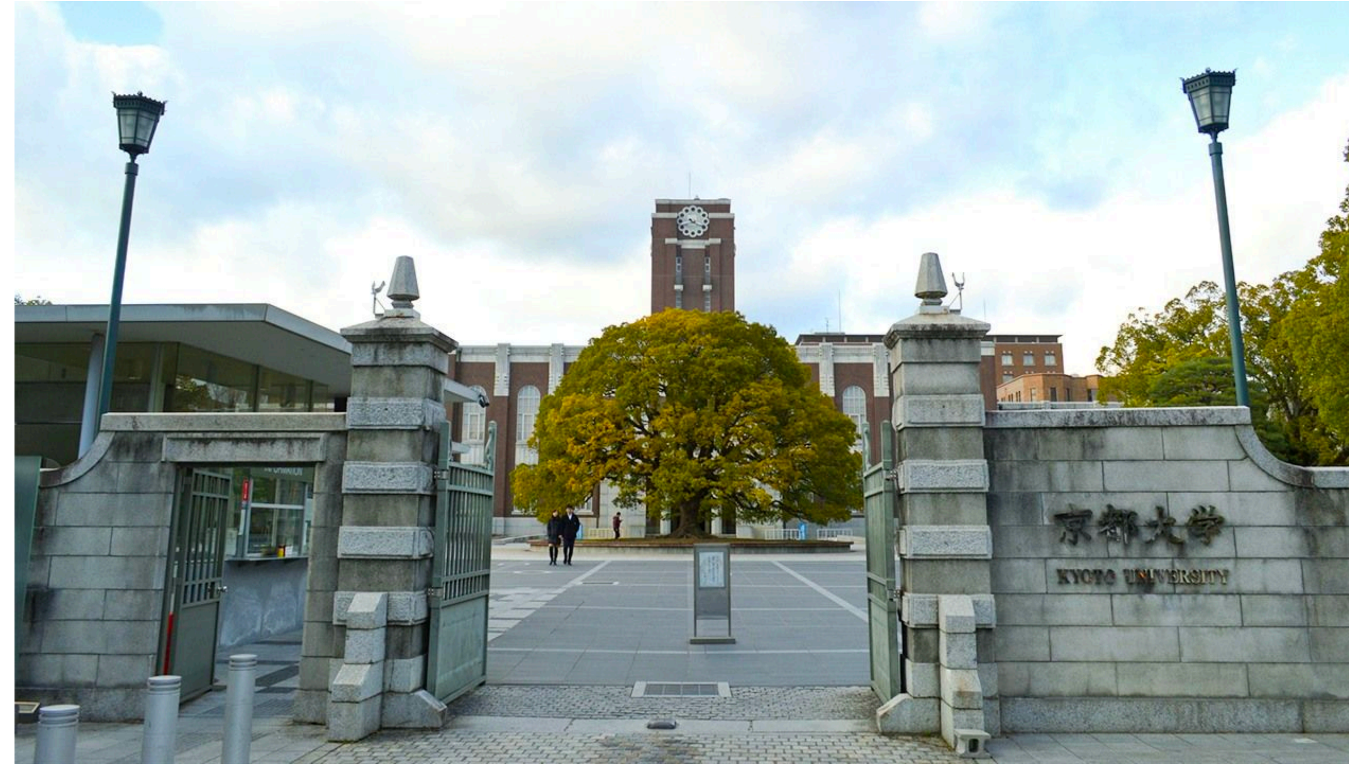

2018

2019

Got Ph.D in Kyoto!

2020

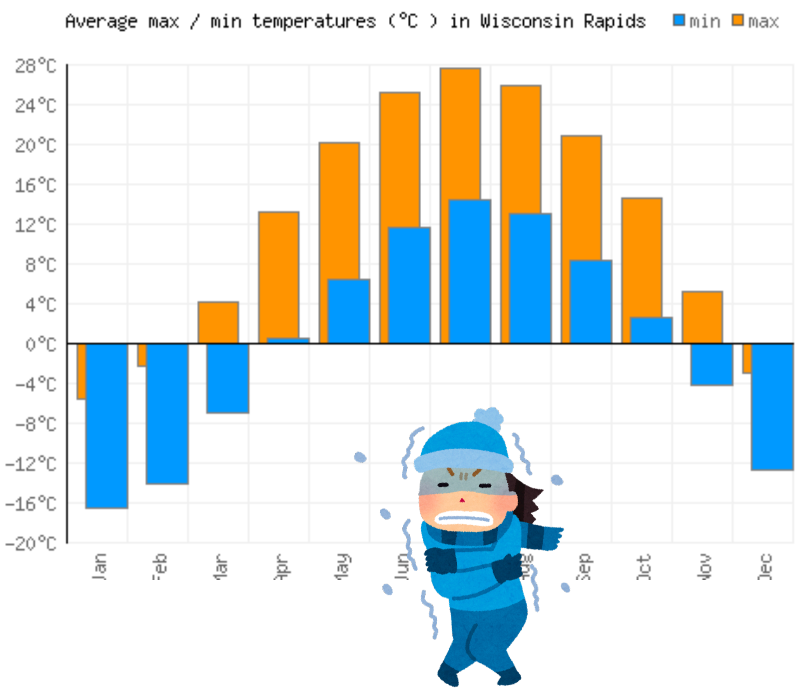

2015

2016

2017

2019

2020

2021

Moved to Madison, Wisconsin!

T2K

↓

Super-Kamiokande

↓

IceCube

2015

Measurement of **γ-rays from neutron-oxygen reactions** for improving understanding of neutron behavior in water

2016

2017

T2K **muon beam monitor** studies:
Current monitor investigations, New detector EMT R&D

2018

Neutrino **neutral-current quasielastic-like** interaction measurement by T2K beams

2019

Diffuse supernova neutrino background search at Super-Kamiokande

2020

IceCube researches for **high-energy astrophysical neutrino detections**

2021

Supernova Explosion

- A Star which is more than ~8 times heavier than the Sun ends its life by an explosion.
  - kinetic energy: **~10^{51} erg** (1 erg = 1×10^{-7} J = 6.2×10^{11} eV)
  - luminosity: ~galaxy
  - rate: 1–3/century/galaxy
- Classification by spectral characteristics
  - Ia, Ib, Ic, II
- Classification by explosion mechanism
  - thermonuclear (= Ia)
  - **core-collapse** (= Ib, Ic, II)

  → **neutrino emission**

Crab Nebula by NASA

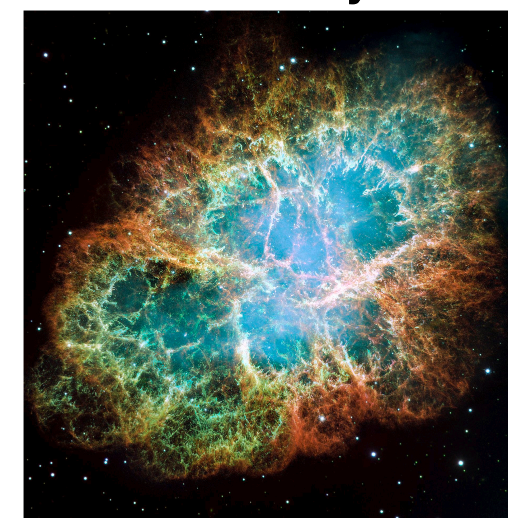

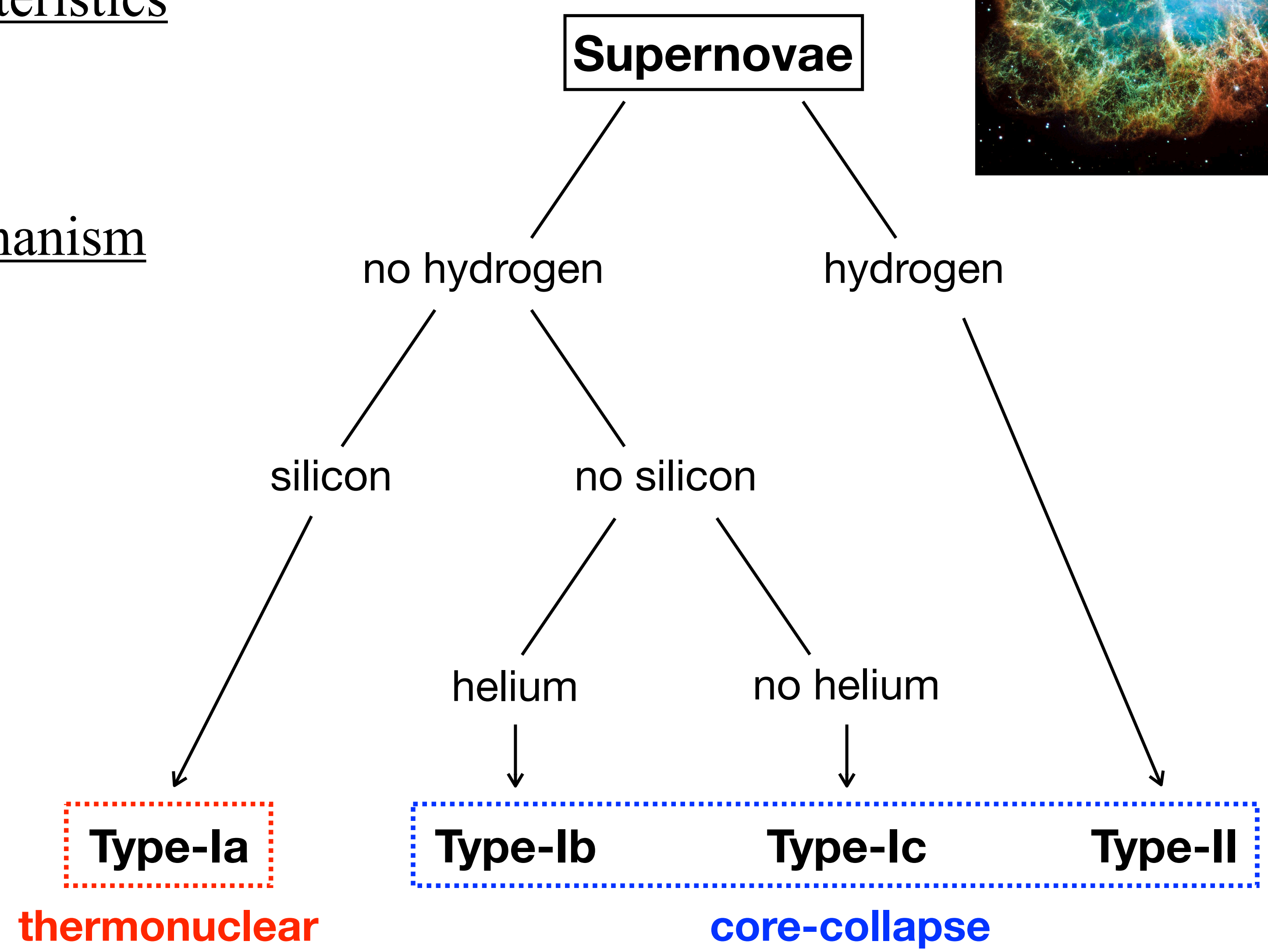

Neutrinos from Core-Collapse Supernovae

- ***Experiment*** There is only one observation of neutrinos from a supernova ("SN1987A" in the Large Magellanic Cloud).
- ***Theory*** There are many numerical simulations about CCSNe, but the explosion mechanism is not completely revealed.

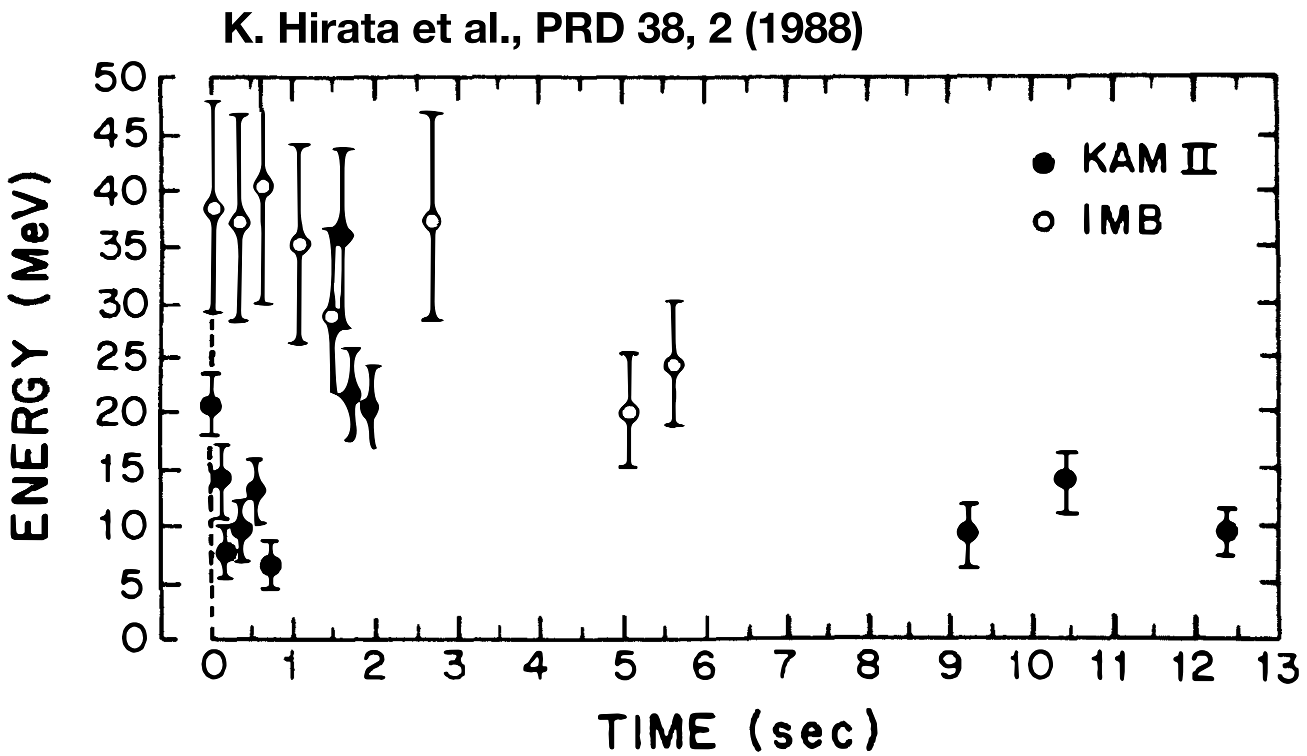

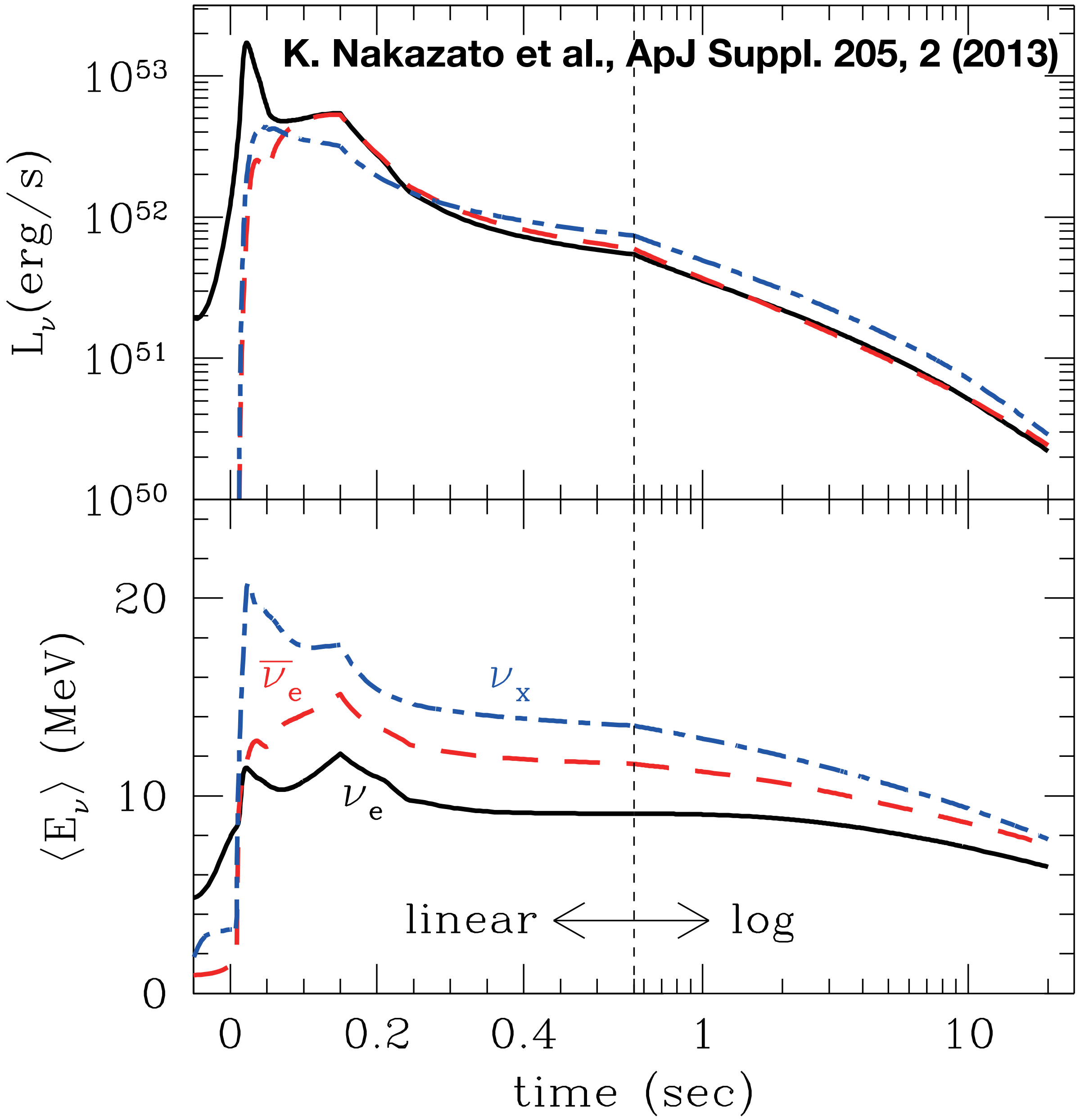

Diffuse Supernova Neutrino Background

- Neutrinos from all past CCSNe are accumulated to form an integrated flux.

  = **Diffuse Supernova Neutrino Background (DSNB)** or **Supernova Relic Neutrinos (SRNs)**

- Various factors affect the DSNB flux on Earth.
  - Neutrino oscillation (mass ordering)
  - Galactic evolution (star formation rate, initial mass function, binary interactions, etc)
  - Black hole formation rate (metallicity, equation-of-state, etc)
  - etc

DSNB flux

$$\frac{d\Phi(E_\nu)}{dE_\nu} = c\int_0^\infty \frac{dz}{H_0\sqrt{\Omega_m(1+z)^3+\Omega_\Lambda}} \times \left[R_{\mathrm{CCSN}}(z)\int_0^{Z_{\max}} \Psi_{\mathrm{ZF}}(z,Z)\left\{\int_{M_{\min}}^{M_{\max}} \Psi_{\mathrm{IMF}}(M)\frac{dN(M,Z,E'_\nu)}{dE'_\nu}dM\right\}dZ\right].$$

cosmological parameters

neutrino number spectrum per CCSN

CCSN rate

metallicity distribution of progenitors

initial mass function of progenitors

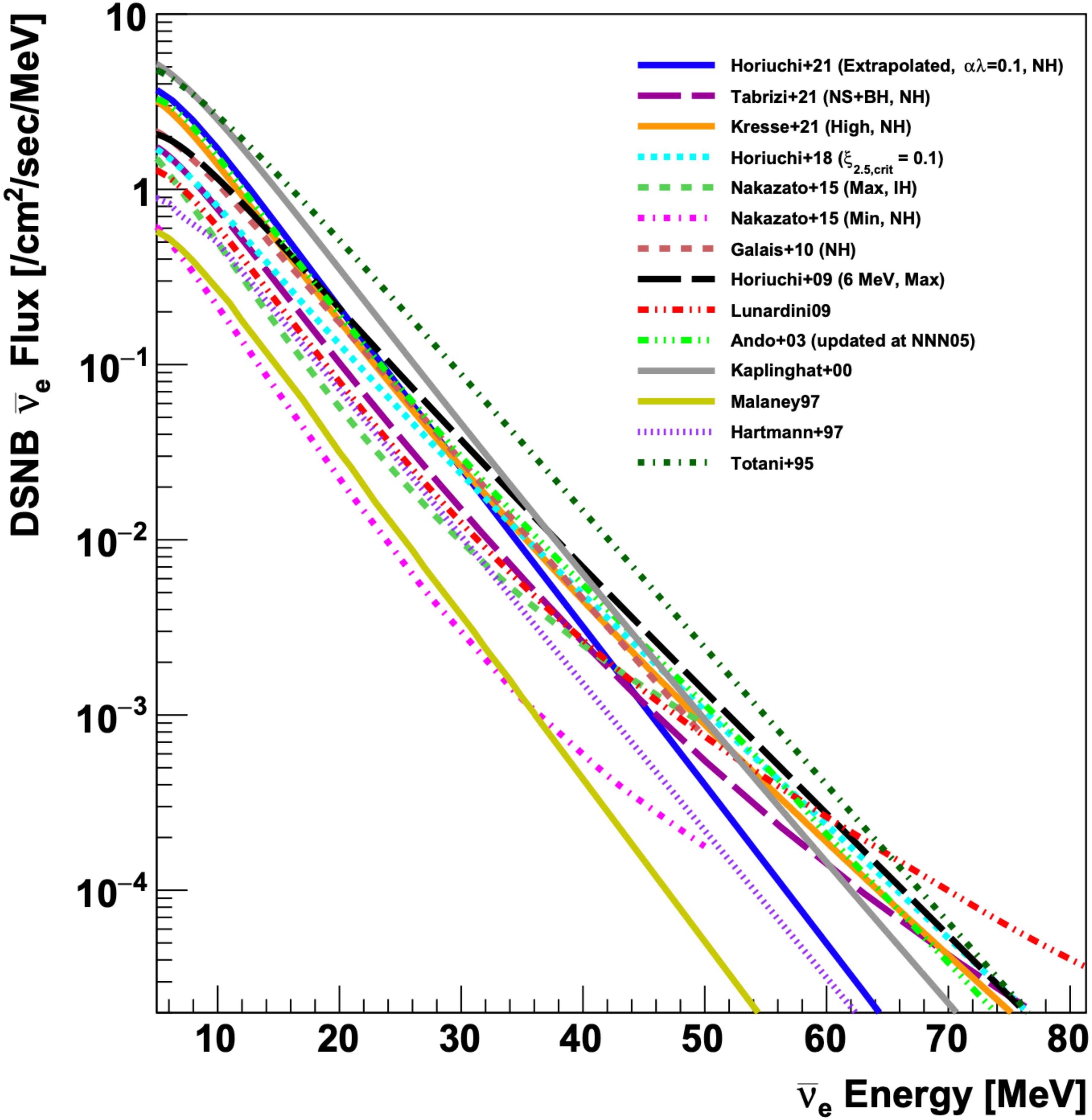

Horiuchi+21 (Extrapolated, αλ=0.1, NH)
Tabrizi+21 (NS+BH, NH)
Kresse+21 (High, NH)
Horiuchi+18 (ξ2.5,crit = 0.1)
Nakazato+15 (Max, IH)
Nakazato+15 (Min, NH)
Galais+10 (NH)
Horiuchi+09 (6 MeV, Max)
Lunardini09
Ando+03 (updated at NNN05)
Kaplinghat+00
Malaney97
Hartmann+97
Totani+95
DSNB ν̄e Flux [/cm²/sec/MeV]
ν̄e Energy [MeV]

Experimental Searches

- **Signal in experimental searches** = inverse beta decay (**$\bar{\nu}_e + p \rightarrow e^+ + n$**)
- Most sensitive searches have been performed at **Super-Kamiokande** and **KamLAND**.
- Search at SK (water)
  - SK-I/II/III (spectral fitting analysis): fitting by atmospheric spectra for E_ν > 17.3 MeV
  - SK-IV (neutron tagging analysis): low energy threshold, tagging efficiency ~20%
- Search at KamLAND (oil)
  - very low energy threshold, tagging efficiency ~ 100%

K. Nakazato et al., ApJ 804, 75 (2015)

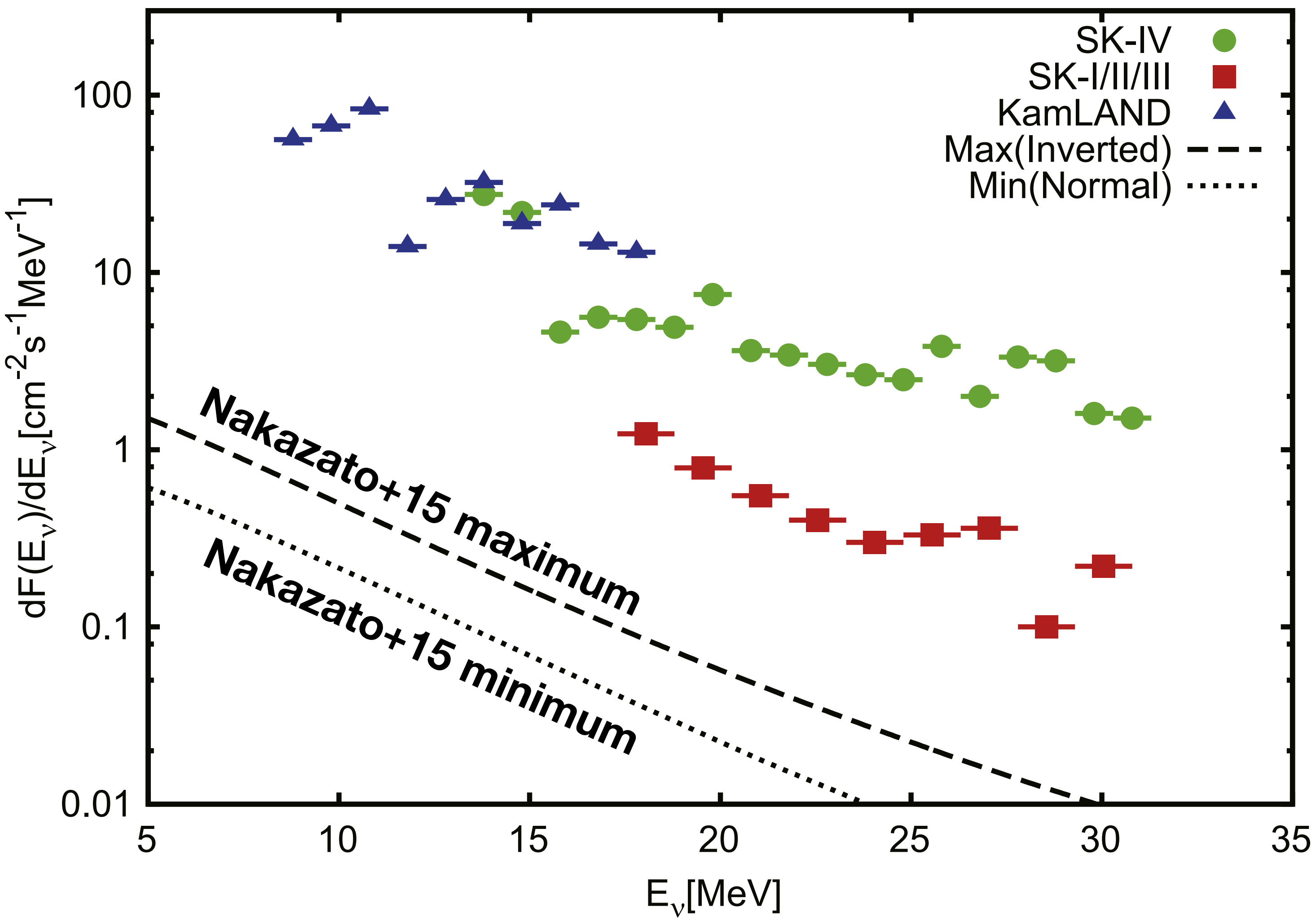

Recent Result from KamLAND

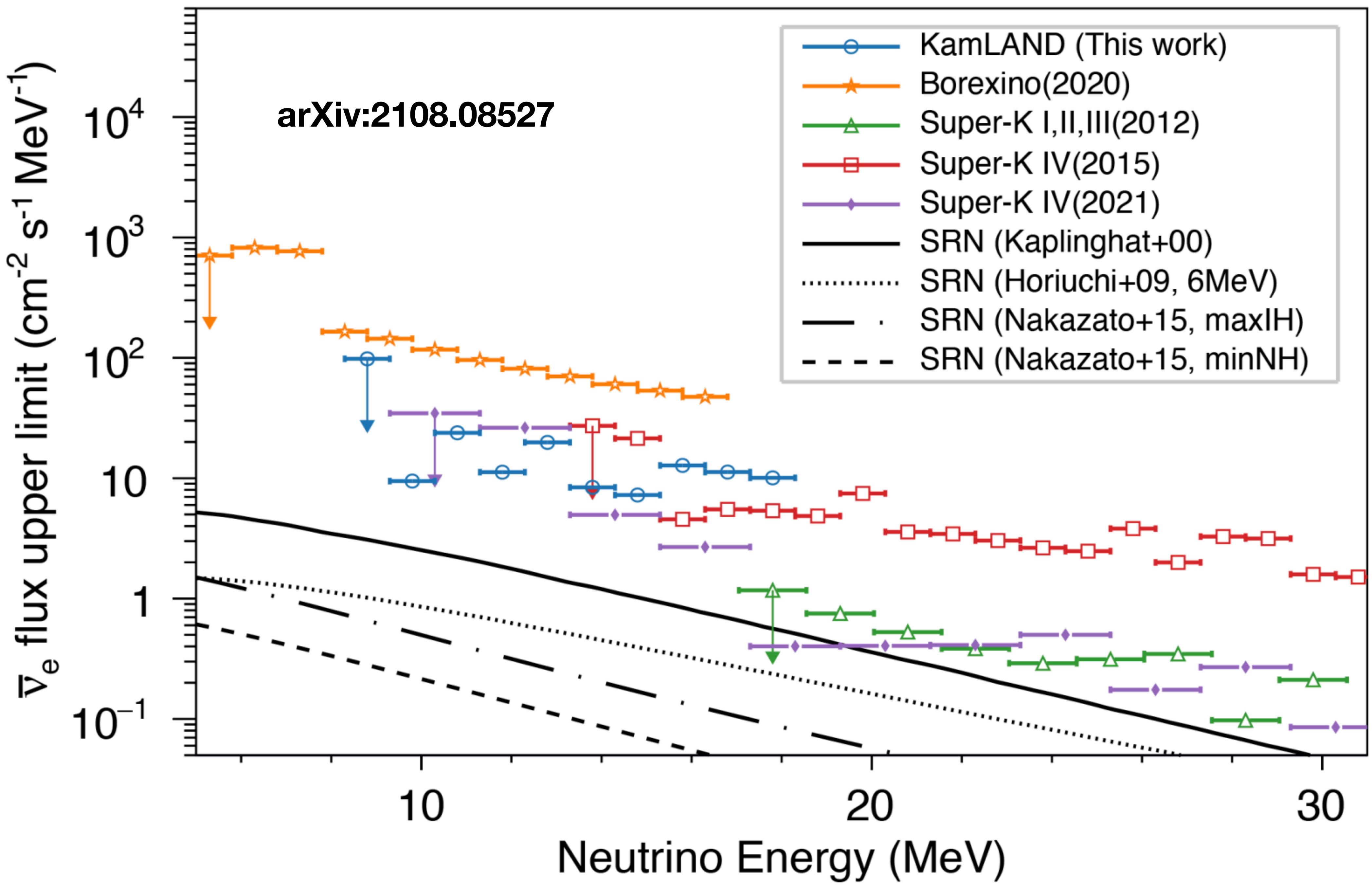

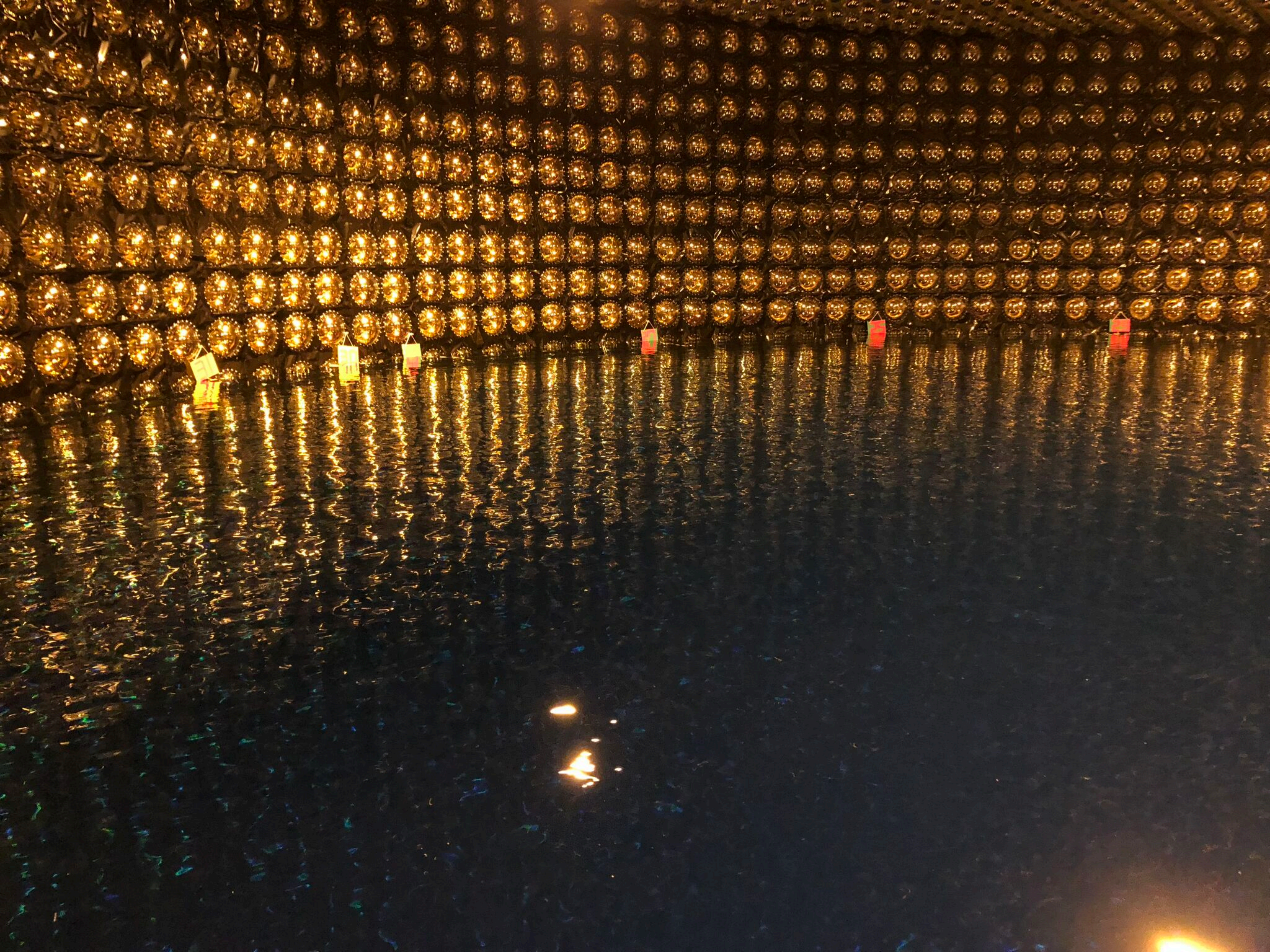

Super-Kamiokande

- A water Cherenkov detector located 1,000 m under the mountain.
- Fiducial volume: 22.5 kton
- Inner detector: 11,129 20-inch PMTs
- Outer detector: 1,885 8-inch PMTs, used for cosmic muon veto
- Operated since 1996 in five periods.
  - This work uses data from **SK-IV** (2008–2018).

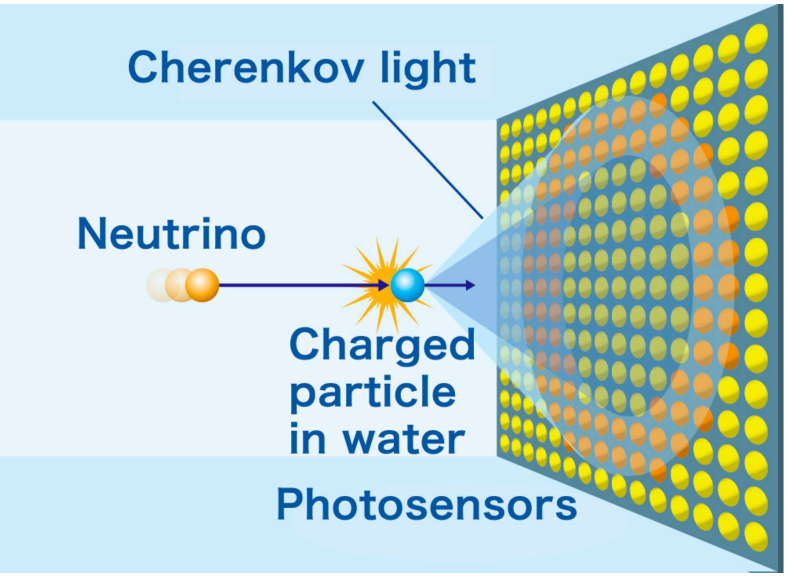

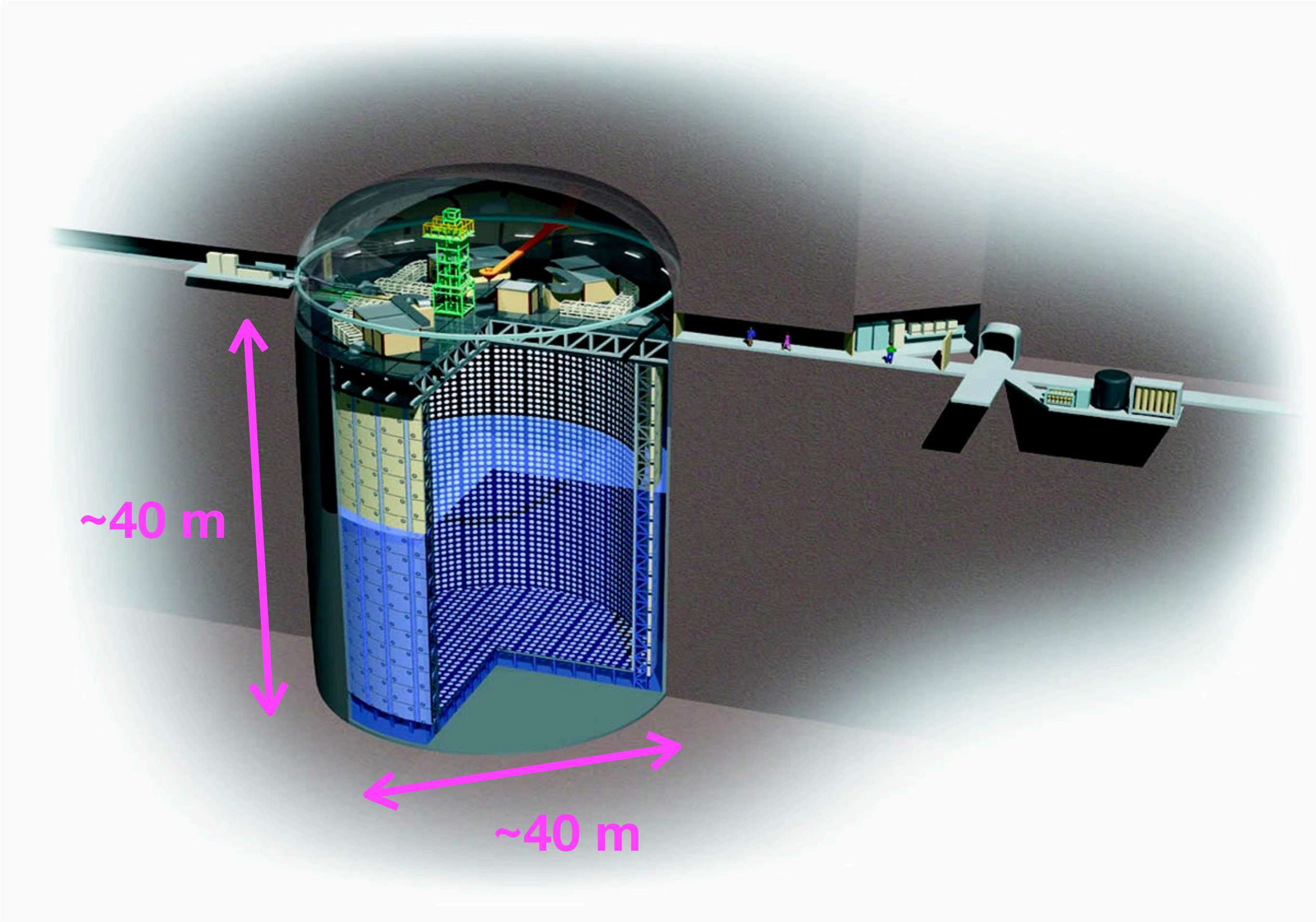

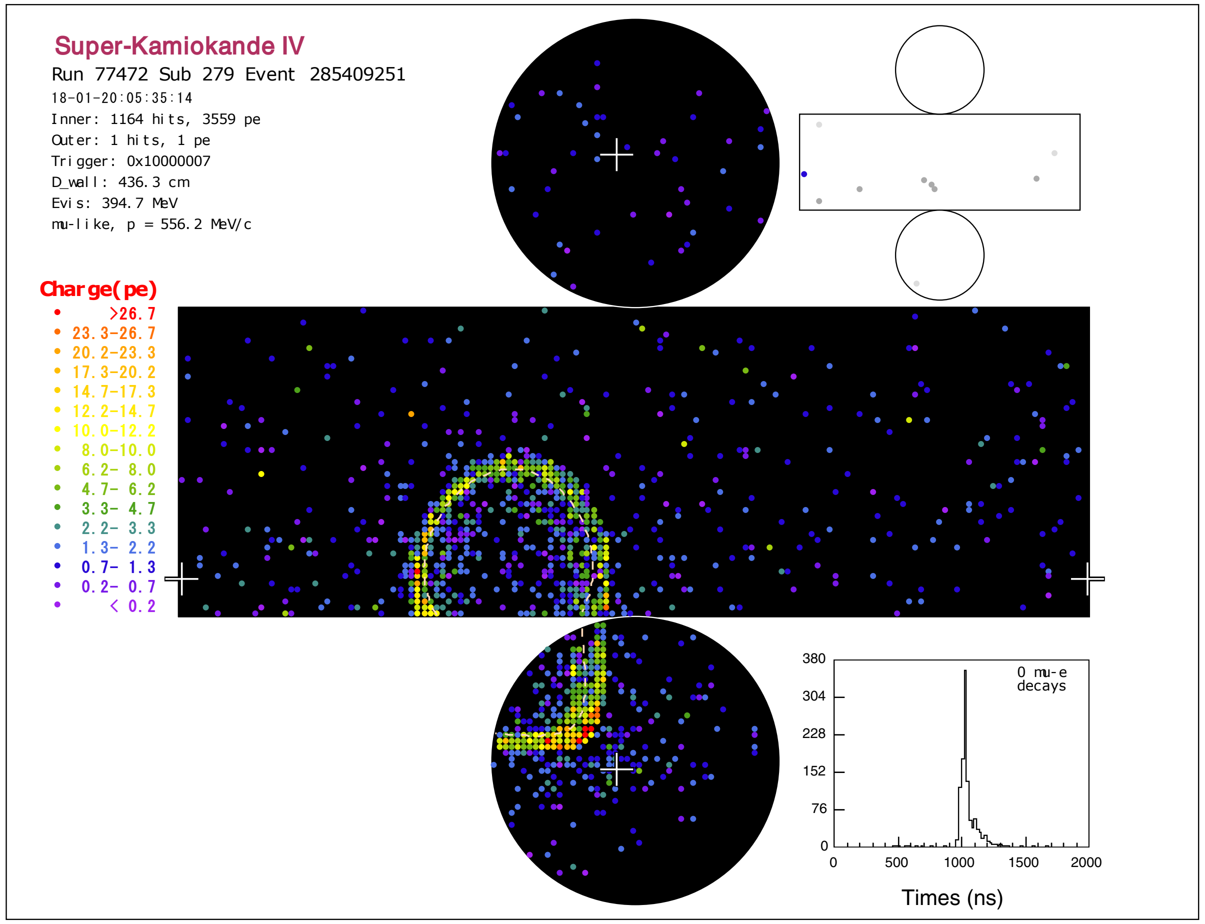

Signal

- Inverse beta decay of electron antineutrinos (**$\bar{\nu}_e + p \rightarrow e^+ + n$**) is searched.
  - <u>Larger than the other mode by >2 orders of magnitude.</u>
  - Search region = [7.5, 29.5] MeV in visible energy (E_ν = [9.3, 31.3] MeV)
- Signal: "***β+n***" events
  - Prompt signal = β
  - Delayed signal = **2.2 MeV γ** from neutron capture

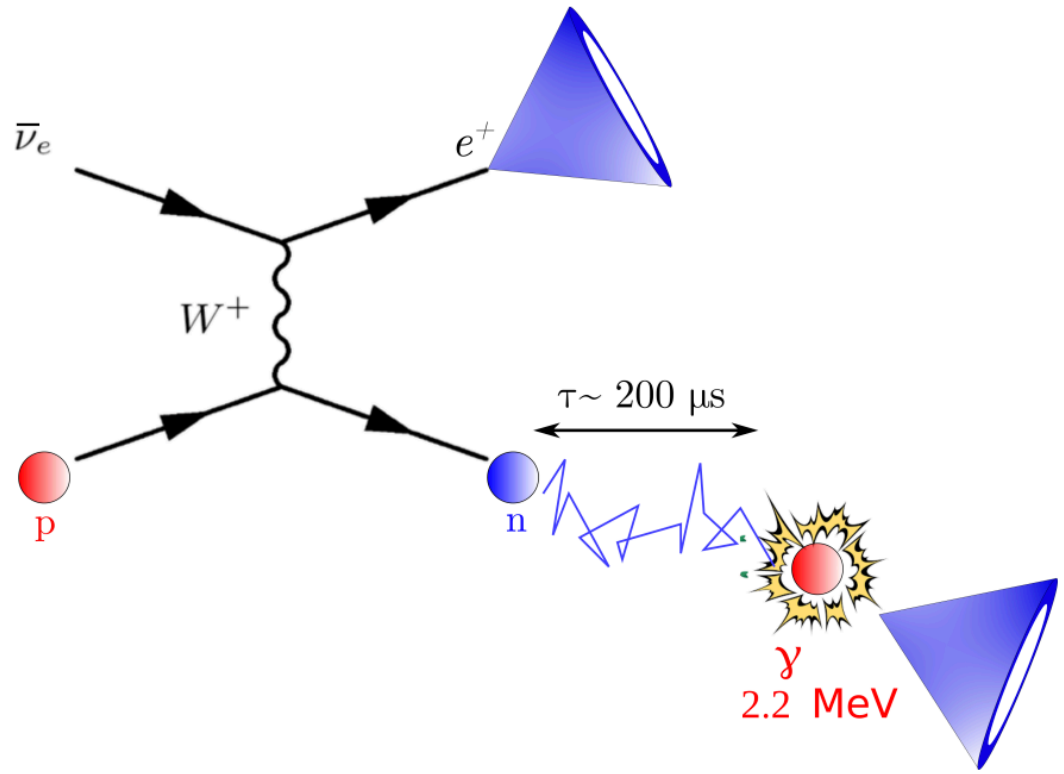

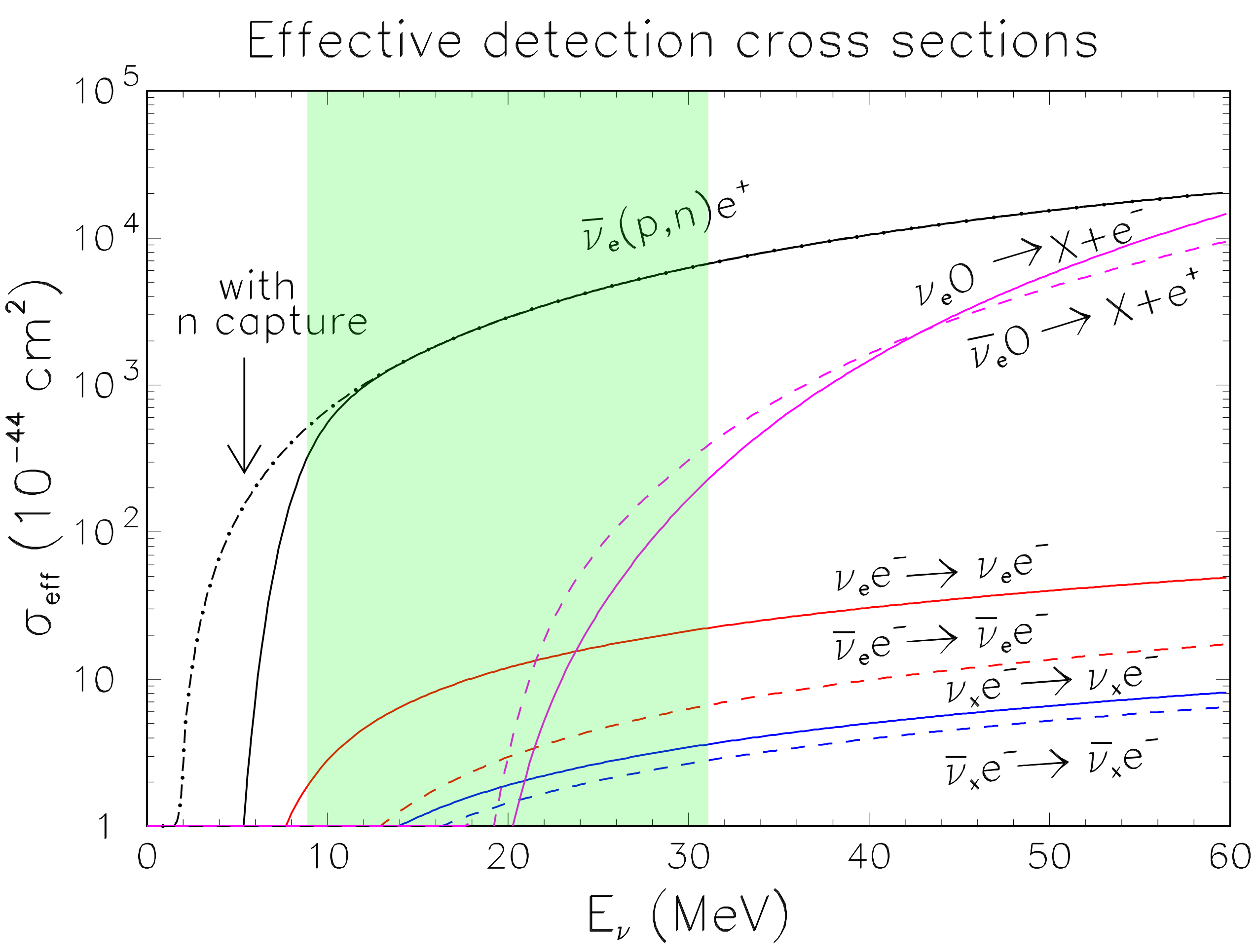

Background (1): Atmospheric Neutrinos

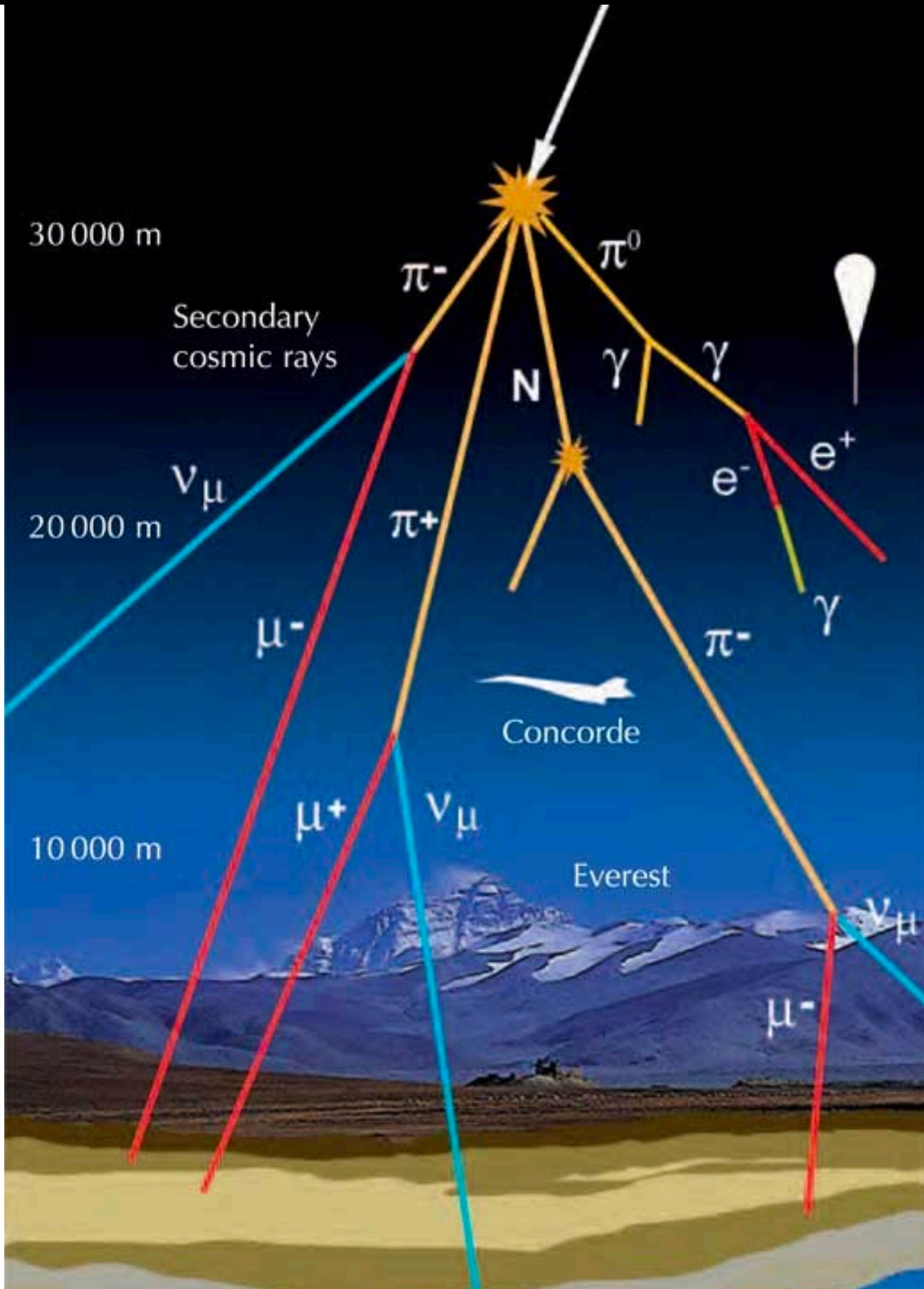

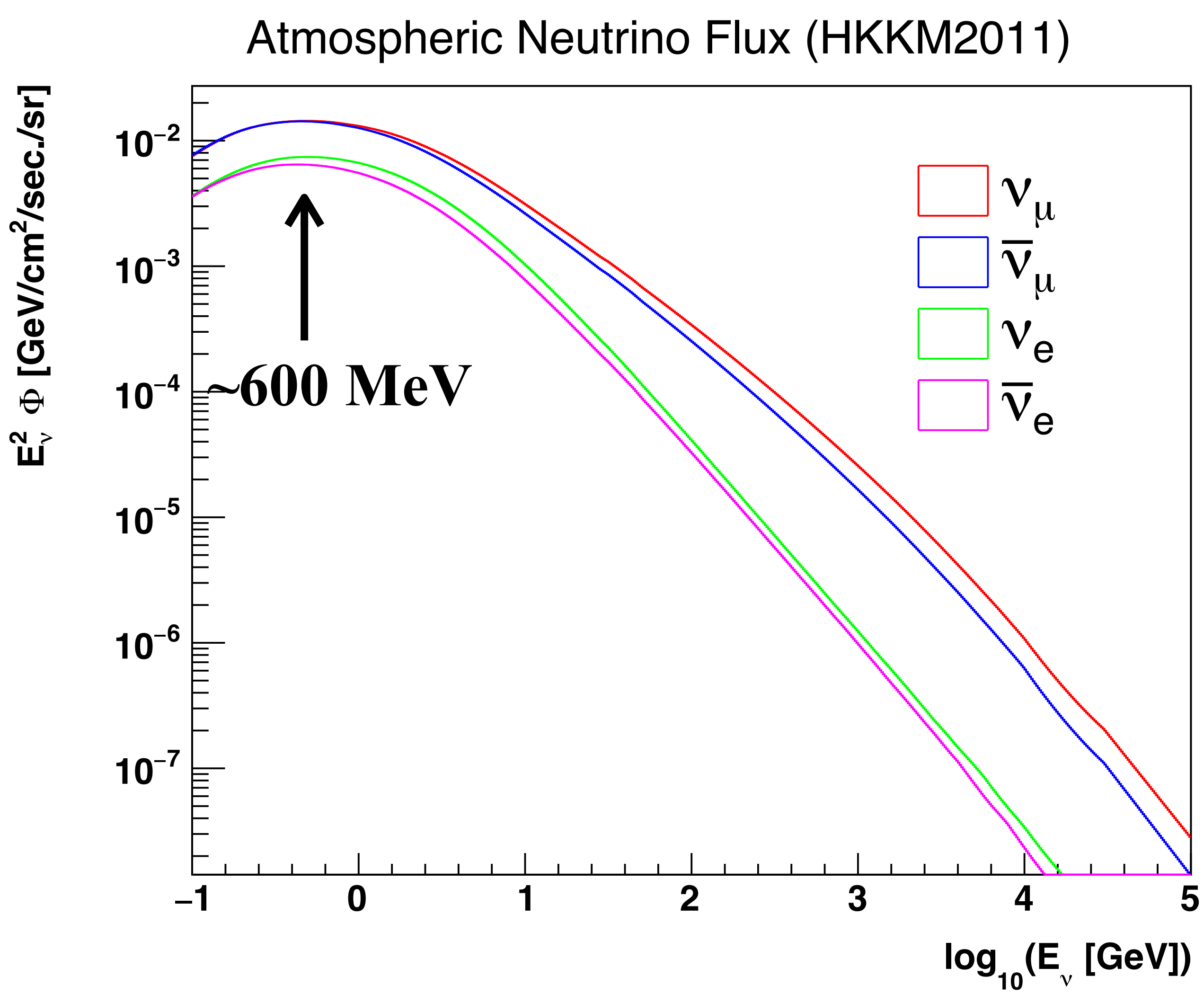

Background (1): Atmospheric Neutrinos

- **Neutral-current quasielastic (NCQE) interactions**
  - de-excitation γ-ray (+*n*)
  - dominant below ~20 MeV

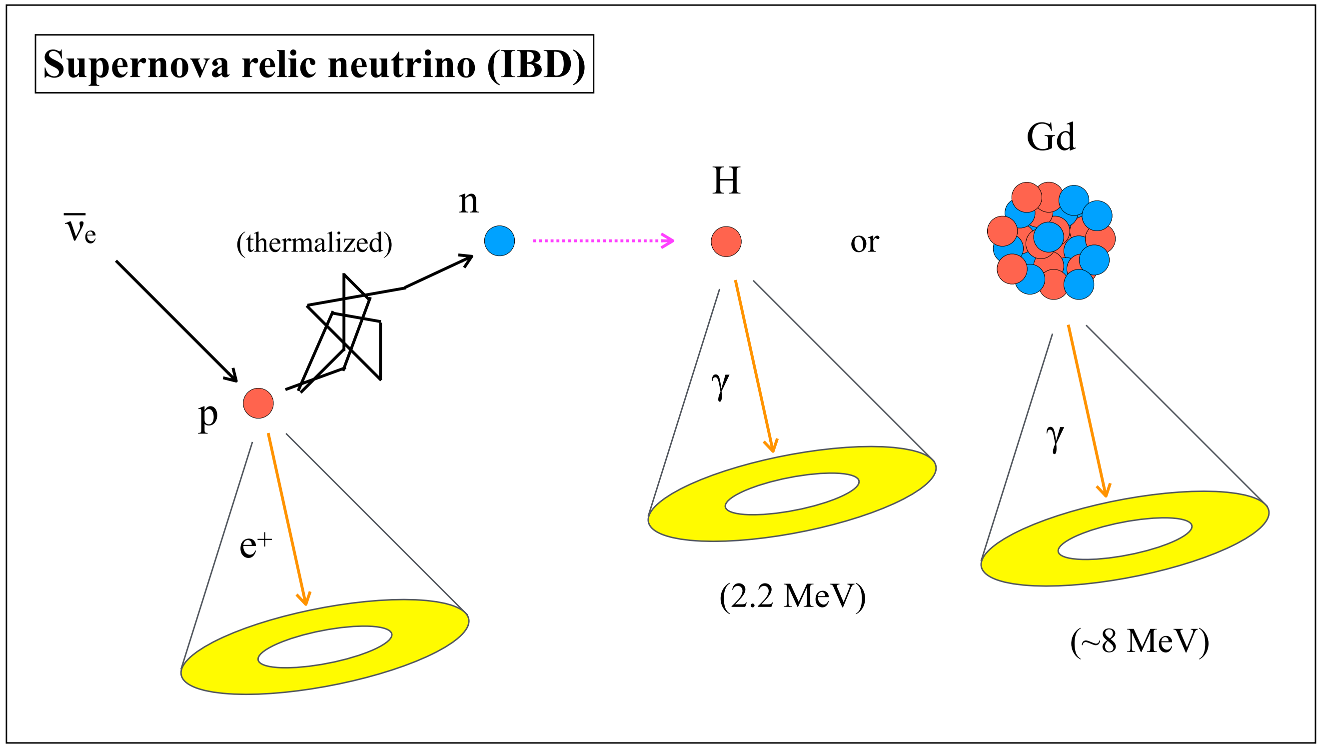

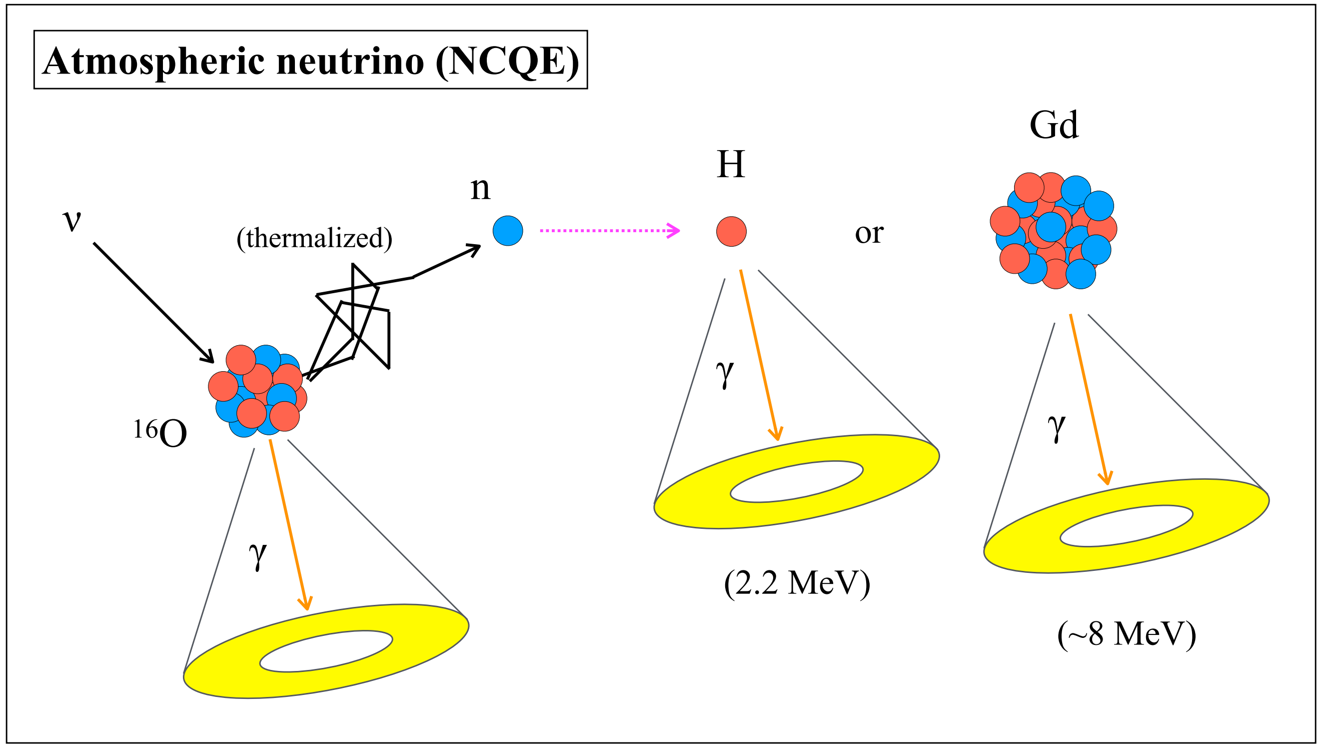

- **Muon-producing interactions (CC, NC)**
  - (invisible muon →) decay electron (+*n*)
  - dominant above ~20 MeV

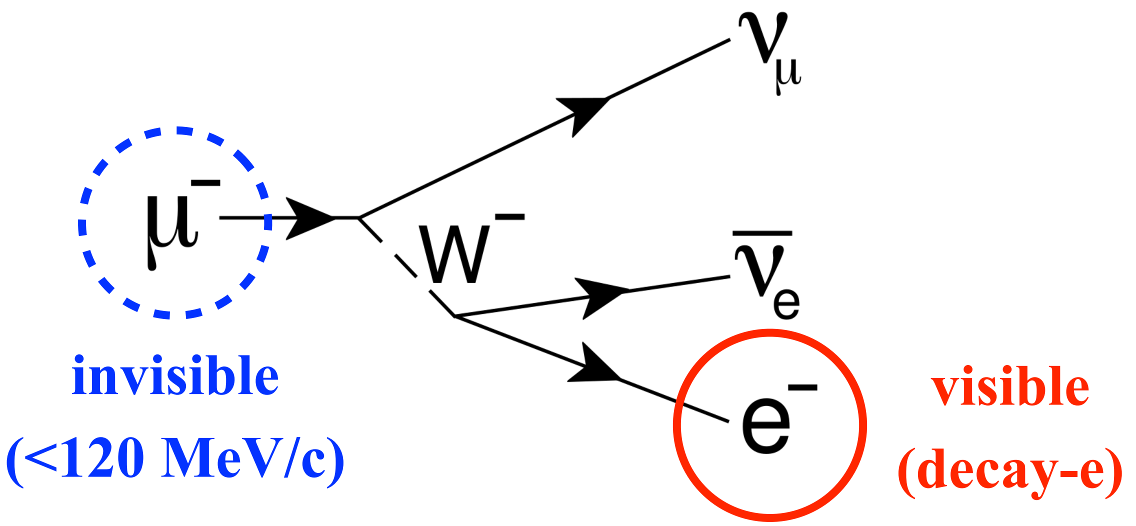

Background (2): Muon Spallation

- Cosmic-ray muons are coming at Super-K with ~2 Hz.
- Some of them break nuclei in water, producing radioactive isotopes.
- This is huge below 20 MeV, and especially ^{9}Li decays into β+n.

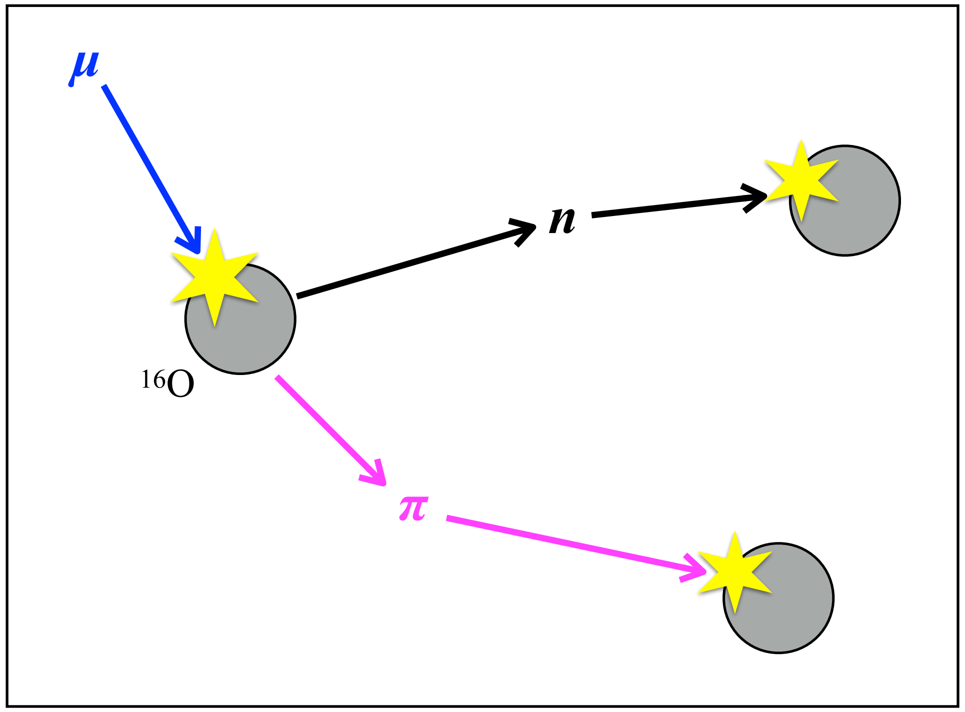

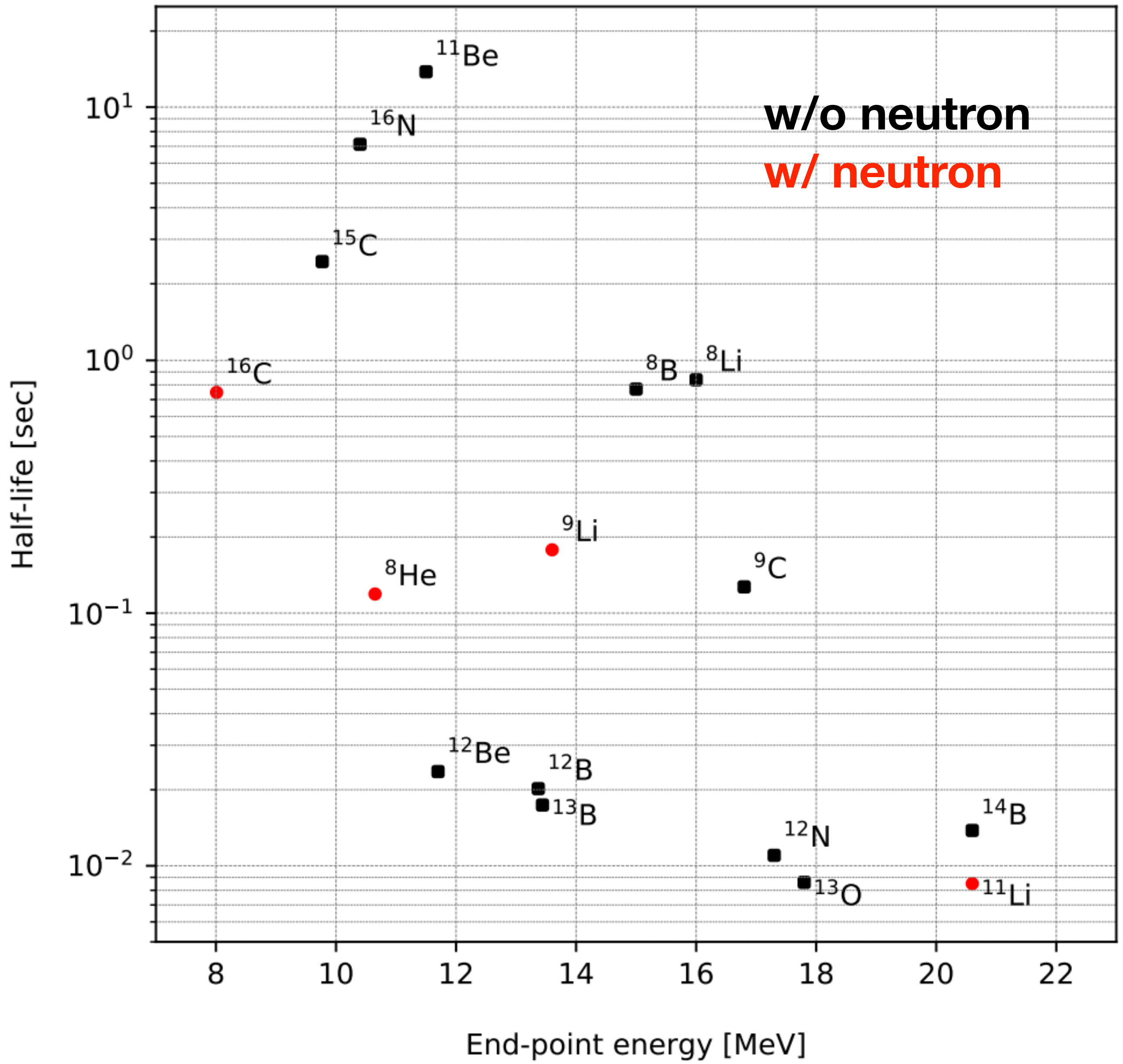

Background (3): Other Sources

- **Solar neutrinos**
  - Electron neutrinos from Sun.
  - Would make an accidental pair with a neutron-like signal.

- **Reactor neutrinos**
  - Electron antineutrinos from reactor plants
  - Only below 10 MeV

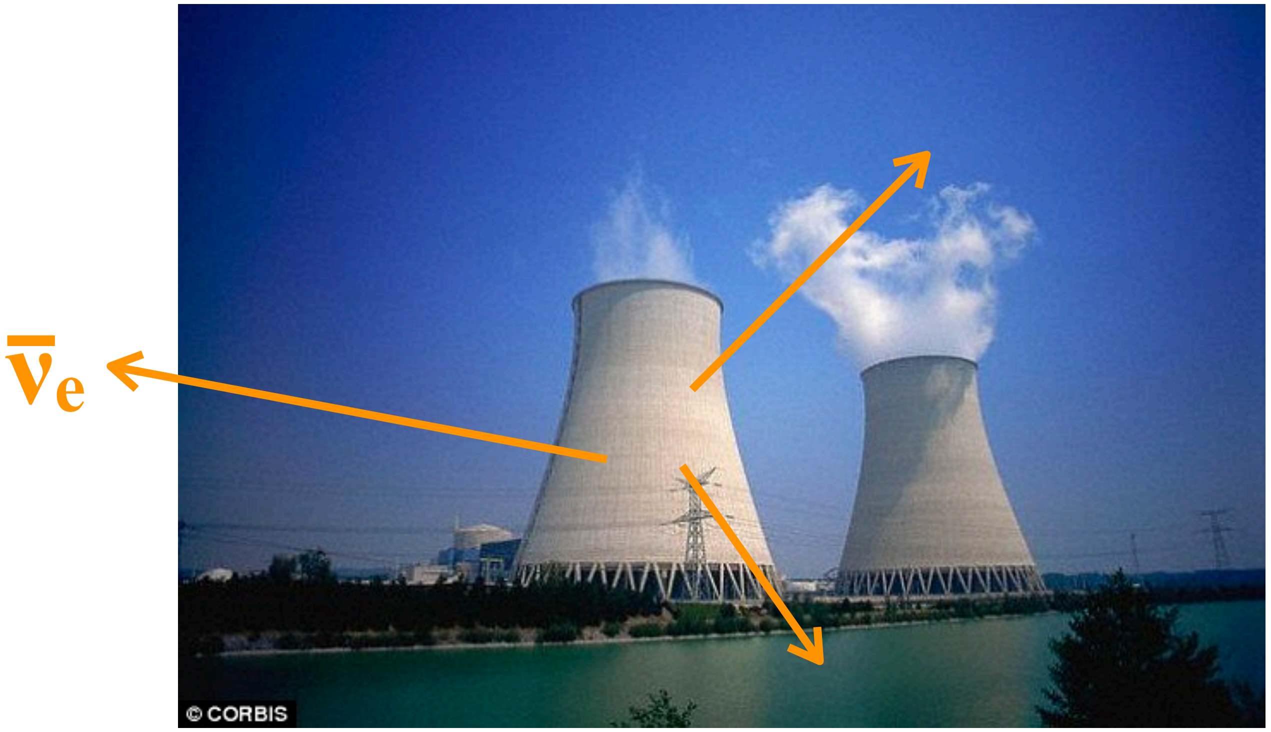

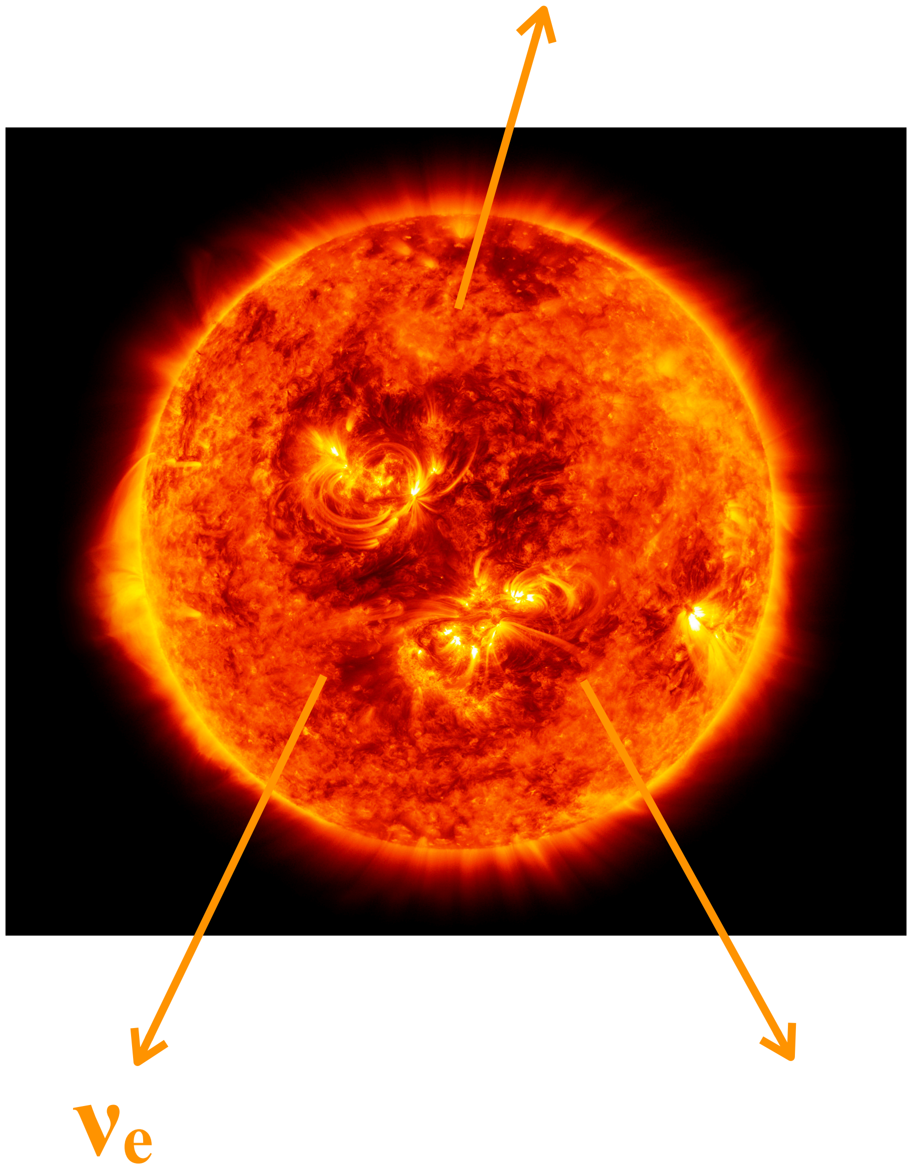

Energy at LowE

- Energy is reconstructed from the number of PMT hits.
- Detector calibration is performed in many ways.
    - Electron linear accelerator (LINAC): up to ~19 MeV
    - γ-ray source: ~O(10) MeV
    - Electrons from cosmic-ray muon decay (decay electrons): >O(10) MeV

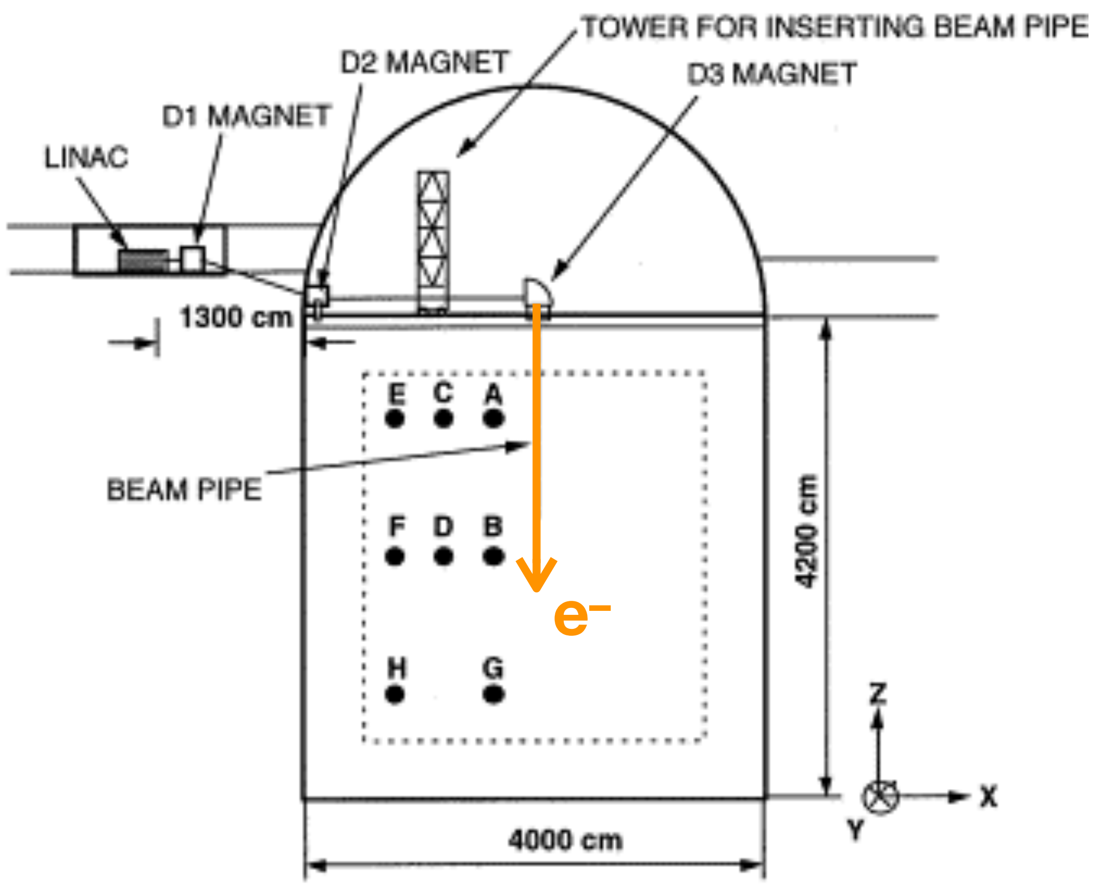

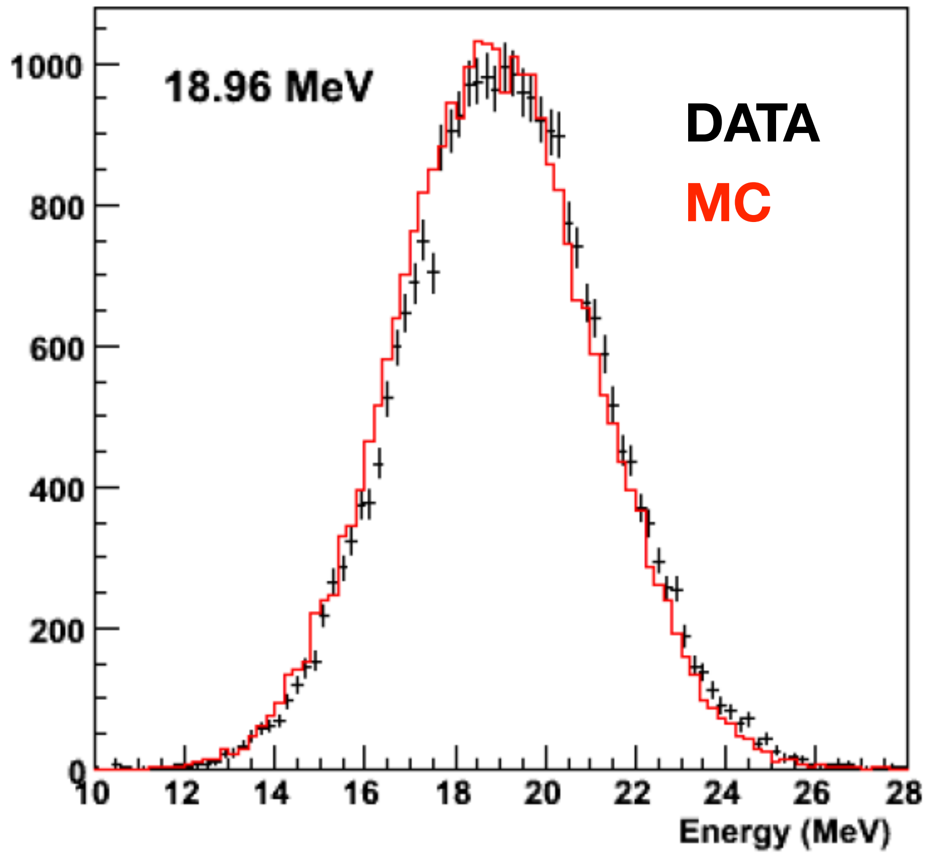

Position and Direction

- Huge amount of radioactive backgrounds near the wall.
- We require >2 m away from the wall and additional cuts on "effective wall distance".

$$d_{\rm eff} > \max\left\{300,\ 500 - \frac{E_{\rm rec} - 15.5\ {\rm MeV}}{1\ {\rm MeV}} \times 50\right\}\ {\rm cm.}$$

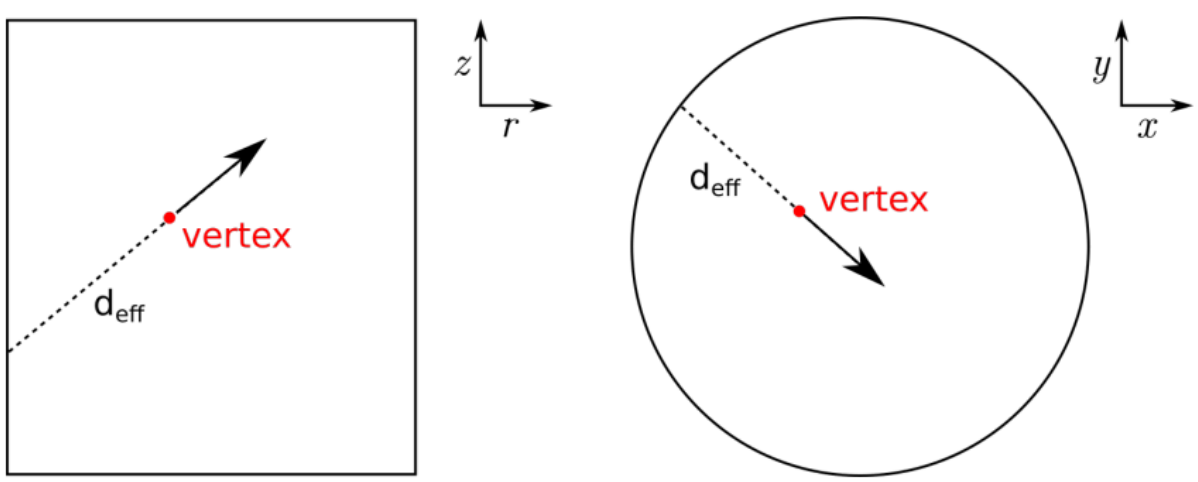

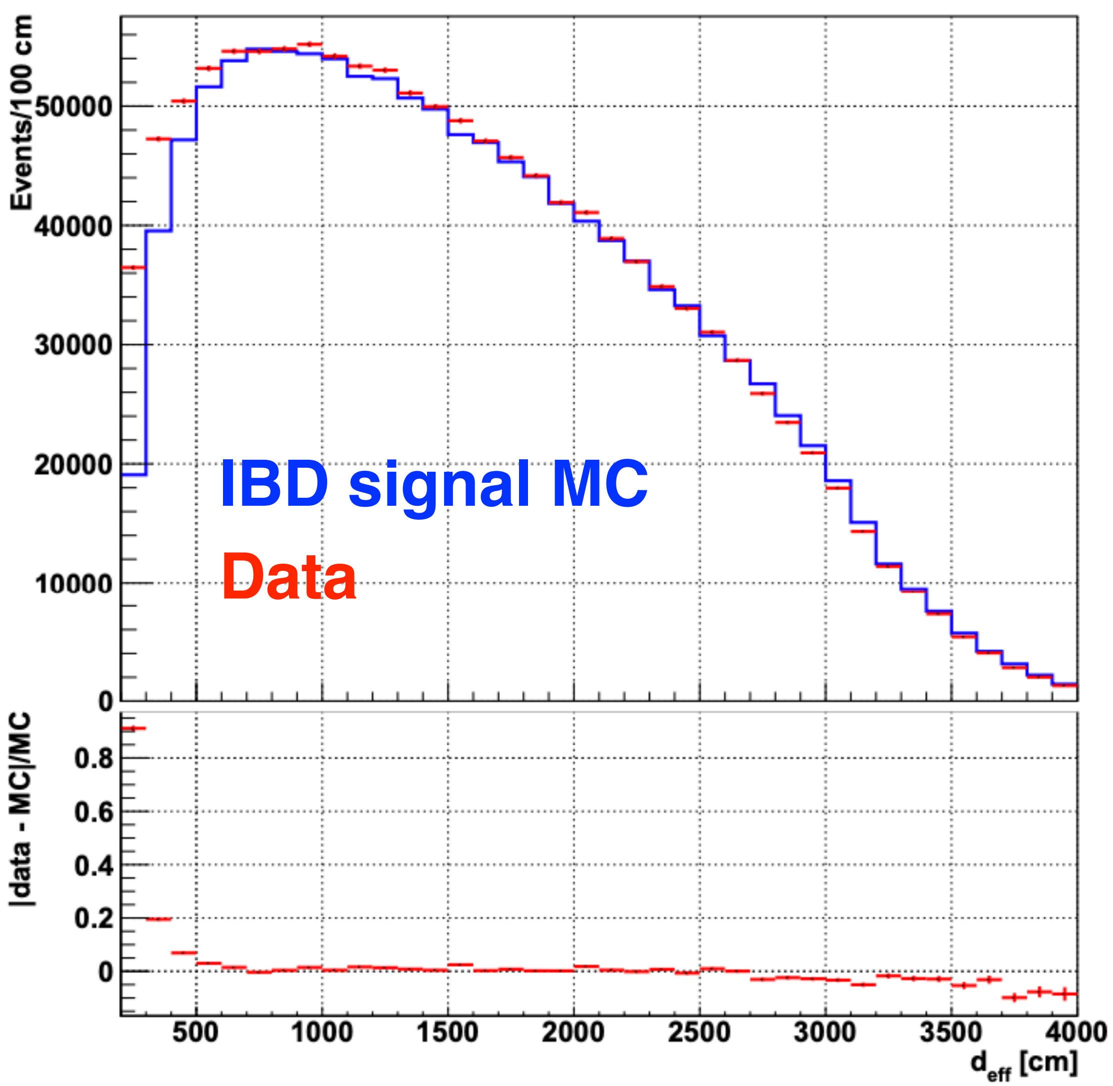

Particle Identification

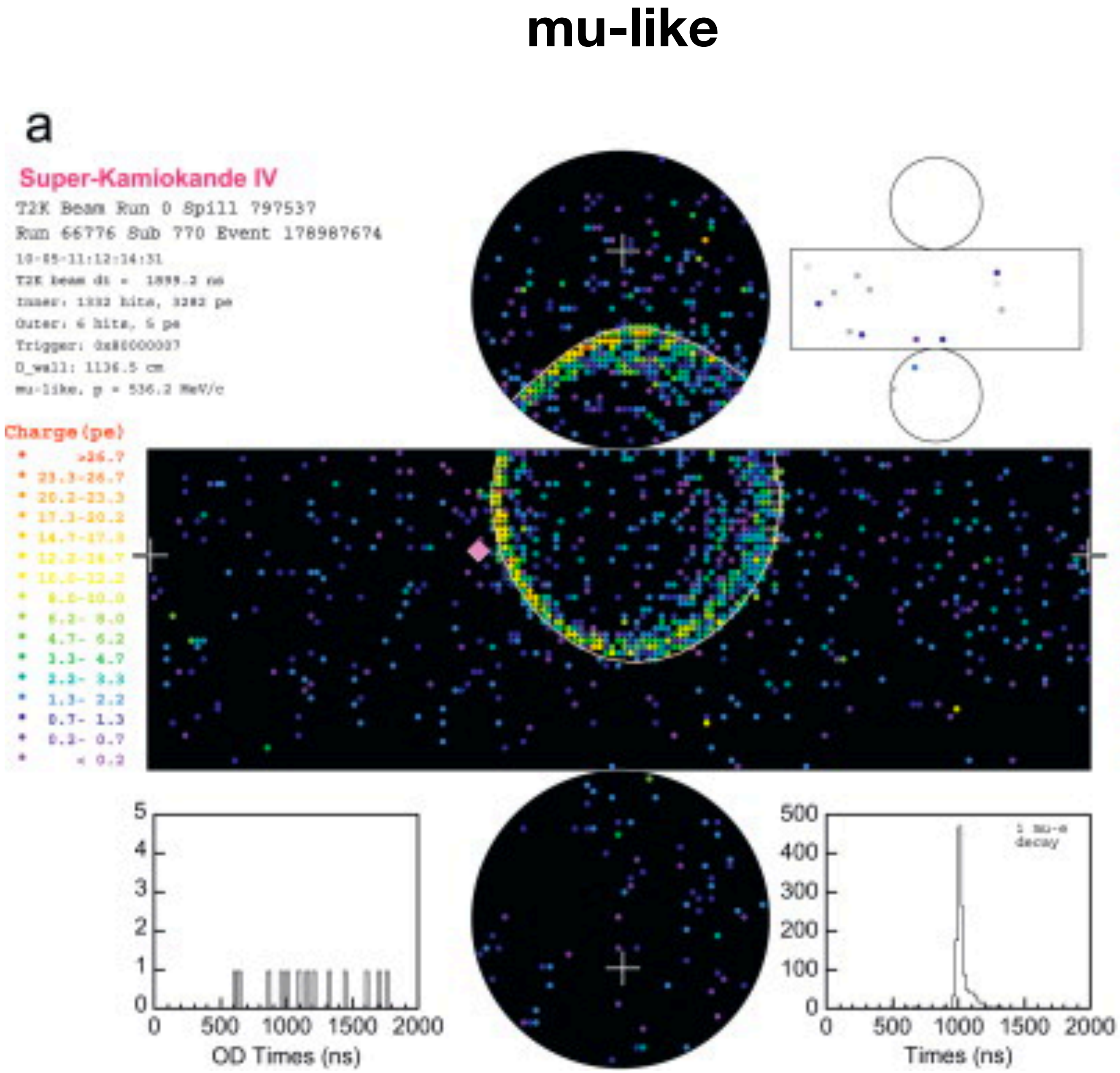

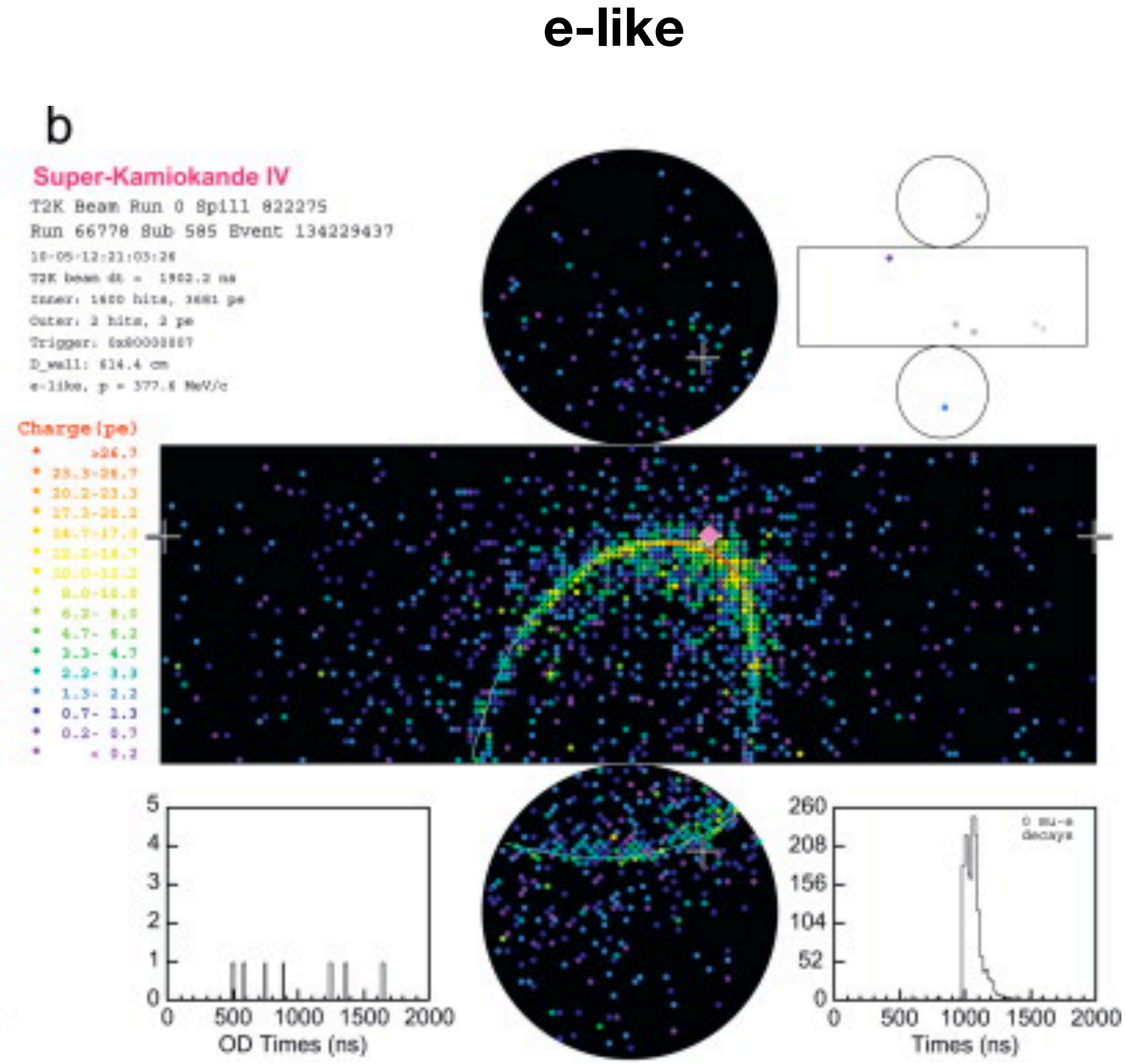

Particle Identification

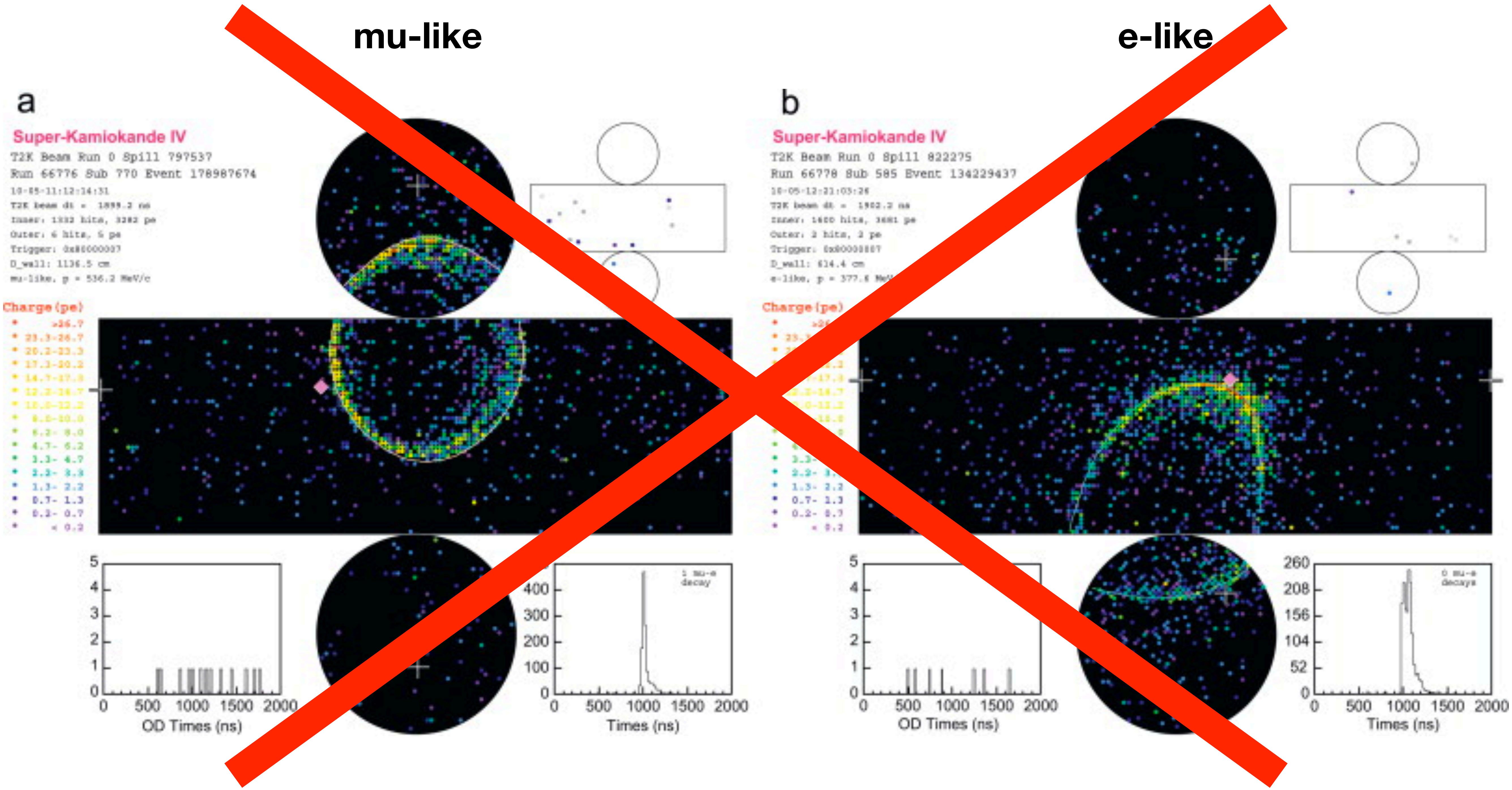

The current analysis region (<30 MeV) has only 100~200 hits!

Almost all PMTs have single p.e. hit.

Cherenkov Angle & Decay Electron

- Low energy muon events are likely to have their decay electrons at later times.
- Cherenkov opening angle is a nice discriminant for particle identification.

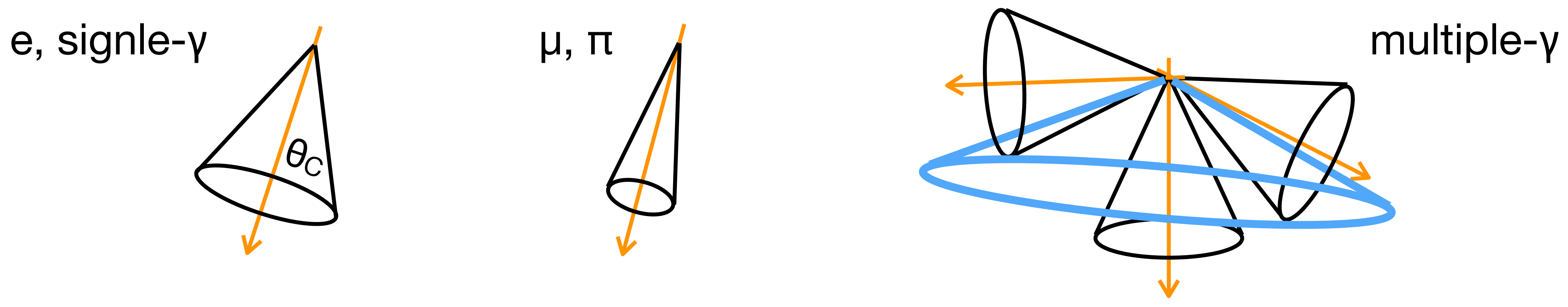

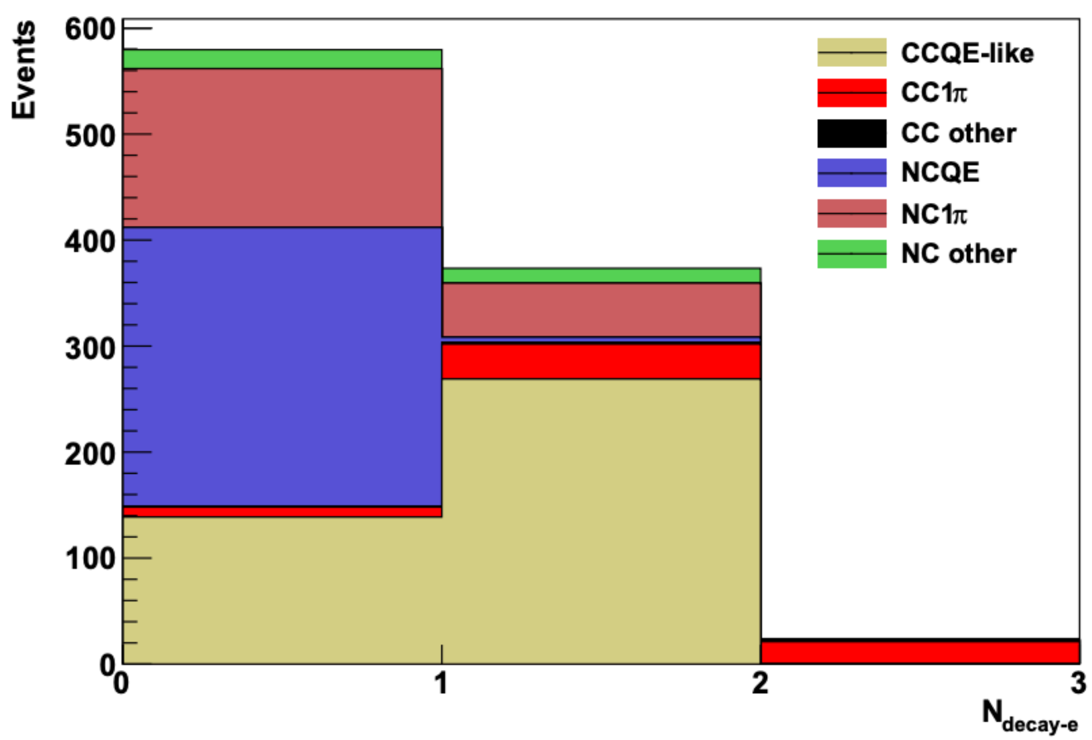

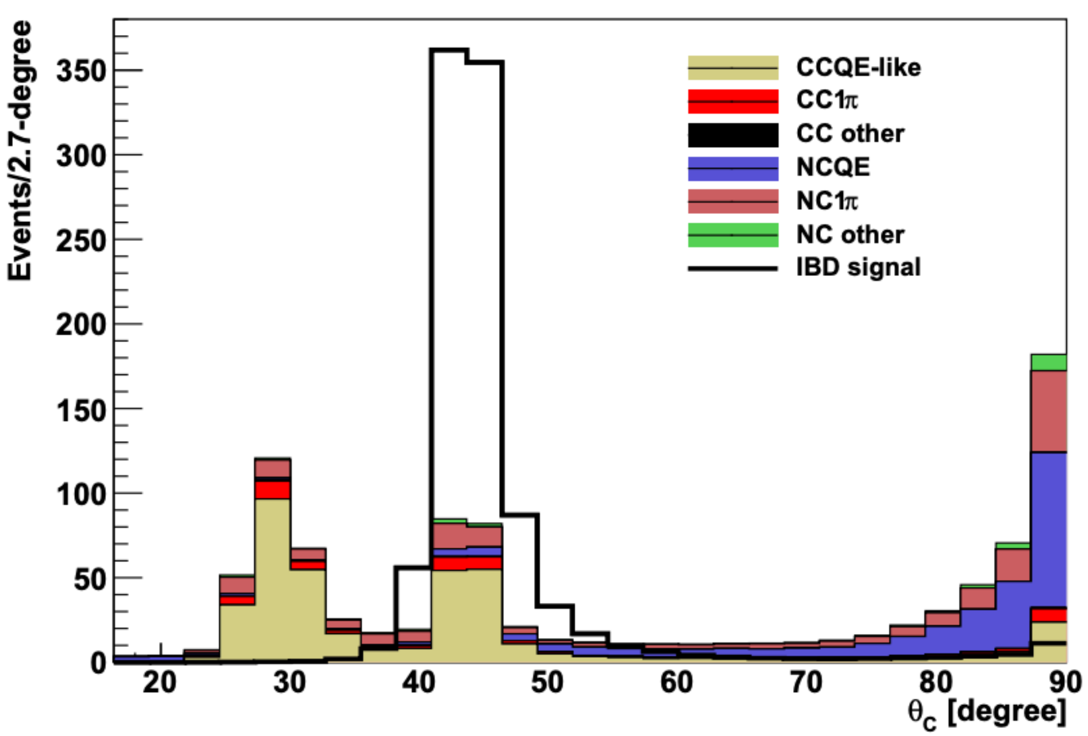

Spallation Cuts

- Clustered events (in time and position) are likely to be spallation products.
- More powerful cuts are made by using muon reconstruction information.
  - Events close to muon track in time and position are likely spallation.
  - Large energy depositing muons would produce spallation.
  - **These efforts achieved to reject >95% spallation background.**

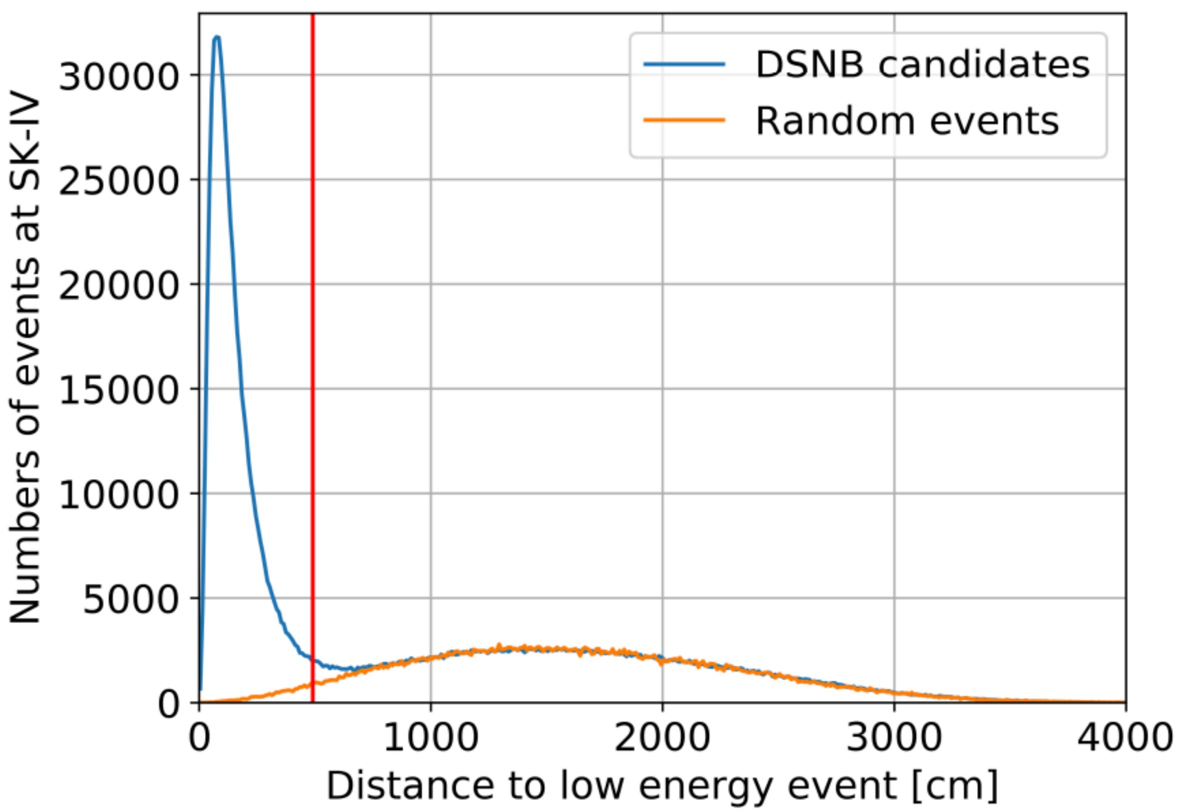

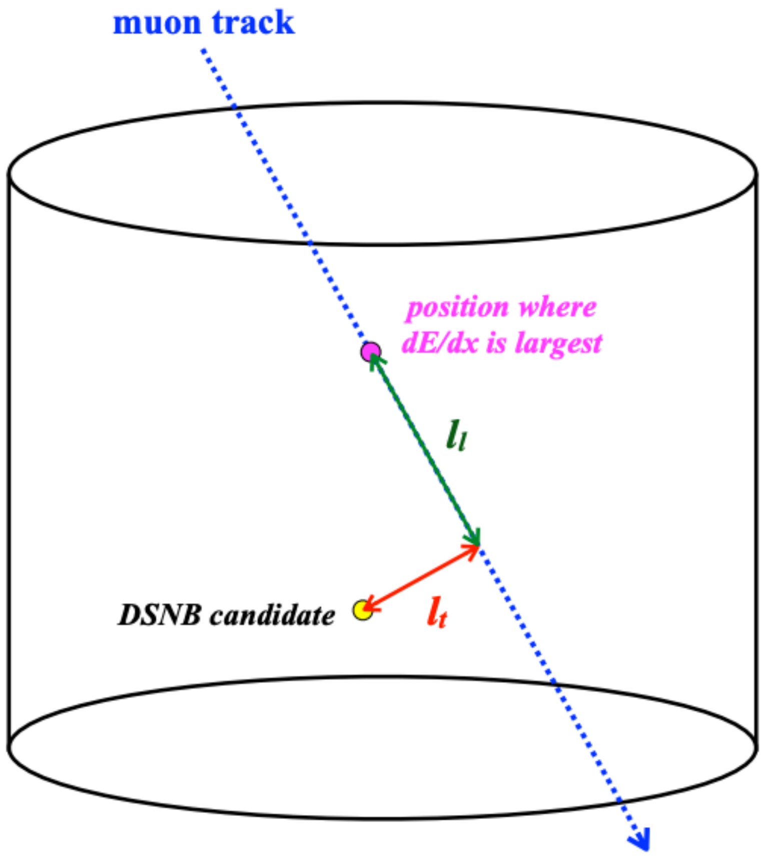

Neutron Tagging

- An additional DAQ window is taken until 500 μs later than the primary event (≥SK-IV).
- Very subtle sign for the 2.2 MeV γ (visible is <2.2 MeV; only ~10 hits).
  - SK reconstruction is possible above 3.5 MeV visible energy.
  - **BDT** is implemented to catch this subtle sign.
  - The 22 variables: hit pattern, geometrical information, etc
- **20~30%** signal (=neutron) efficiency against **10^{-3}~10^{-4}** background (=no neutron) rejection.

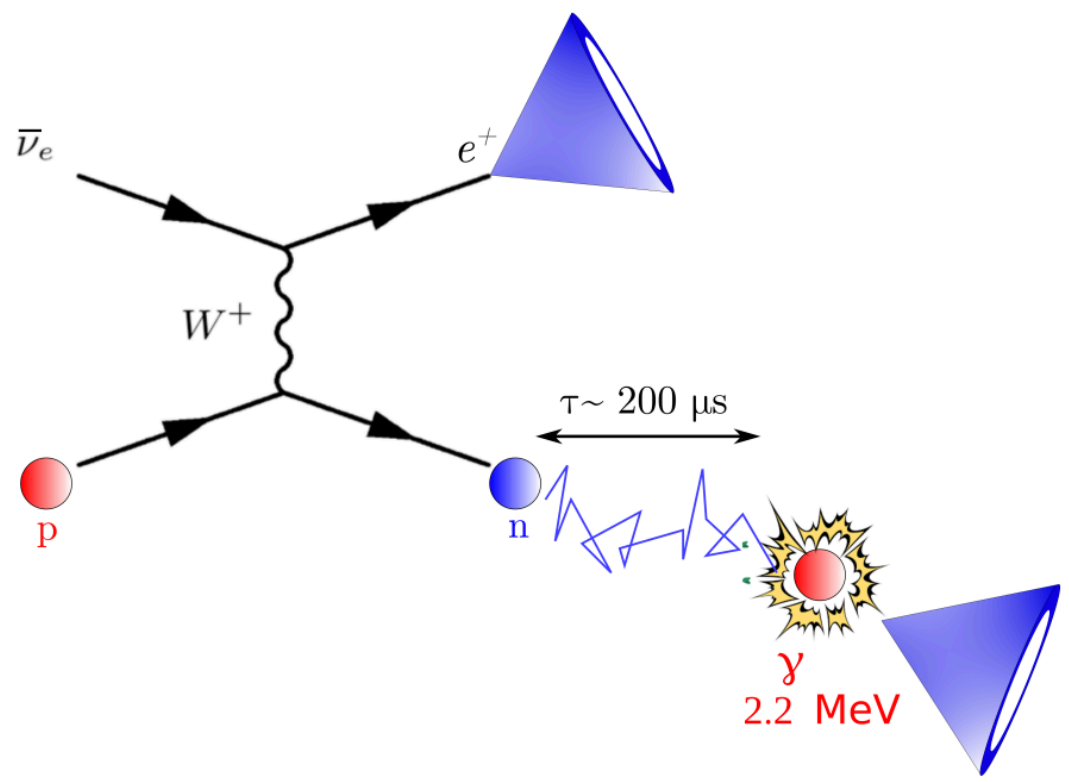

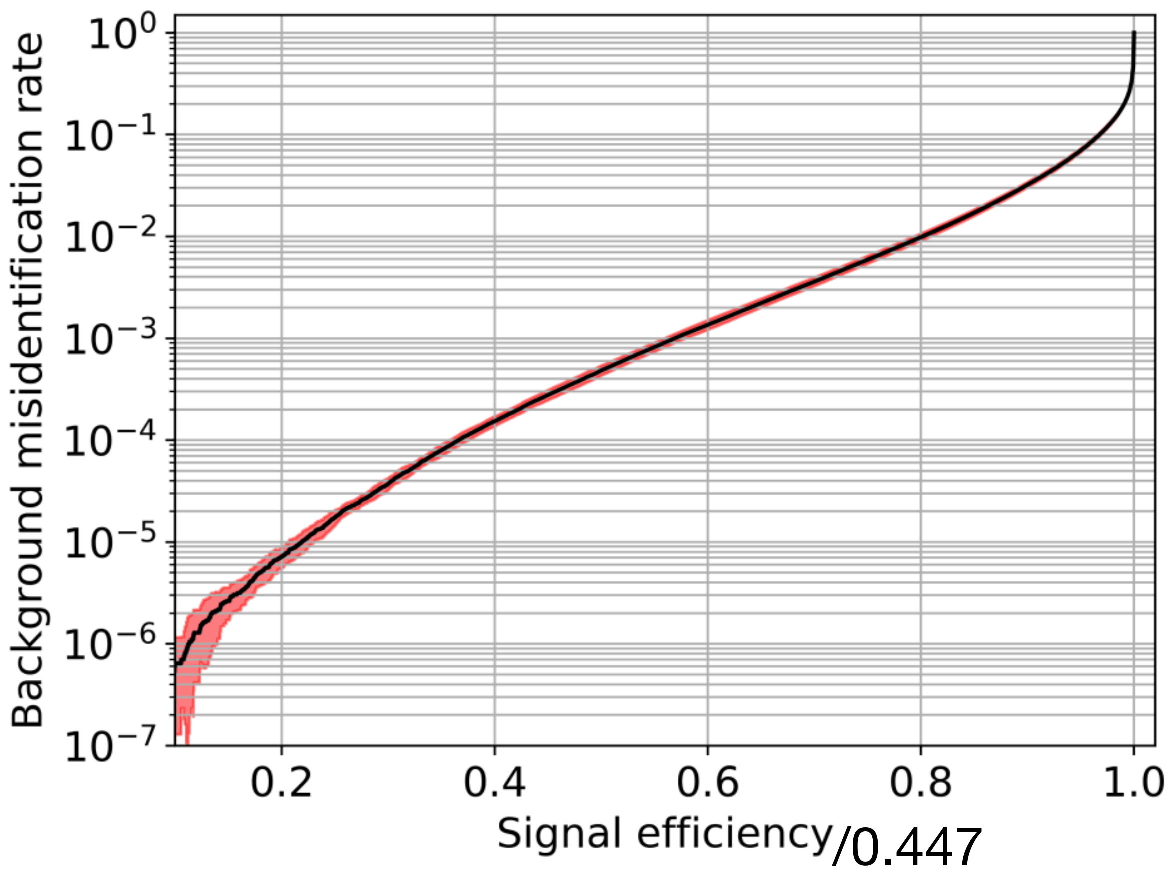

Neutron Tagging: The 22 Variables for BDT

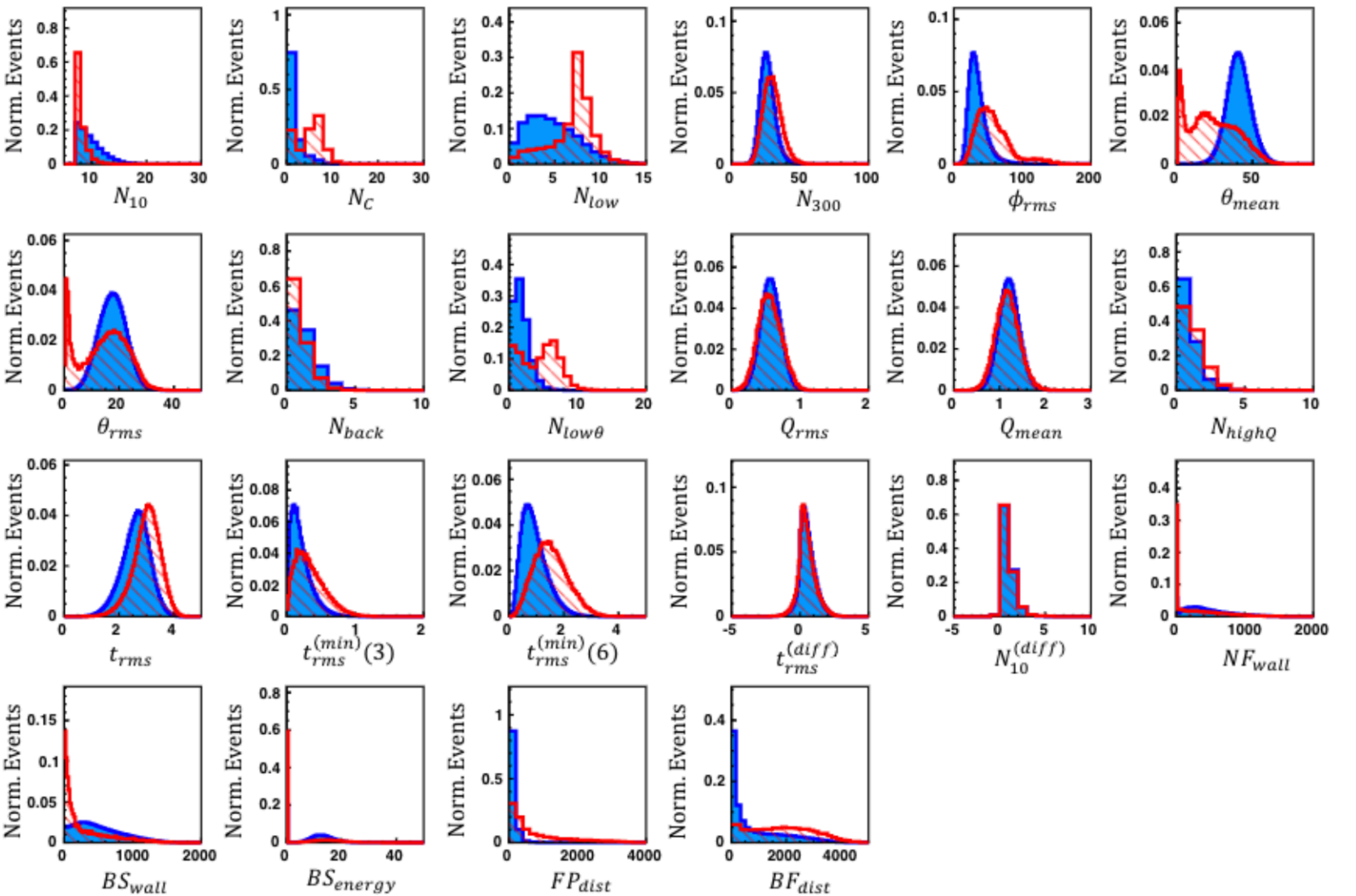

Selected Events

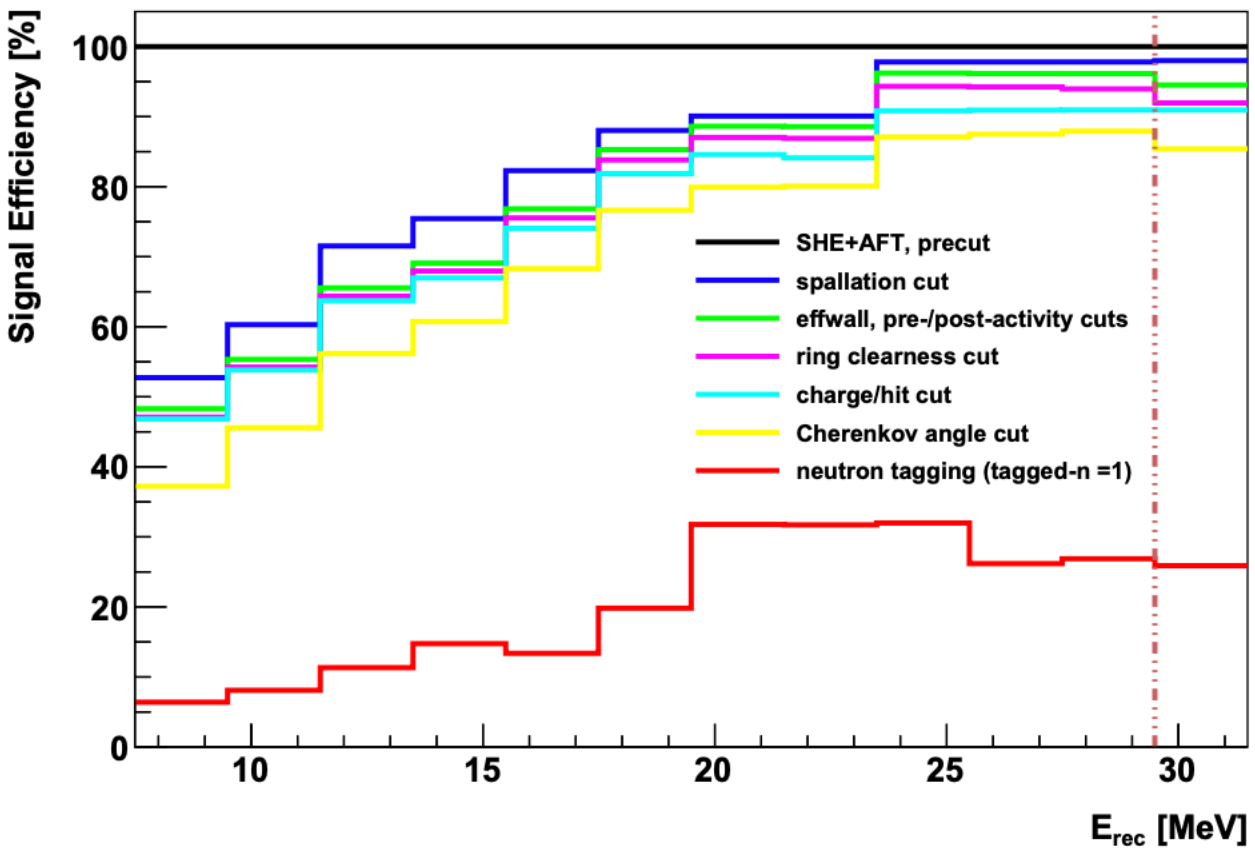

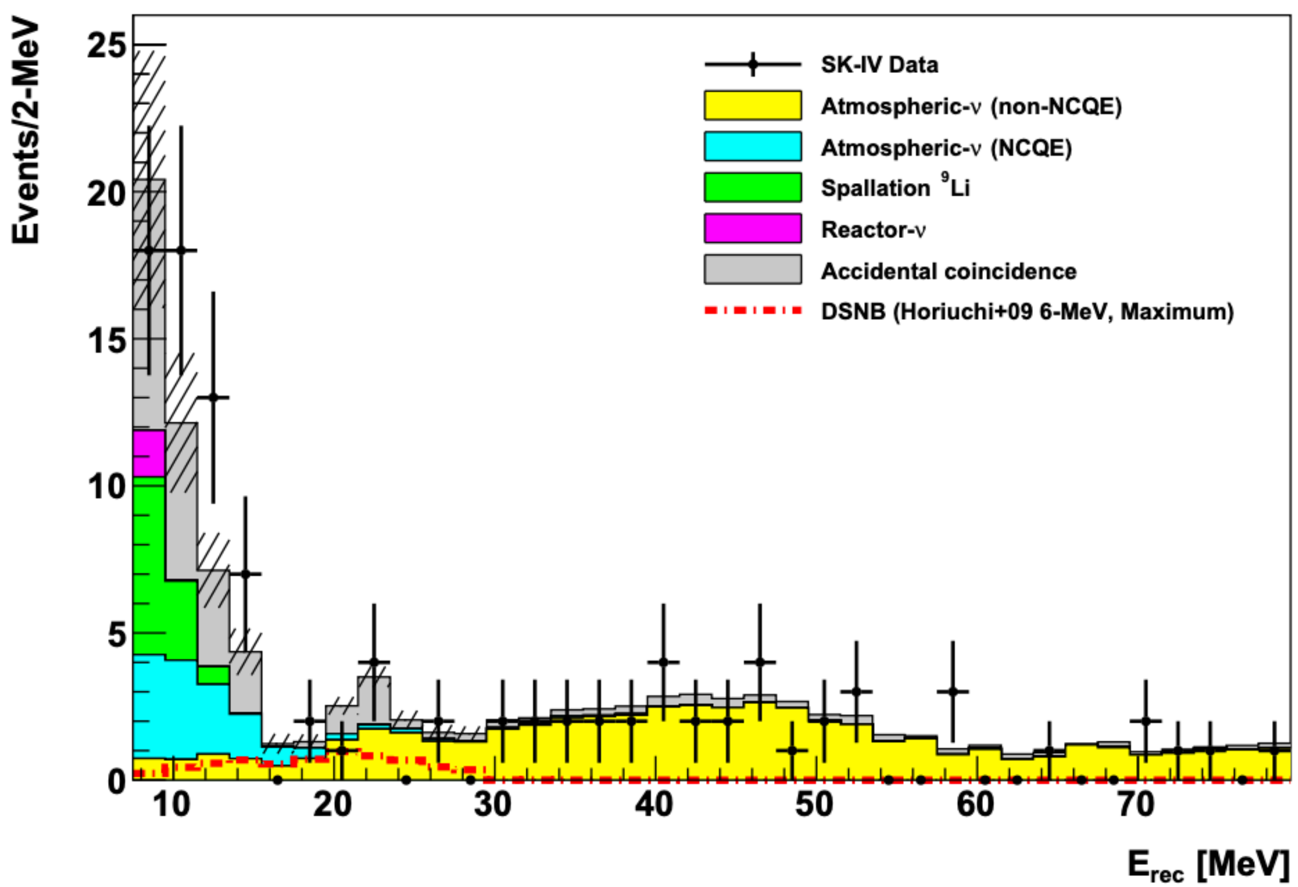

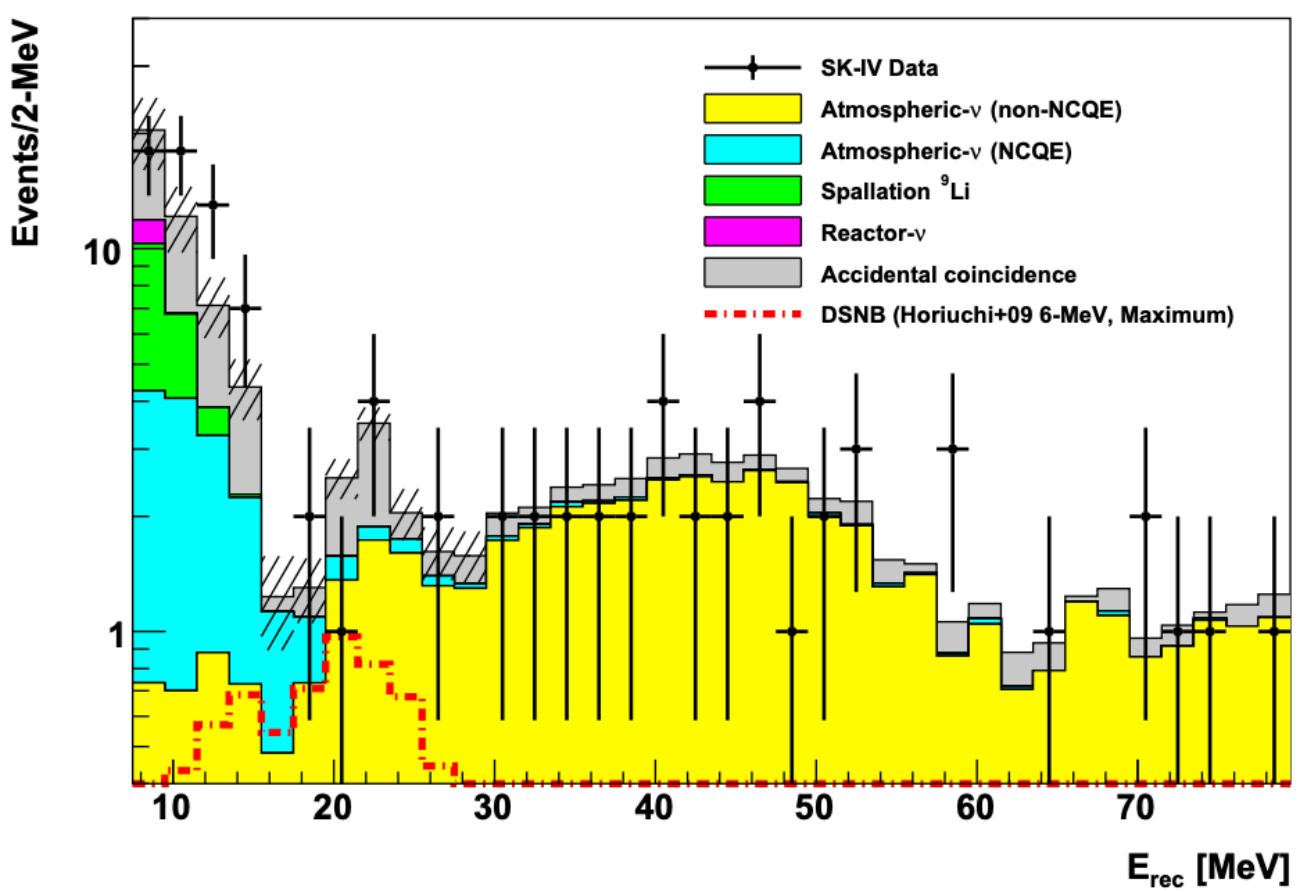

Model-Independent Upper Limit

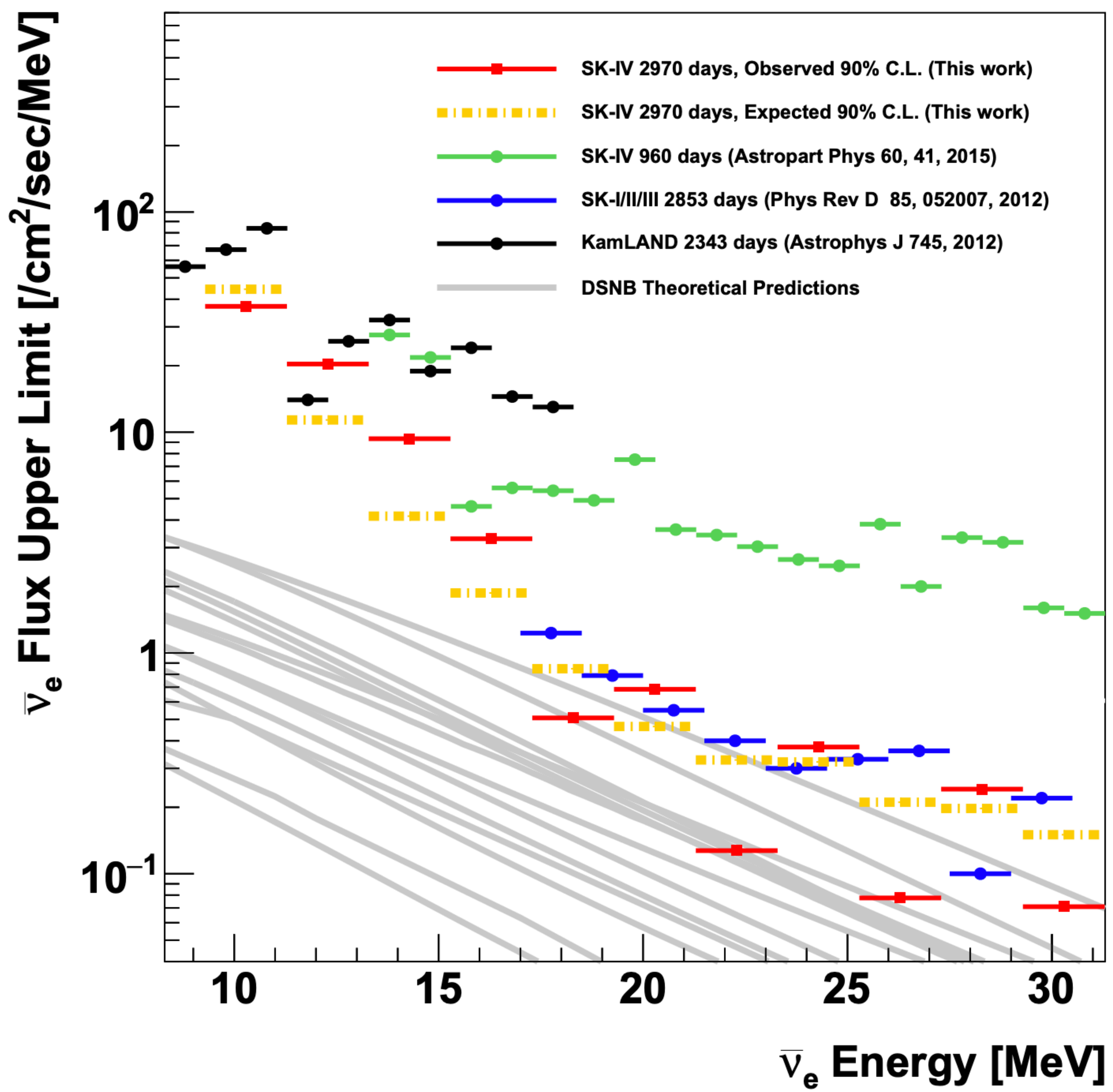

Spectrum Fitting

- We also performed more dedicated analysis for each DSNB model.
- We fit our observed data with signal and background PDFs.
- Here we make use of no tagged region as well.
- This fitting can be combined with SK-I,II,III data (where neutron tagging could not be used).

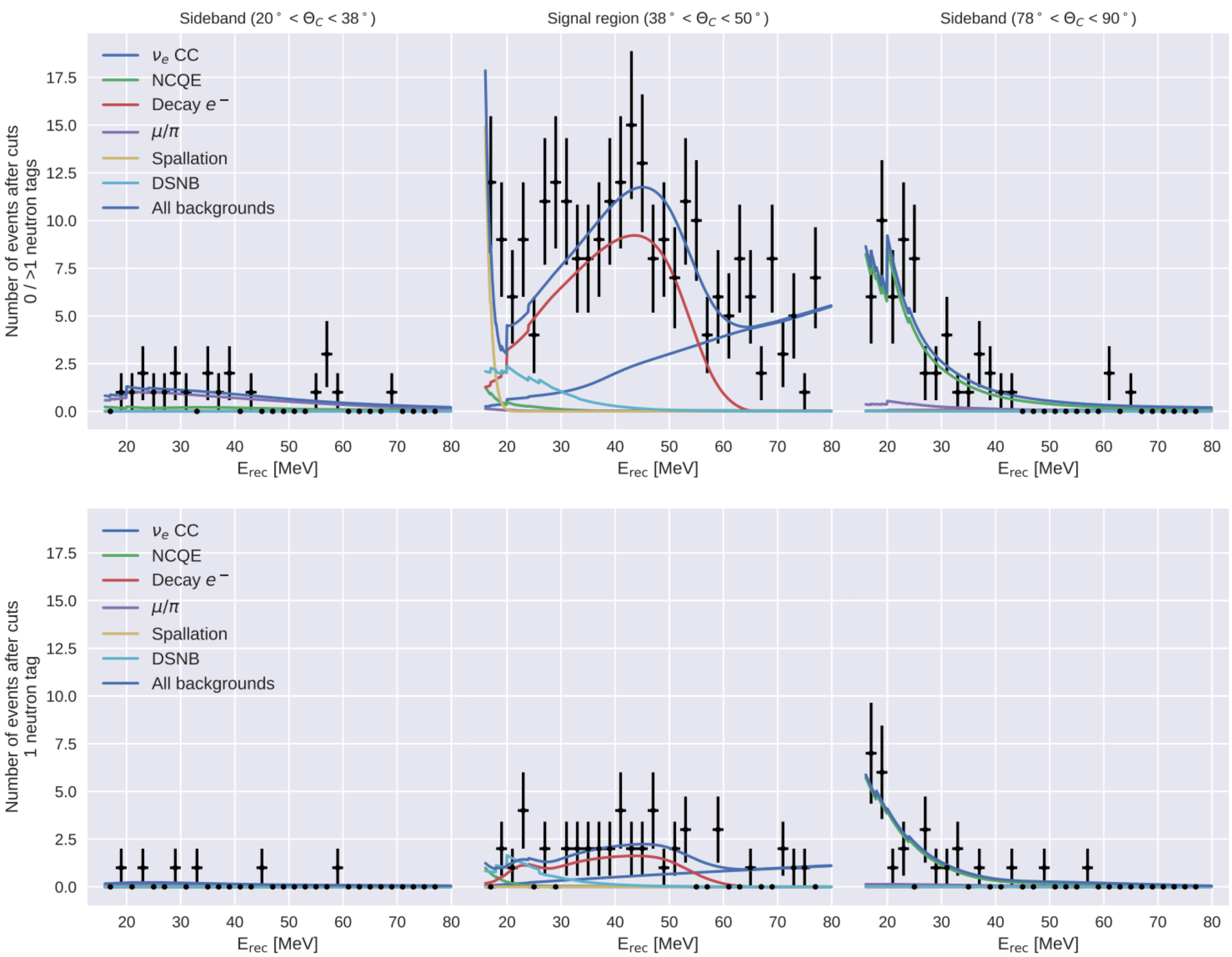

Combination with SK-I,II,III

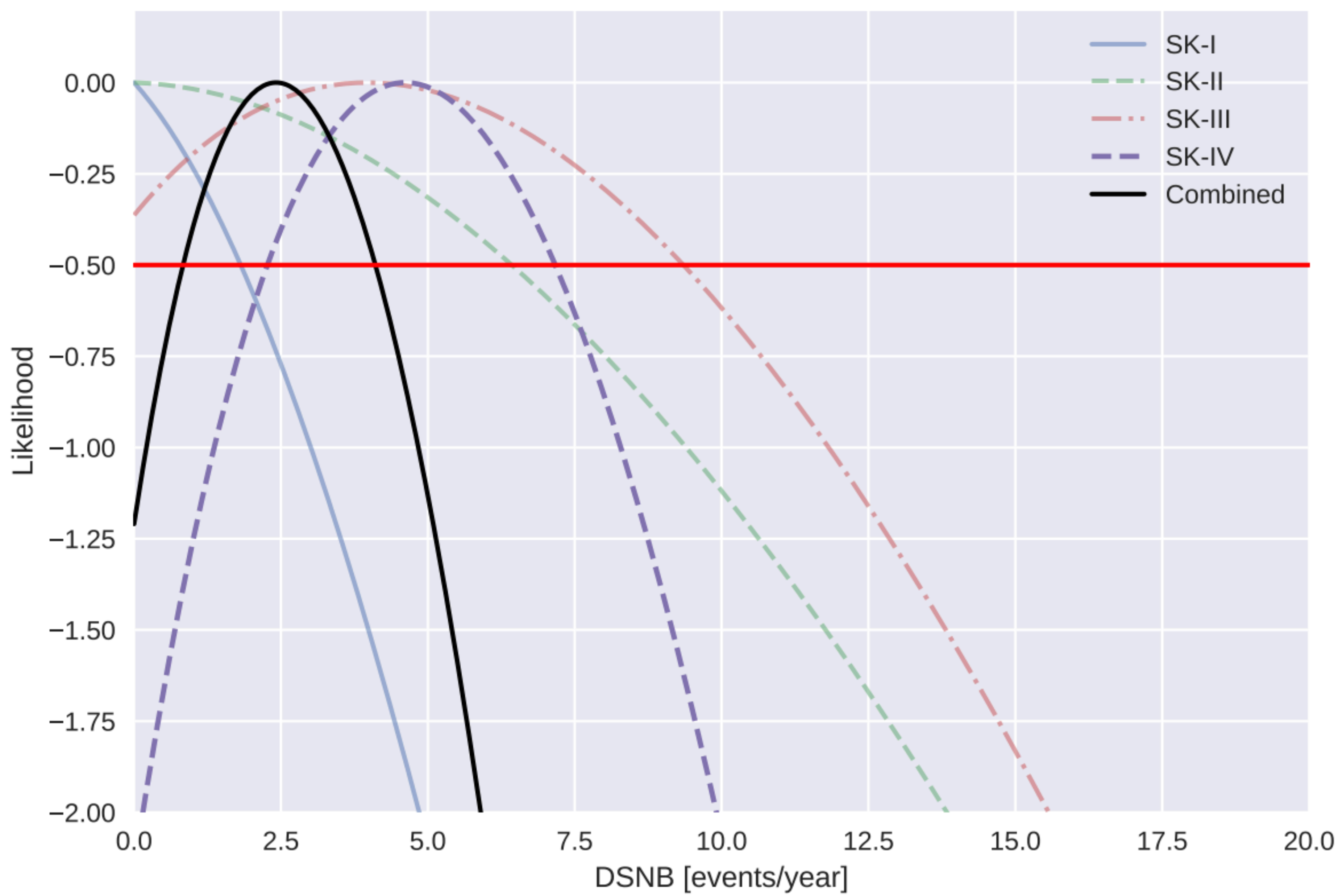

Upper Limits by Spectral Fitting

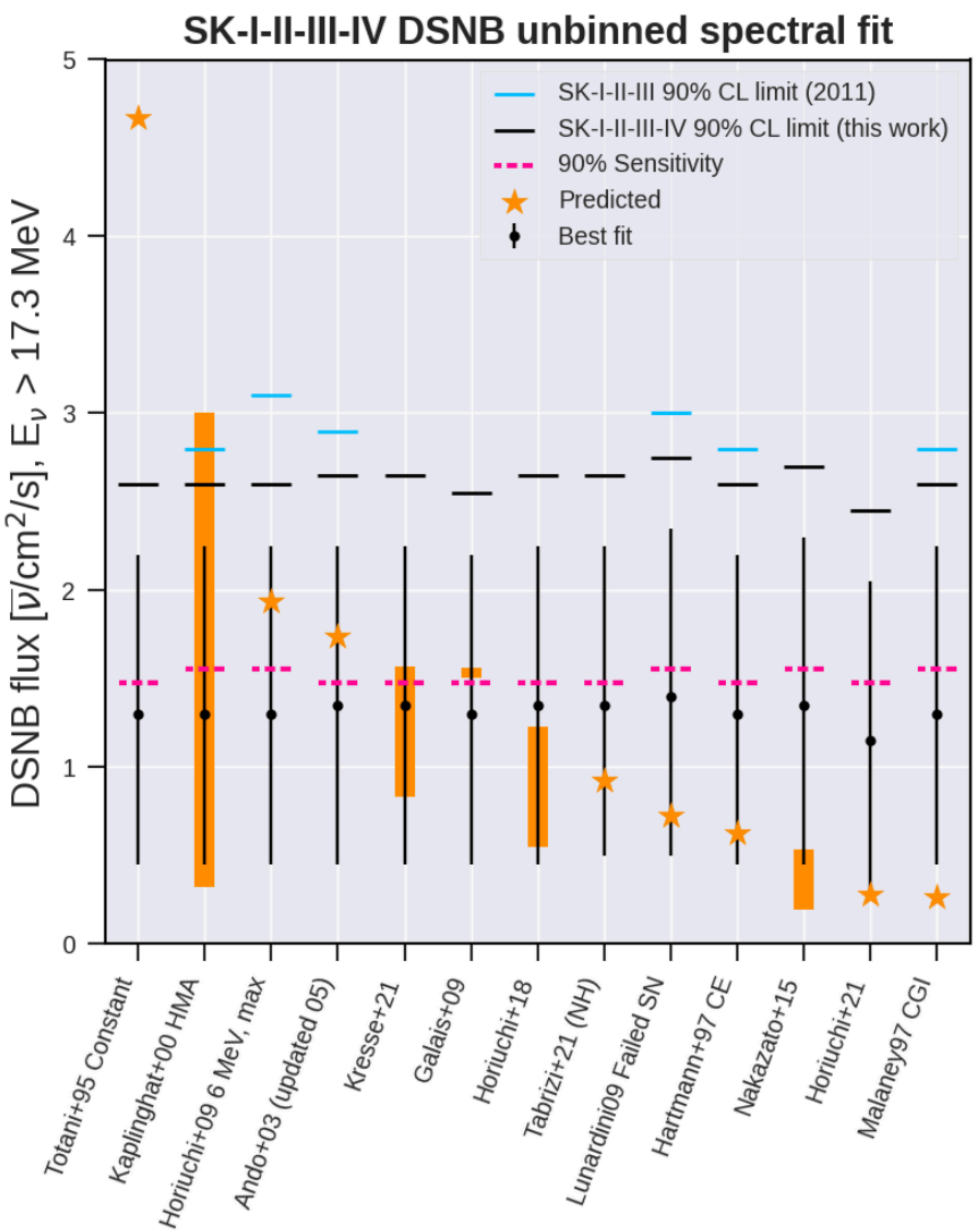

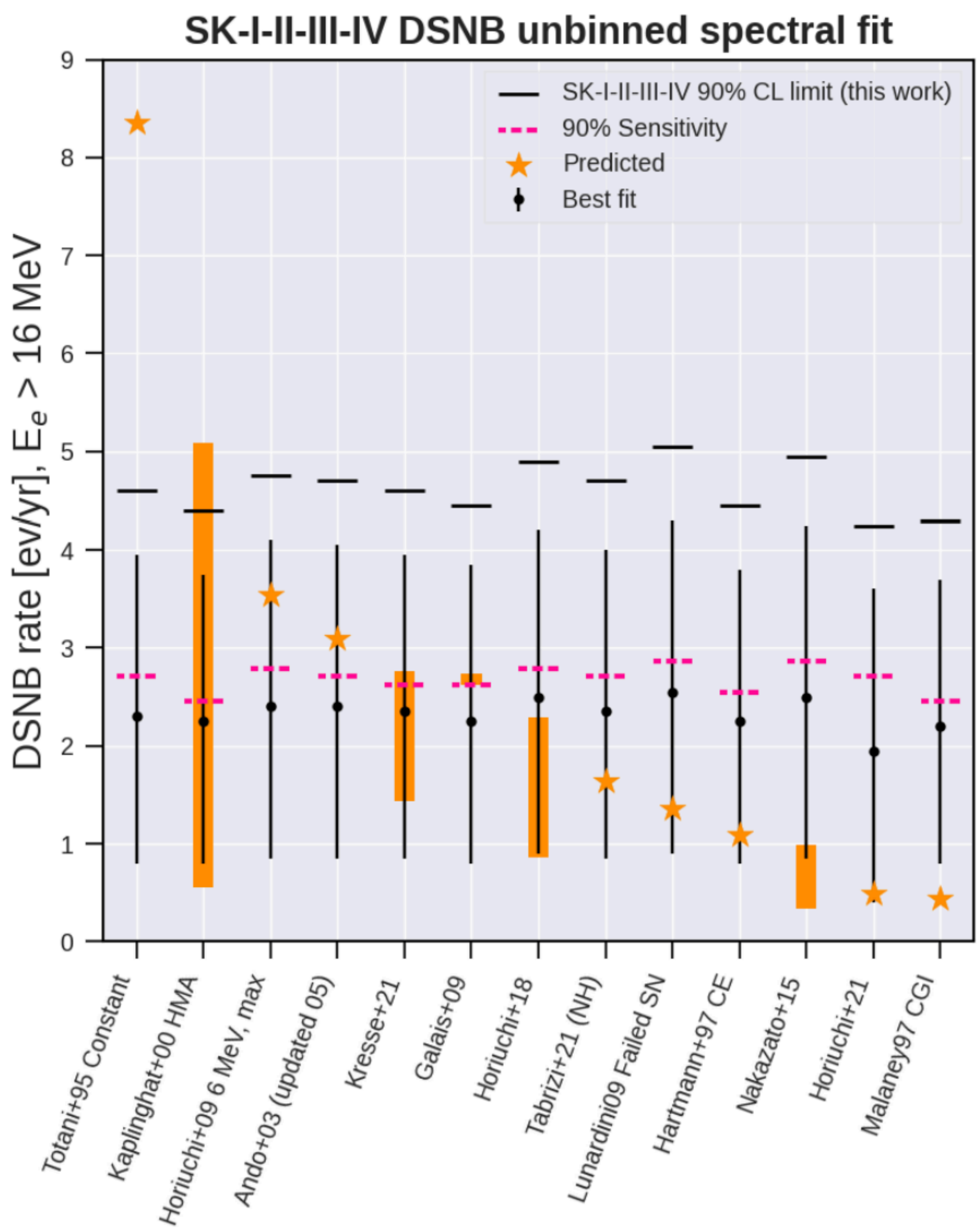

Future Prospects

J. Beacom and M. Vagins, PRL 93, 171101 (2004)
K. Abe et al. (HK Proto-Collaboration), arXiv:1109.3262

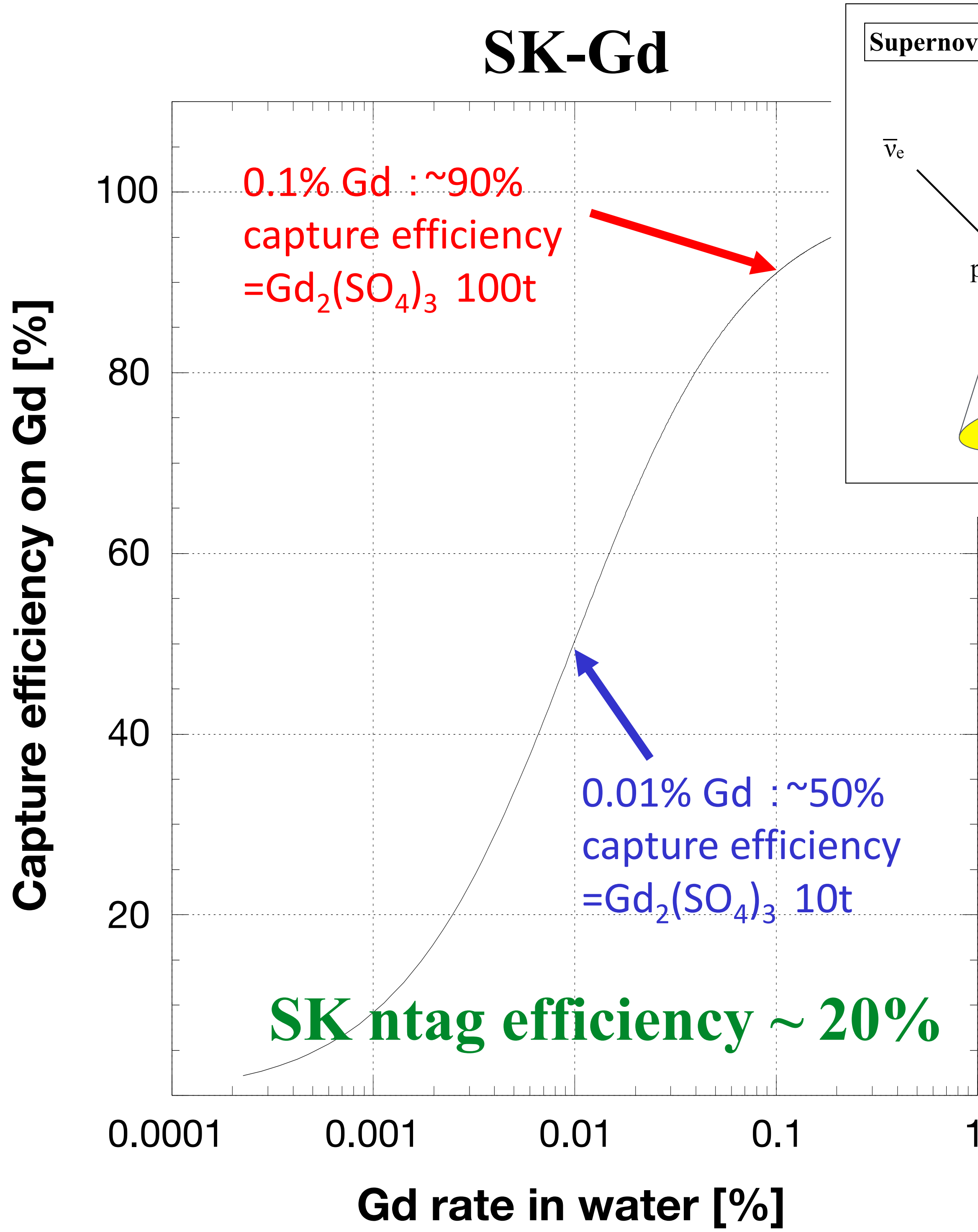

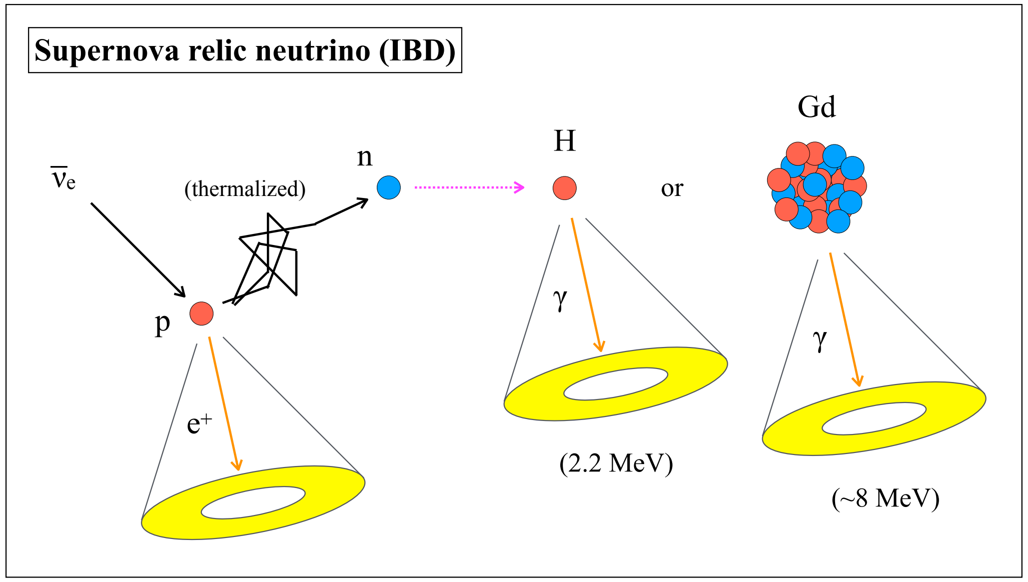

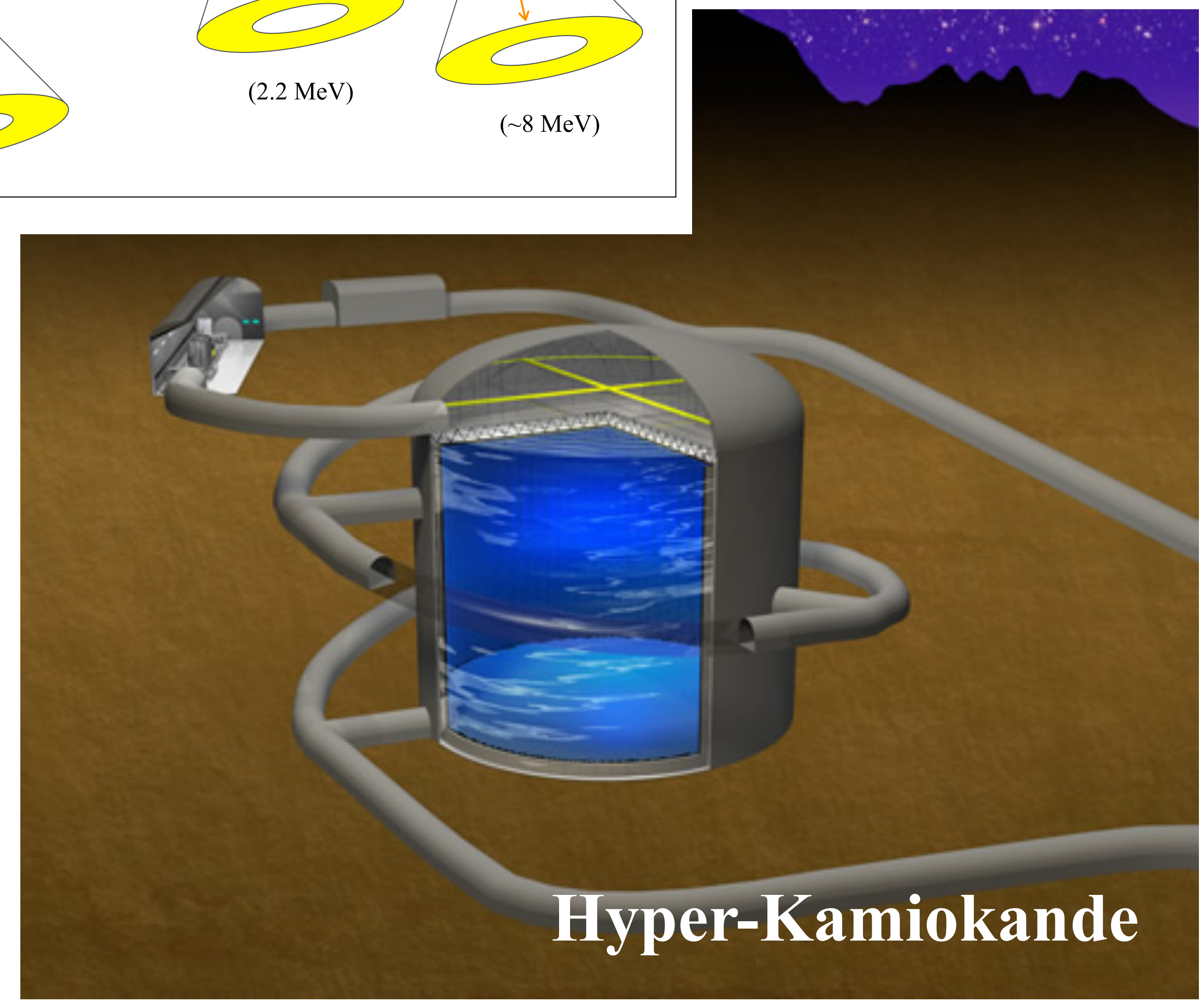

H: ~0.3 barn, 2.2 MeV γ
Gd: ~50 kbarn, ~8 MeV γ

Fiducial mass: ~8.4 times larger than SK
Better photosensor: higher ntag efficiency

Improvement from Beam Experiments

- Bunched proton beams (8 bunch per spill) are injected on the graphite target to produce hadrons (pions and kaons).
- Hadrons are focused by magnetic fields and decay to produce neutrino beams.
- Beam polarity (neutrino or antineutrino) is changed by the magnetic field direction.
- Neutrinos are detected at 295 km away Super-Kamiokande.

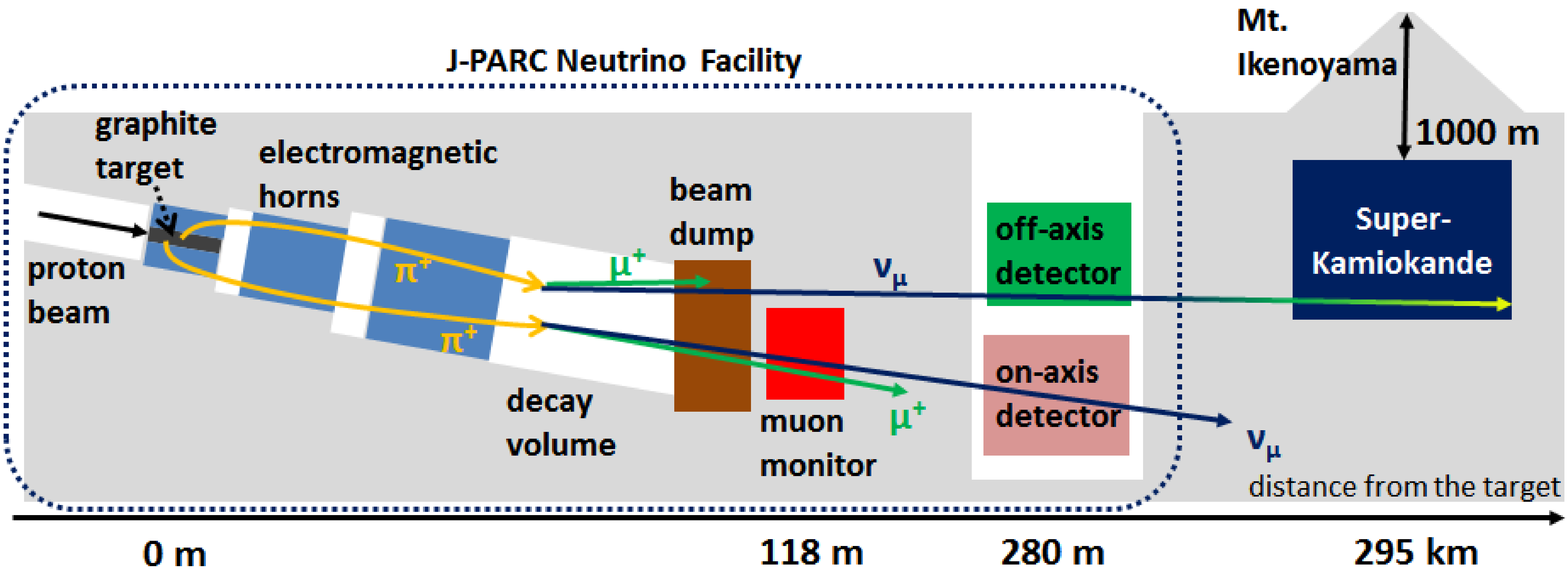

Flux: Atmospheric vs. J-PARC

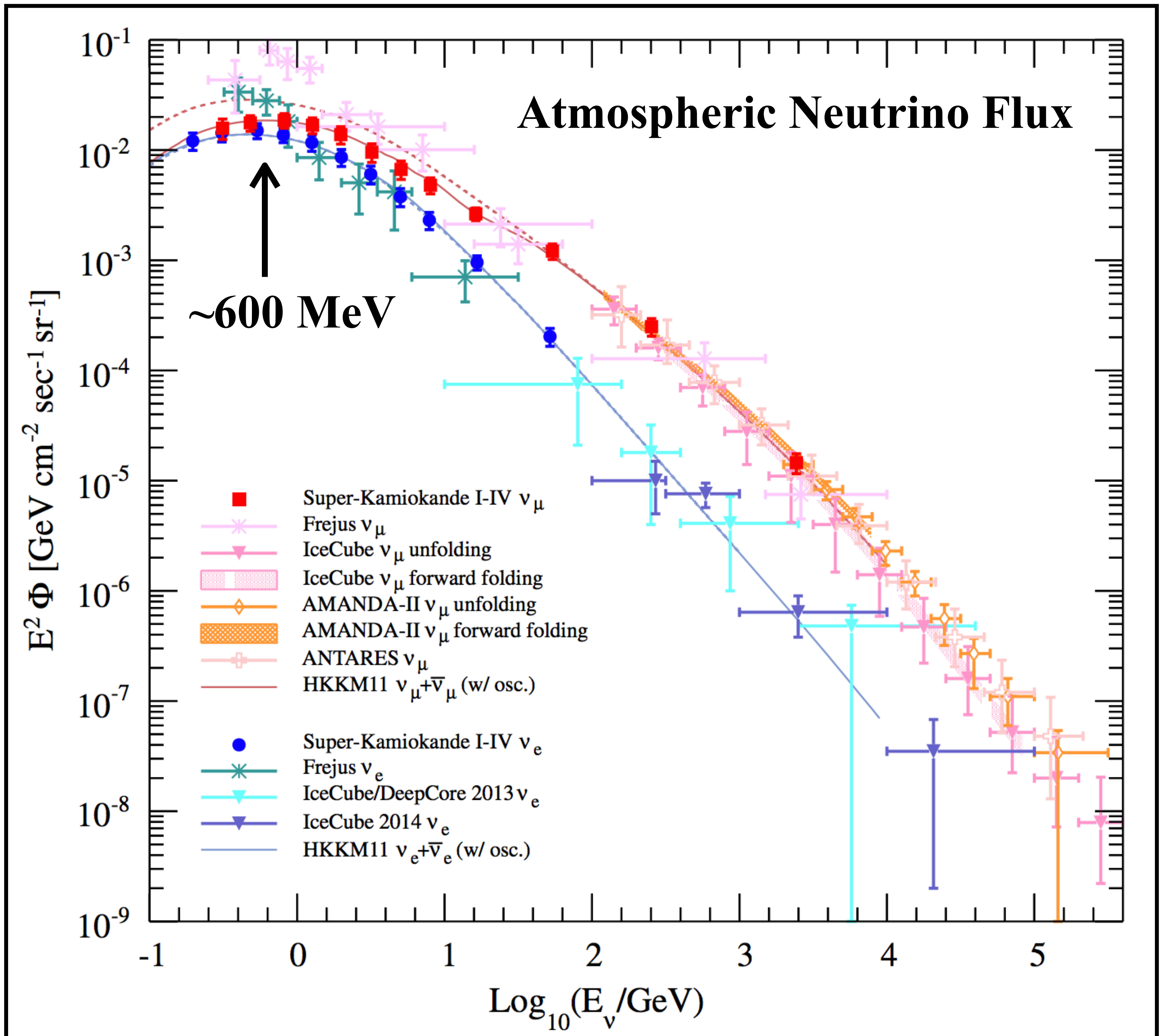

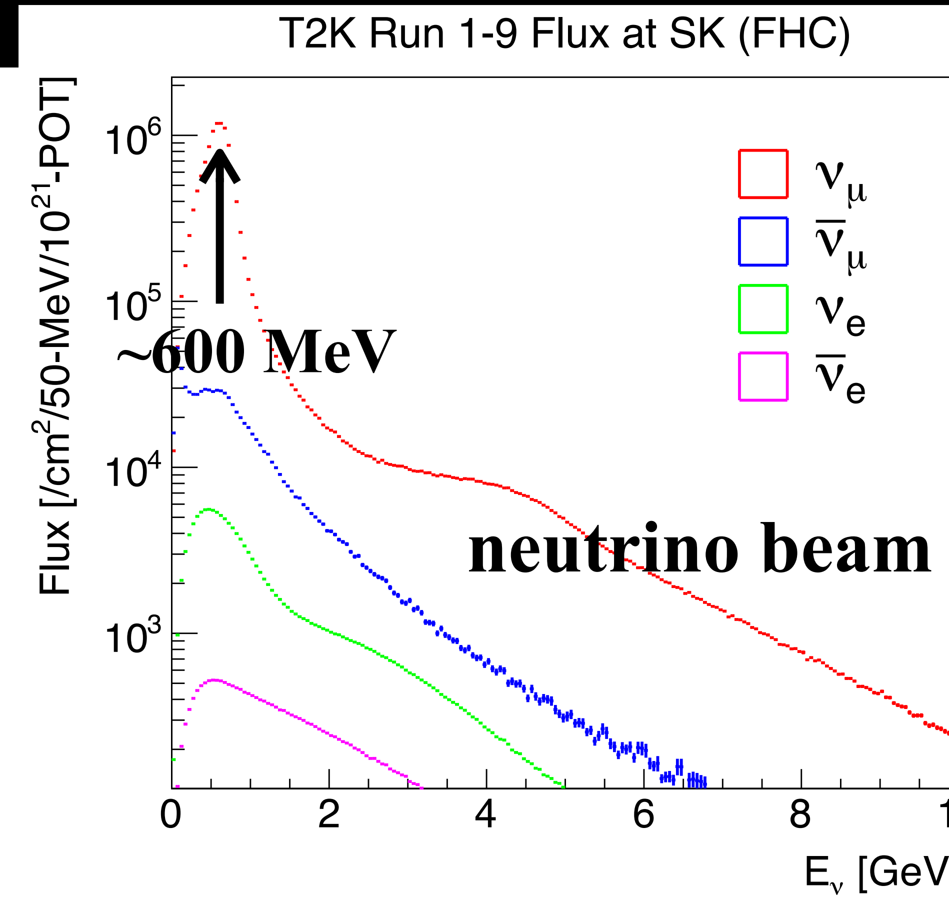

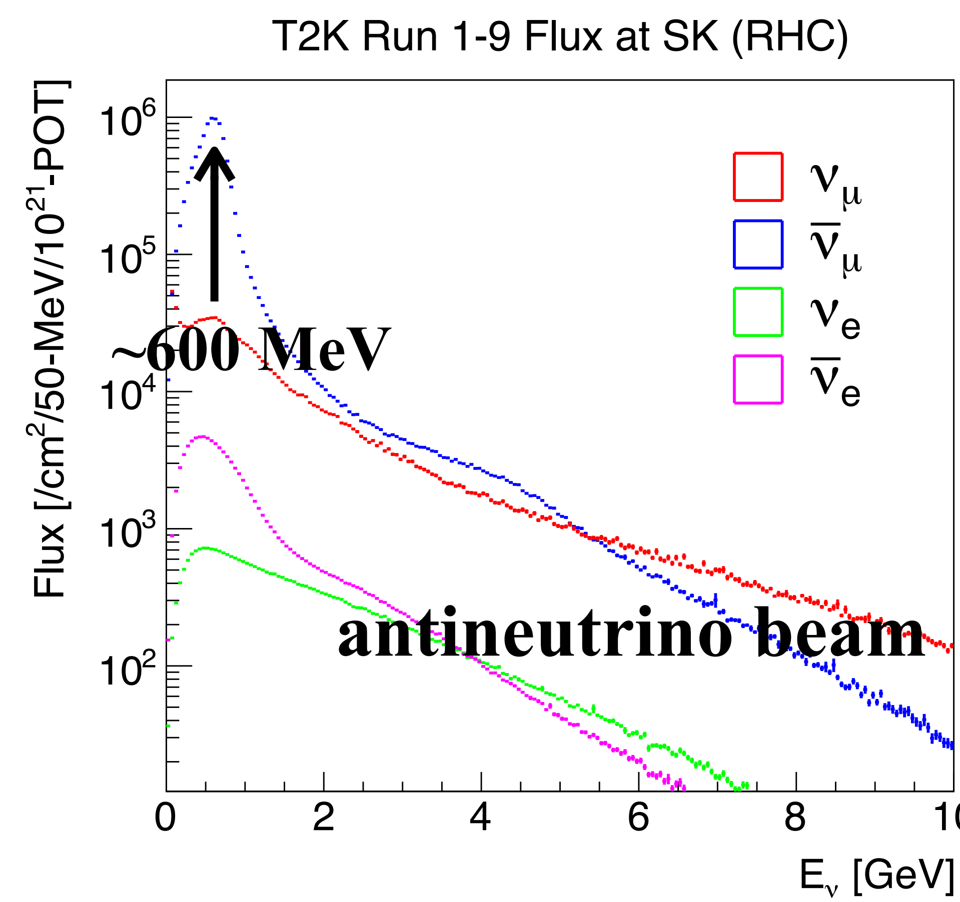

NCQE Estimation with T2K

- So far NCQE background was estimated by the simulation based on theories.
  → A **100%** uncertainty was assigned to this channel because of little experimental data.

- Measurements of neutrino and antineutrino NCQE interactions are performed in T2K.
  - Similar energy region, large statistics, well known flux, pure sample
  - This improves the uncertainty **from 100% to 60%**.

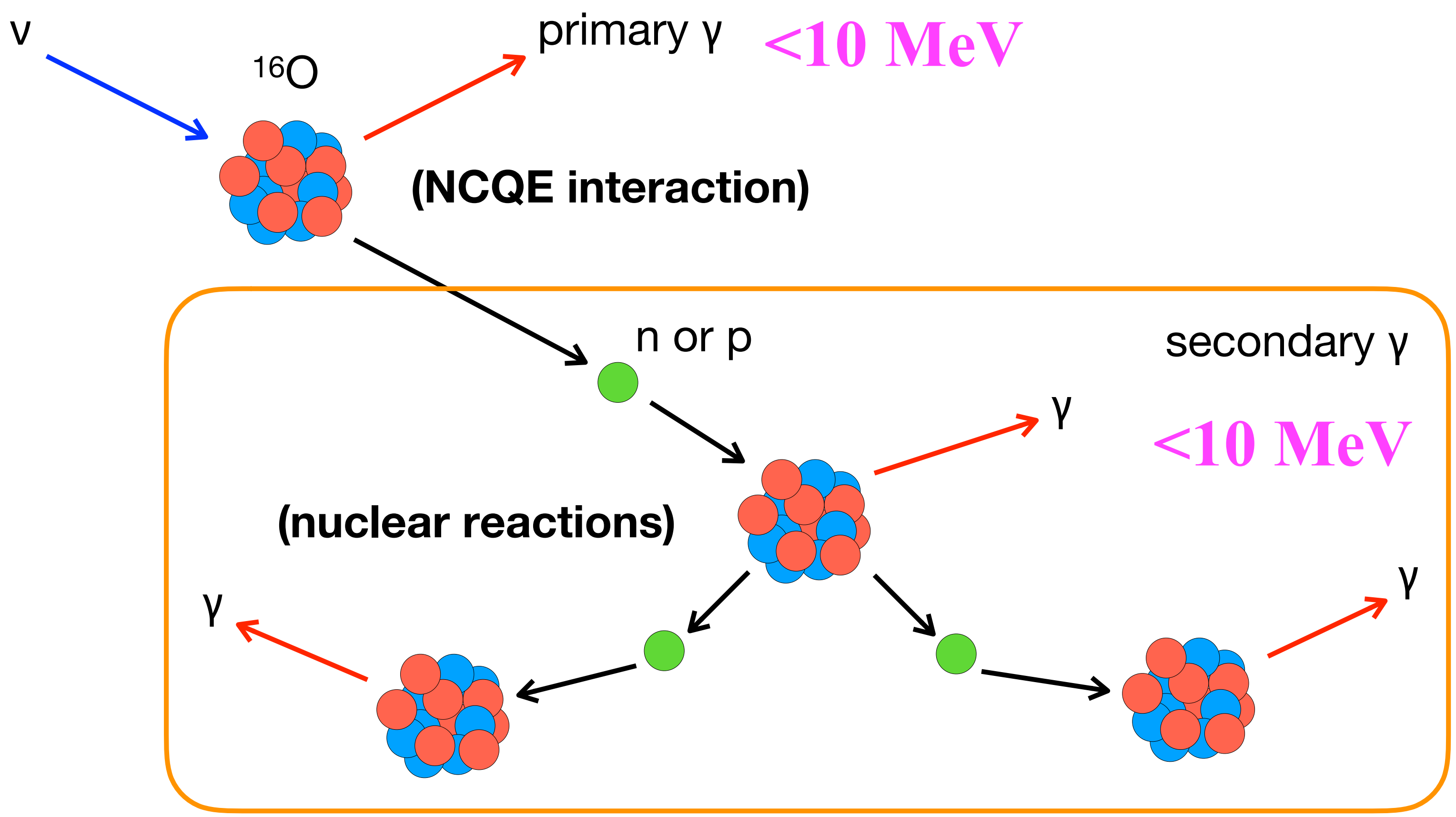

K. Abe et al. (T2K Collaboration), PRD 100, 112009 (2019)

Other Experiments …

KamLAND, JUNO, DUNE? **SK-Gd, HK, HK-Gd?**

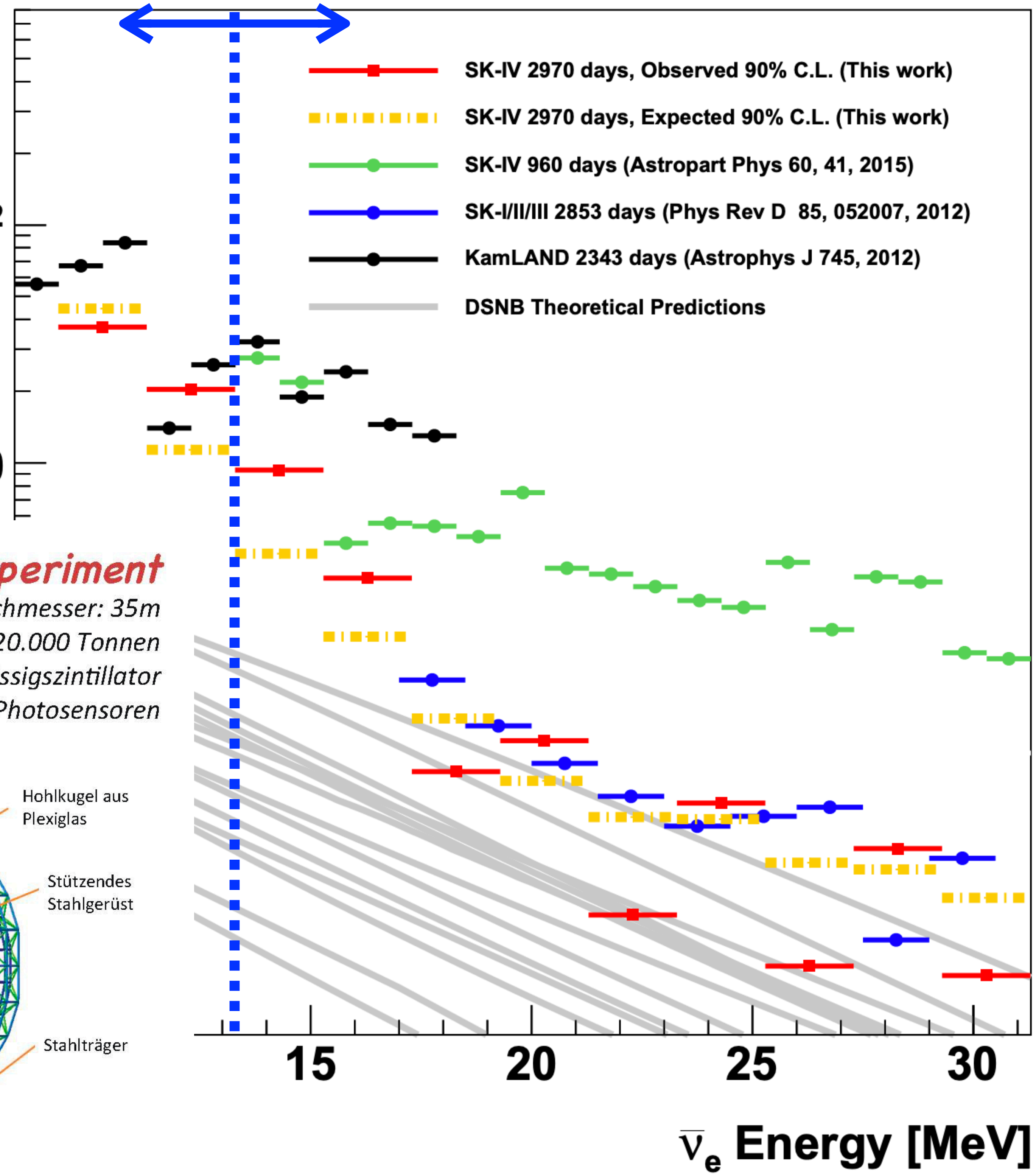

JUNO Experiment

Durchmesser: 35m
20.000 Tonnen
Flüssigszintillator
15.000 Photosensoren

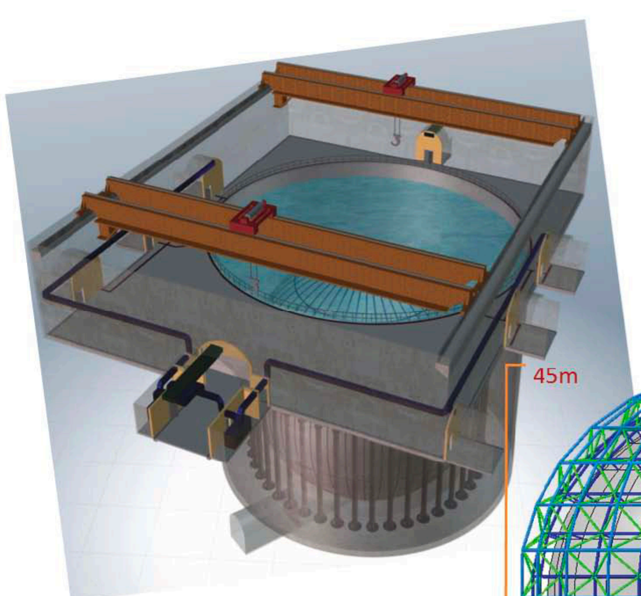

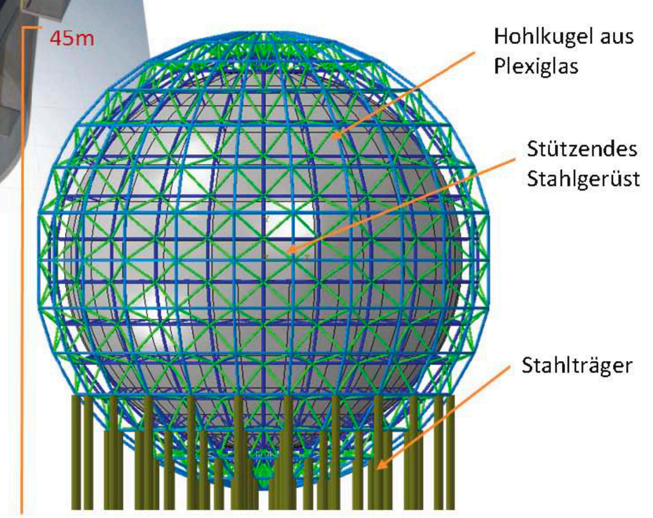

Summary

- A new DSNB search was performed at Super-Kamiokande with a lot of improvements on event selection and background estimation as well as larger statistics.
- Limits from both of model-independent and spectral fitting analyses excluded most optimistic models and are close to more realistic model predictions (within a factor).
- SK-Gd starting now, and Hyper-Kamiokande approved. ***Future is bright!***

Thanks for your attention!

Same Neutrinos, but …

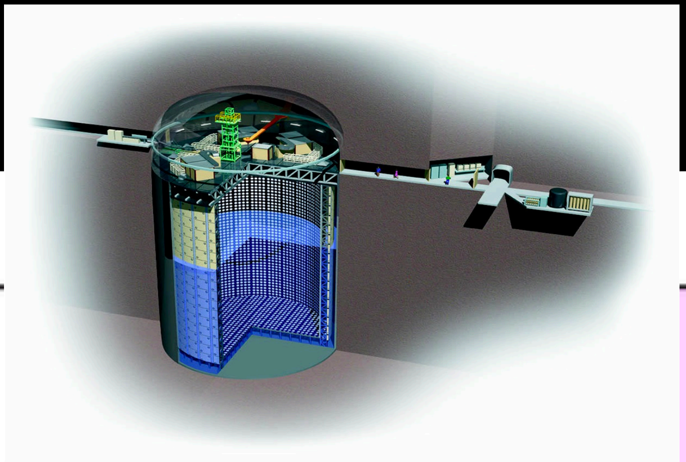

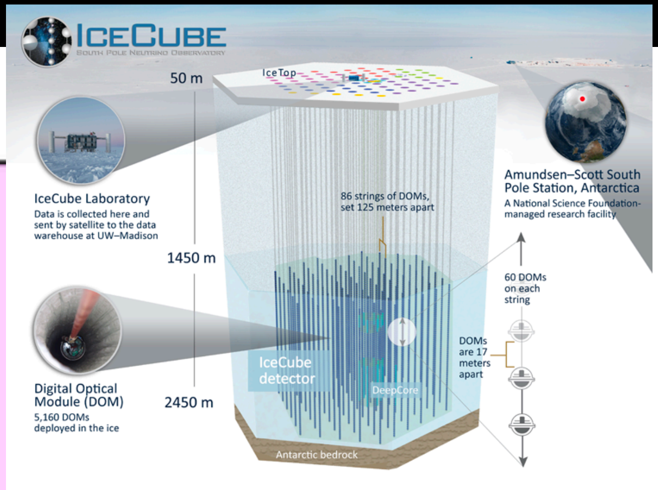

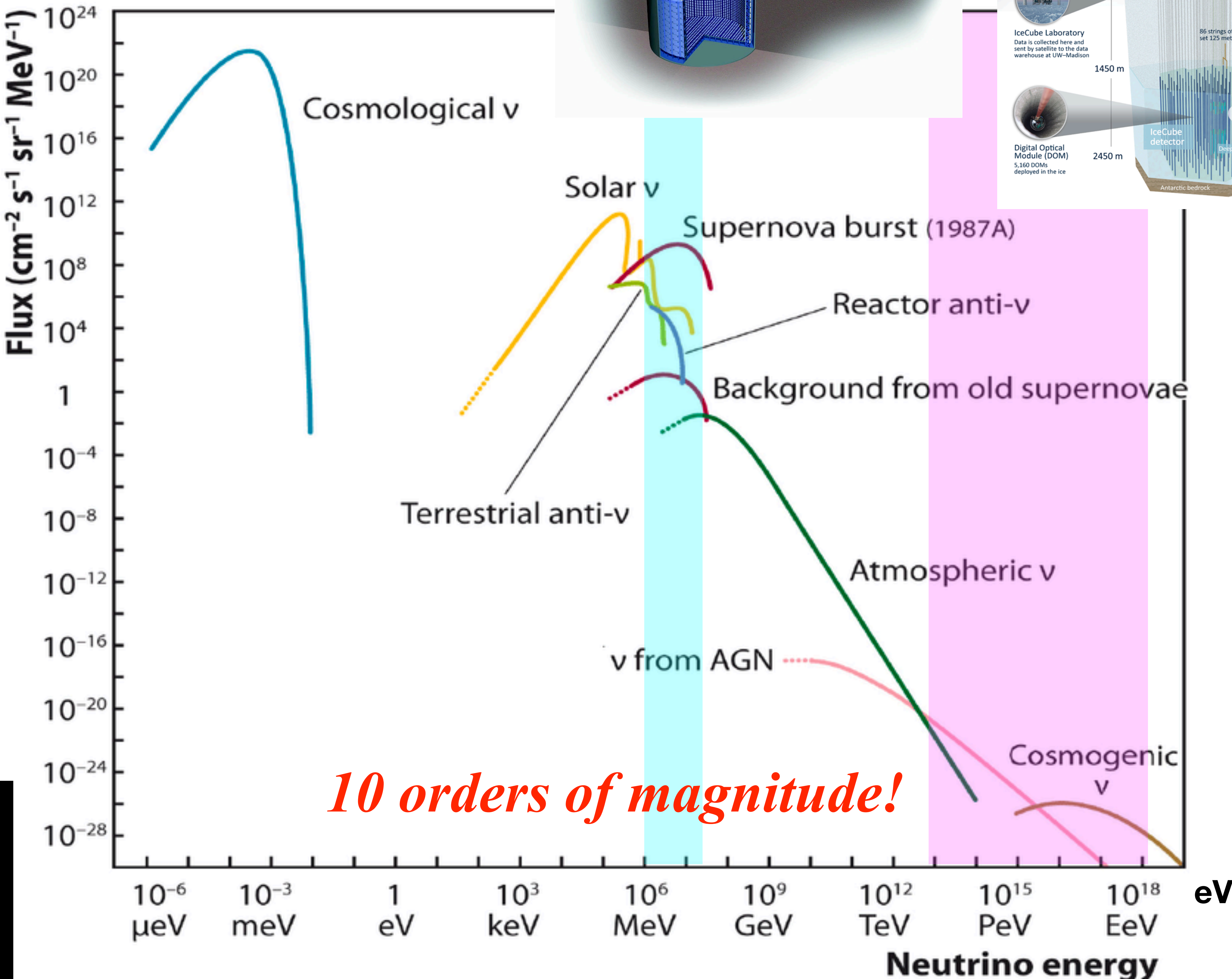

Supplements

Neutrino Heating Scenario

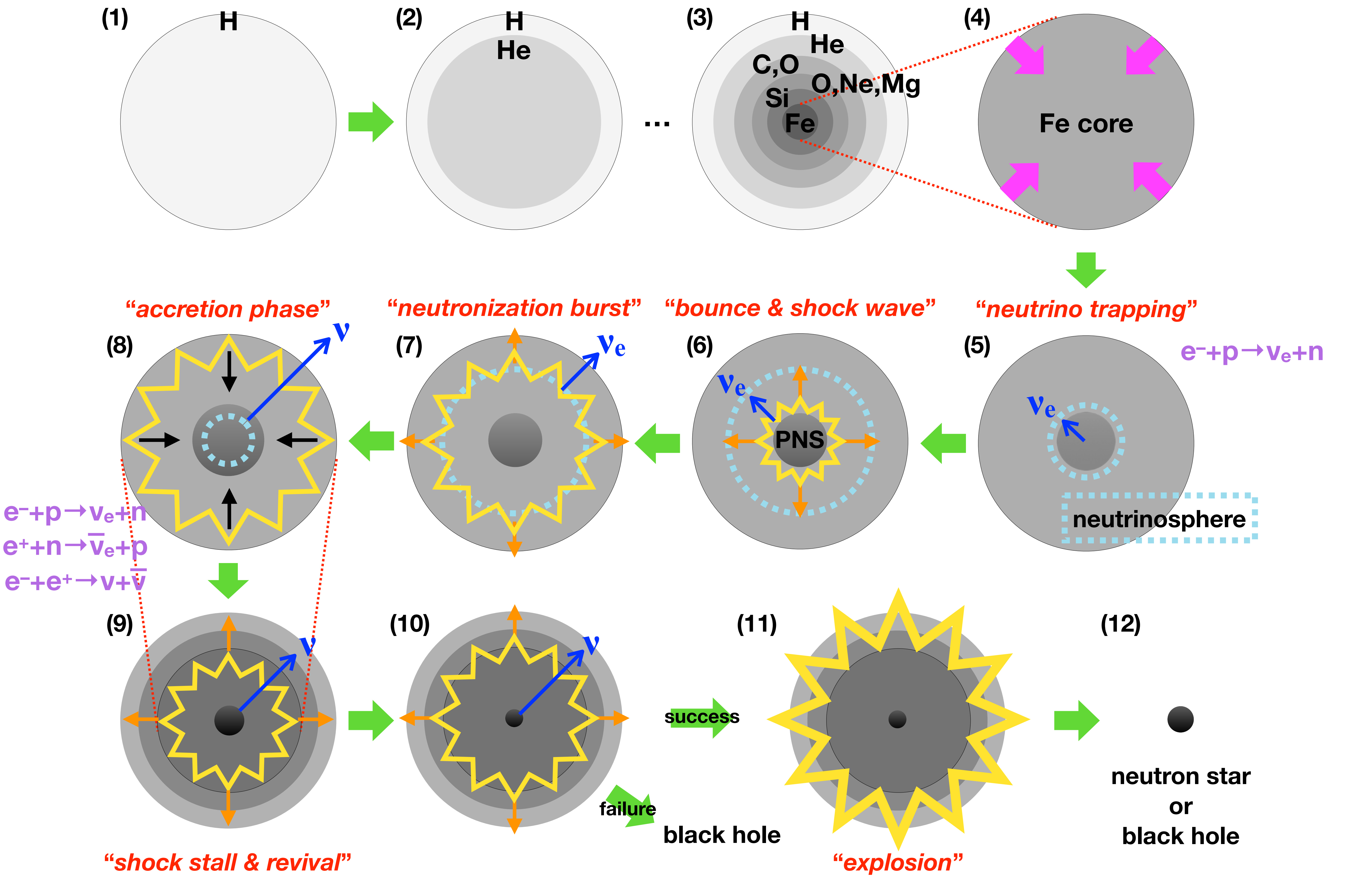

Nakazato+15 Flux Summary

K. Nakazato et al., ApJ 804, 75 (2015)

Table 3
SRN Event Rates in Various Ranges of Positron Energy in Super-Kamiokande Over 1 yr (i.e., per 22.5 kton yr) for Models With Metallicity Evolution of DA08+M08

			Normal Mass Hierarchy			Inverted Mass Hierarchy			
CSFRD	t_{revive}	EOS for BH	18–26	10–18	10–26 MeV	18–26	10–18	10–26 MeV	Figure 12
HB06	100 ms	Shen	0.286	0.704	0.990	0.375	0.832	1.207	···
		LS	0.227	0.635	0.863	0.351	0.806	1.156	···
	200 ms	Shen	0.361	0.833	1.193	0.429	0.920	1.349	···
		LS	0.302	0.764	1.066	0.404	0.893	1.297	···
	300 ms	Shen	0.432	0.938	1.370	0.463	0.967	1.431	Maximum
		LS	0.374	0.869	1.242	0.439	0.941	1.379	···
DA08	100 ms	Shen	0.219	0.515	0.734	0.286	0.598	0.885	···
		LS	0.178	0.464	0.642	0.269	0.578	0.847	···
	200 ms	Shen	0.274	0.604	0.879	0.326	0.660	0.986	Reference
		LS	0.233	0.554	0.787	0.308	0.640	0.948	···
	300 ms	Shen	0.326	0.677	1.003	0.350	0.694	1.044	···
		LS	0.285	0.627	0.911	0.333	0.674	1.007	···
K13	100 ms	Shen	0.203	0.443	0.645	0.264	0.505	0.769	···
		LS	0.171	0.410	0.581	0.252	0.492	0.744	Minimum
	200 ms	Shen	0.252	0.514	0.767	0.298	0.554	0.853	···
		LS	0.221	0.482	0.703	0.286	0.542	0.827	···
	300 ms	Shen	0.298	0.570	0.868	0.319	0.580	0.899	···
	···	LS	0.266	0.537	0.804	0.306	0.568	0.874	···

Neutrino Oscillation Parameters (2018)

Table 1.1: Best-fit values of the neutrino oscillation parameters from PDG2018 [22]. NH and IH represent the normal and inverted neutrino mass hierarchy, respectively.

Oscillation parameter	Best-fit value
$\sin^2\theta_{12}$	0.307 ± 0.013
$\sin^2\theta_{23}$ (NH, Octant I)	$0.417^{+0.025}_{-0.028}$
$\sin^2\theta_{23}$ (NH, Octant II)	$0.597^{+0.024}_{-0.030}$
$\sin^2\theta_{23}$ (IH, Octant I)	$0.421^{+0.033}_{-0.025}$
$\sin^2\theta_{23}$ (IH, Octant II)	$0.592^{+0.023}_{-0.030}$
$\sin^2\theta_{13}$	$(2.12 \pm 0.08) \times 10^{-2}$
Δm^2_{12}	$(7.53 \pm 0.18) \times 10^{-5}$ eV^2
Δm^2_{32} (NH)	$(2.51 \pm 0.05) \times 10^{-3}$ eV^2
Δm^2_{32} (IH)	$(-2.56 \pm 0.04) \times 10^{-3}$ eV^2

CSFRD

K. Nakazato et al., ApJ 804, 75 (2015)

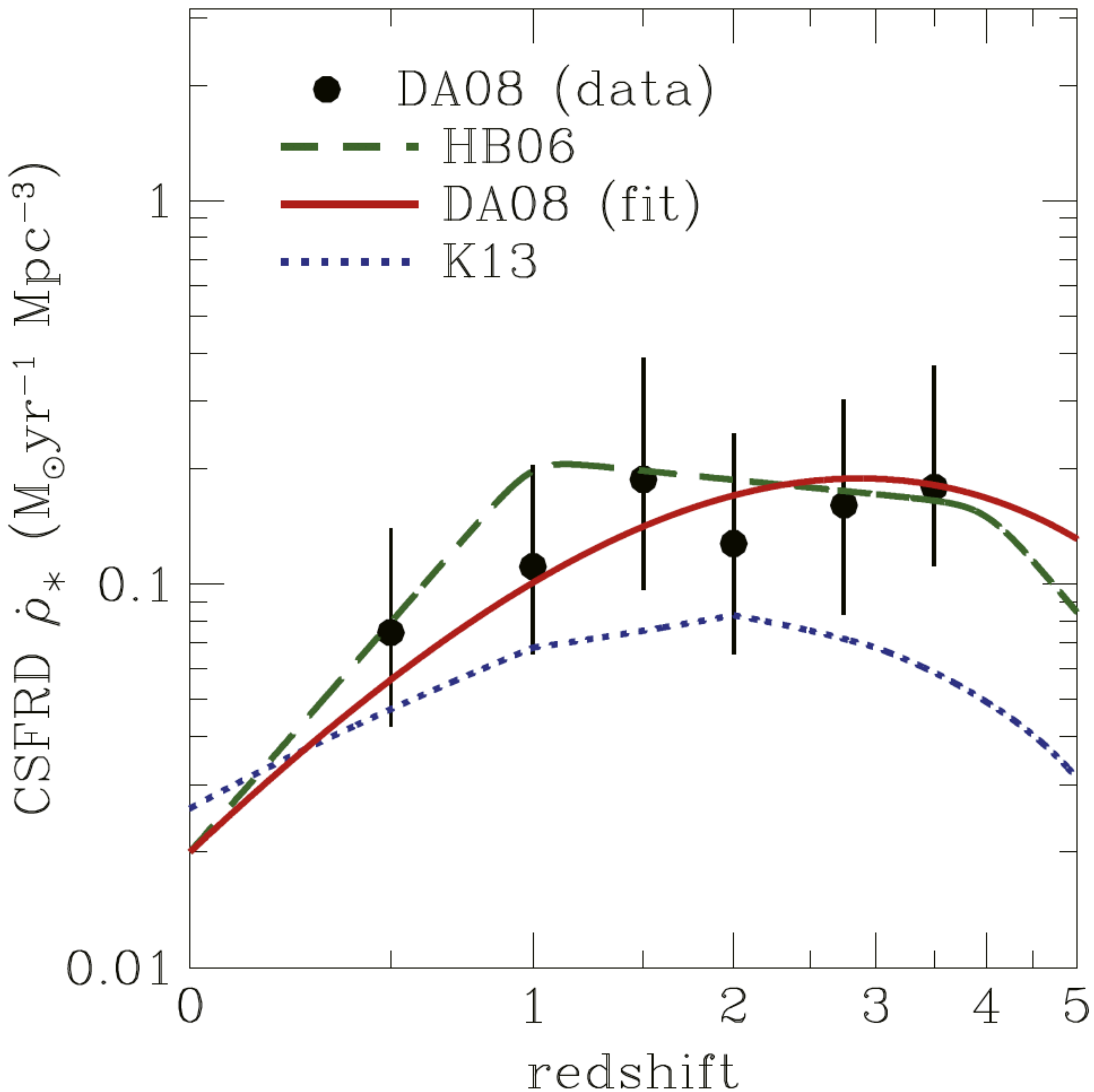

Figure 2. CSFRD as a function of redshift. Dashed, solid and dotted lines correspond to the models in HB06, DA08 and K13, respectively. Plots are calculated from the data in Tables 1 and 2 in DA08.

$$R_{\rm CCSN}(z) = \zeta_{\rm CCSN}\dot{\rho}_*(z),$$

$$\zeta_{\rm CCSN} = \frac{\int_{M_{\rm min}}^{M_{\rm max}} \Psi_{\rm IMF}(M)dM}{\int_{0.1M_{\rm sun}}^{100M_{\rm sun}} M\Psi_{\rm IMF}(M)dM},$$

BH Formation Criteria

K. Nakazato et al., ApJ 804, 75 (2015)

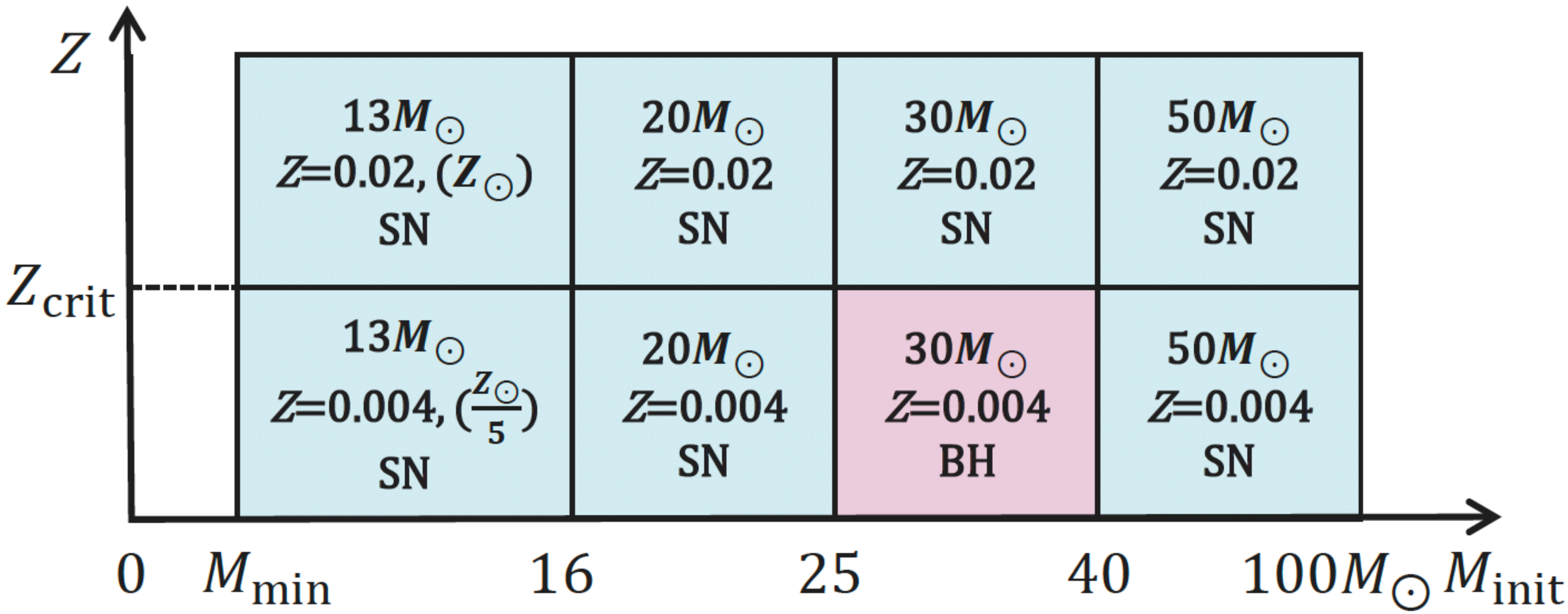

Mass Hierarchy Effect

K. Nakazato et al., ApJ 804, 75 (2015)

$$\begin{aligned}\frac{dN_{\bar{\nu}_e}}{dE_\nu} &= |U_{e1}|^2\frac{dN_{\bar{\nu}_1}}{dE_\nu} + |U_{e2}|^2\frac{dN_{\bar{\nu}_2}}{dE_\nu} + |U_{e3}|^2\frac{dN_{\bar{\nu}_3}}{dE_\nu} \\ &= \cos^2\theta_{12}\cos^2\theta_{13}\frac{dN_{\bar{\nu}_1}}{dE_\nu} + \sin^2\theta_{12}\cos^2\theta_{13}\frac{dN_{\bar{\nu}_2}}{dE_\nu} + \sin^2\theta_{13}\frac{dN_{\bar{\nu}_3}}{dE_\nu} \\ &\sim 0.68\cdot\frac{dN_{\bar{\nu}_1}}{dE_\nu} + 0.30\cdot\frac{dN_{\bar{\nu}_2}}{dE_\nu} + 0.02\cdot\frac{dN_{\bar{\nu}_3}}{dE_\nu},\end{aligned}$$

➡ $$\frac{dN_{\bar{\nu}_e}}{dE_\nu} \sim 0.68\cdot\frac{dN^0_{\bar{\nu}_e}}{dE_\nu} + 0.32\cdot\frac{dN^0_{\bar{\nu}_x}}{dE_\nu}.$$ **Normal Hierarchy**

➡ $$\frac{dN_{\bar{\nu}_e}}{dE_\nu} \sim \frac{dN^0_{\bar{\nu}_x}}{dE_\nu}.$$ **Inverted Hierarchy**

Shock Revival Time Effect

K. Nakazato et al., ApJ 804, 75 (2015)

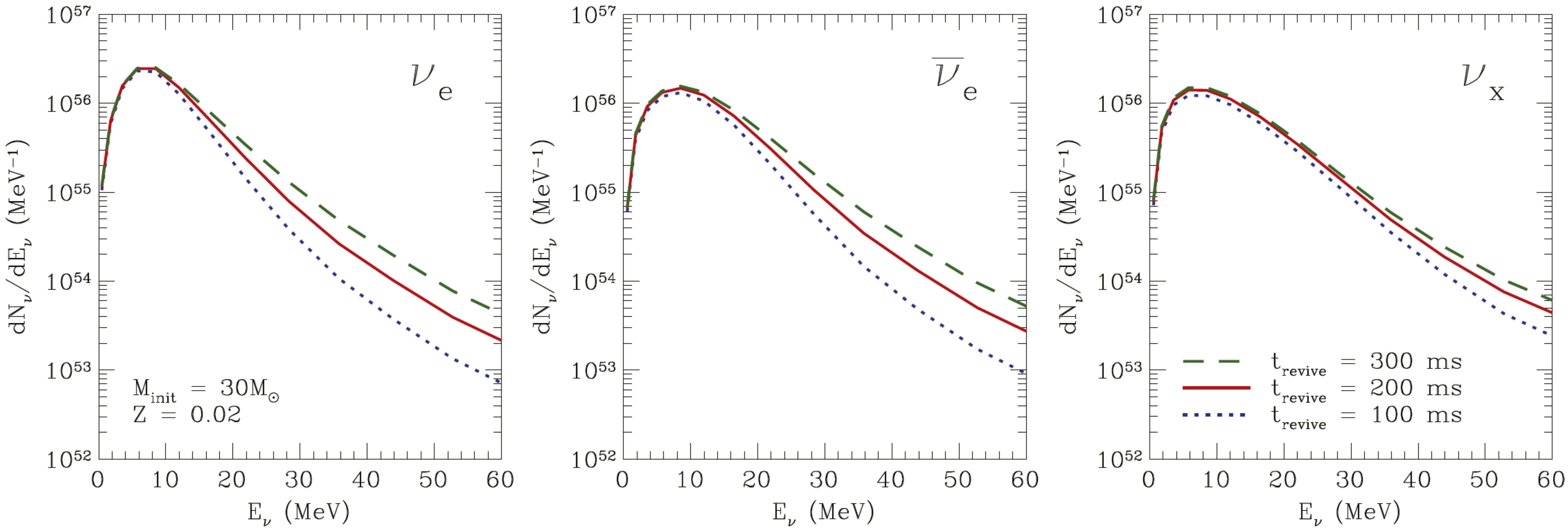

Figure 4. Neutrino number spectra of supernova with $30M_\odot$, $Z = 0.02$ and shock revival times of t_{revive} = 100 ms (dotted), 200 ms (solid), and 300 ms (dashed). The left, central, and right panels correspond to ν_e, $\bar{\nu}_e$, and ν_x $(= \nu_\mu = \bar{\nu}_\mu = \nu_\tau = \bar{\nu}_\tau)$, respectively.

Equation-Of-State Effect

K. Nakazato et al., ApJ 804, 75 (2015)

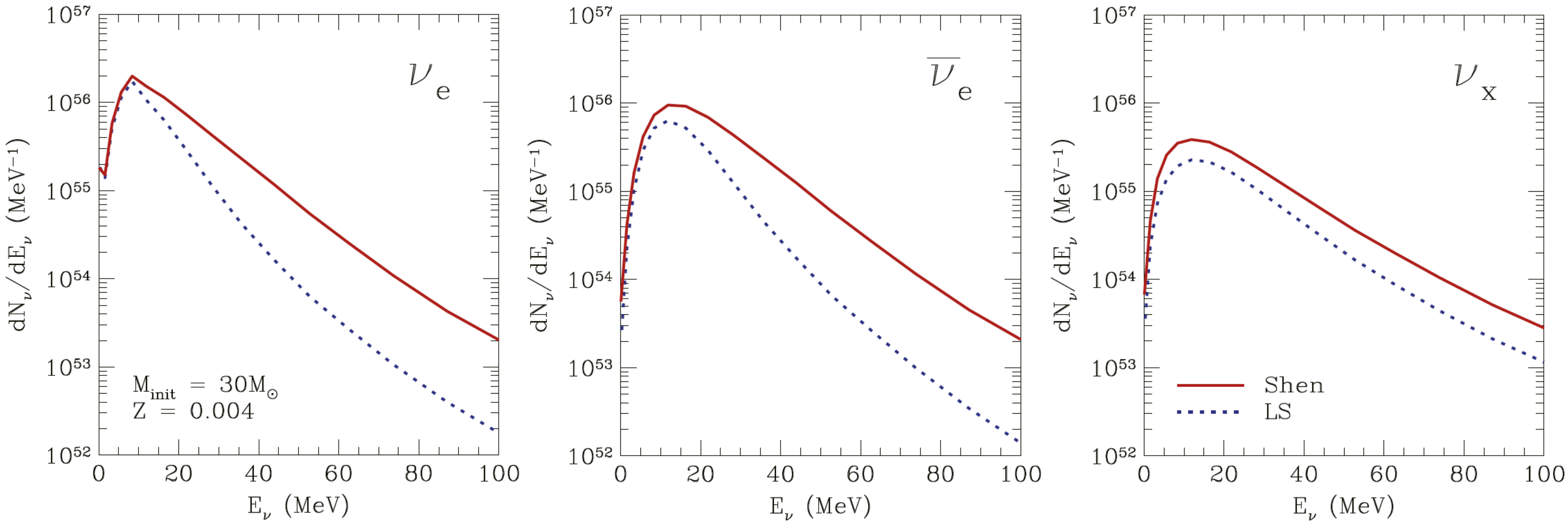

Figure 6. Neutrino number spectra for black hole formation with $30M_\odot$, $Z = 0.004$ and Shen EOS (solid) and LS EOS (dotted). The left, central, and right panels correspond to ν_e, $\bar{\nu}_e$, and ν_x $(=\nu_\mu = \bar{\nu}_\mu = \nu_\tau = \bar{\nu}_\tau)$, respectively.

Redshift Dependence

K. Nakazato et al., ApJ 804, 75 (2015)

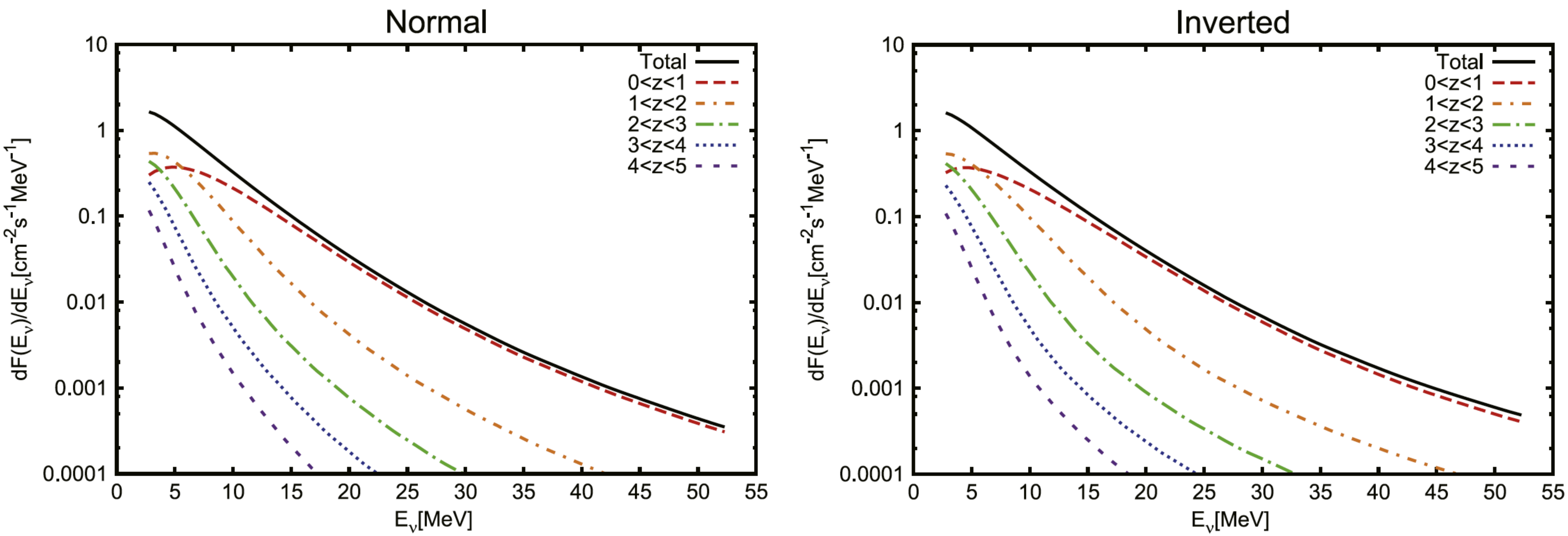

Figure 10. Total fluxes of SRNs (solid) and contributions from various redshift ranges for the reference model. The lines except for the solid line correspond, from top to bottom, to the redshift ranges $0 < z < 1, 1 < z < 2, 2 < z < 3, 3 < z < 4$, and $4 < z < 5$, for $E_\nu > 10$ MeV. The left and right panels show the cases for normal and inverted mass hierarchies, respectively.

Redshift

1 pc ~ 3.26 light-year

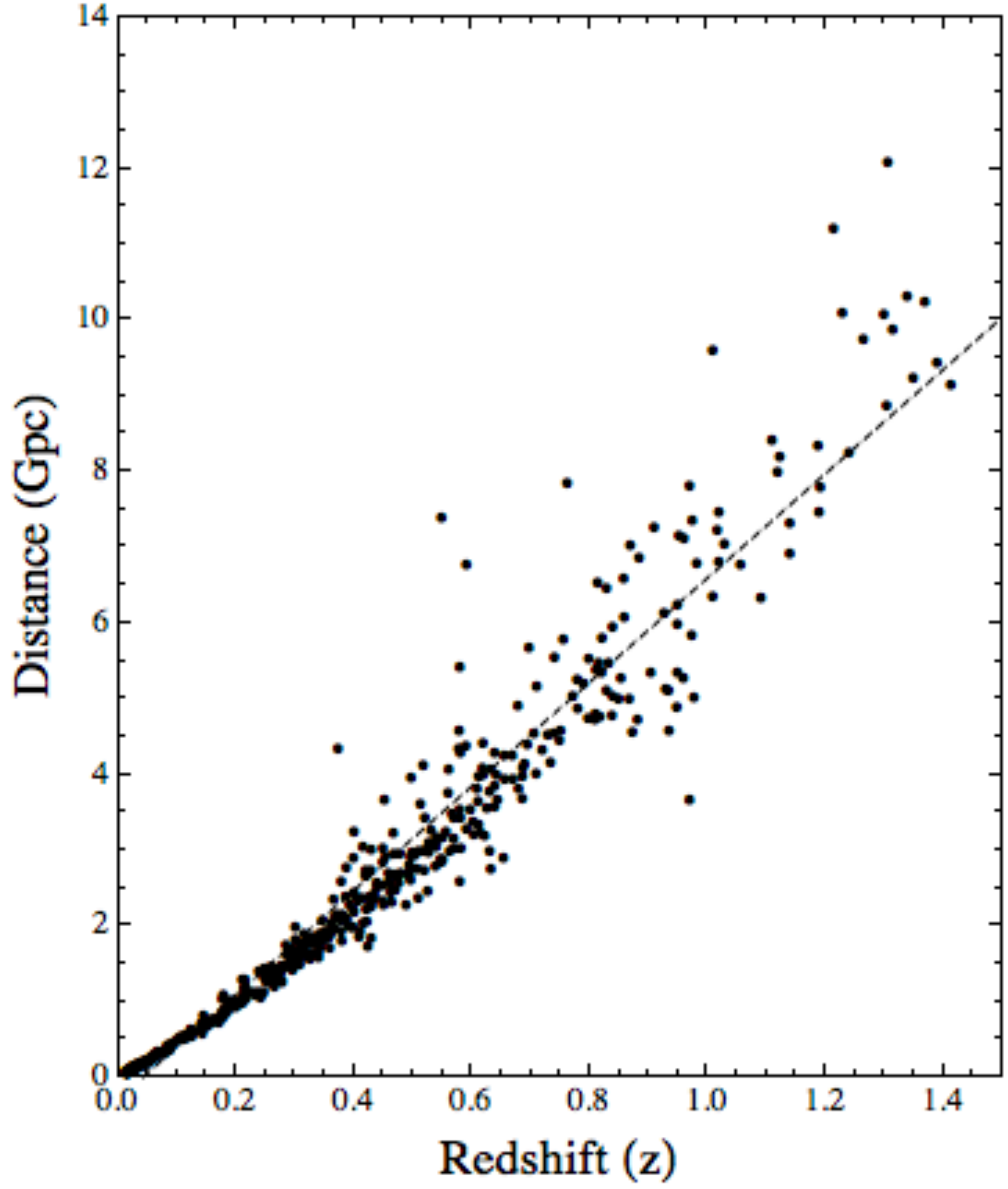

SK Operation Periods

Phase	SK-I	SK-II	SK-III	SK-IV	SK-V
Start	Apr., 1996	Oct., 2002	Jul., 2006	Sep., 2008	Jan., 2019
End	Jul., 2001	Oct., 2005	Aug., 2008	May., 2018	(running)
Live time [days]	1496	791	548	2970	-
Number of ID PMTs	11,146	5,182	11,129	11,129	11,129
ID PMT coverage	40%	19%	40%	40%	40%
Number of OD PMTs	1,885	1,885	1,885	1,885	1,885
PMT protection	No	Yes	Yes	Yes	Yes
Neutron tagging	No	No	No	Yes	Yes
Threshold [MeV]	4.5	6.5	4.0	3.5	3.5

Neutron Tagging: The 22 Variables

from A. Gianpaolo (LLR)

DISCRIMINATING VARIABLES (1)

- N_{10}: number of PMT hits in 10 ns window
- Geometrical variables
  - θ_{mean}, θ_{rms}
  - ϕ_{rms}
  - N_{low}
  - $N_{cluster}$
  - $N_{low\theta}$
  - N_{back}
- PMT noise variables
  - N_{300}
  - N_{highQ}
  - Q_{mean}, Q_{rms}
  - T_{rms}, minT_{rms}(3), minT_{rms}(6)

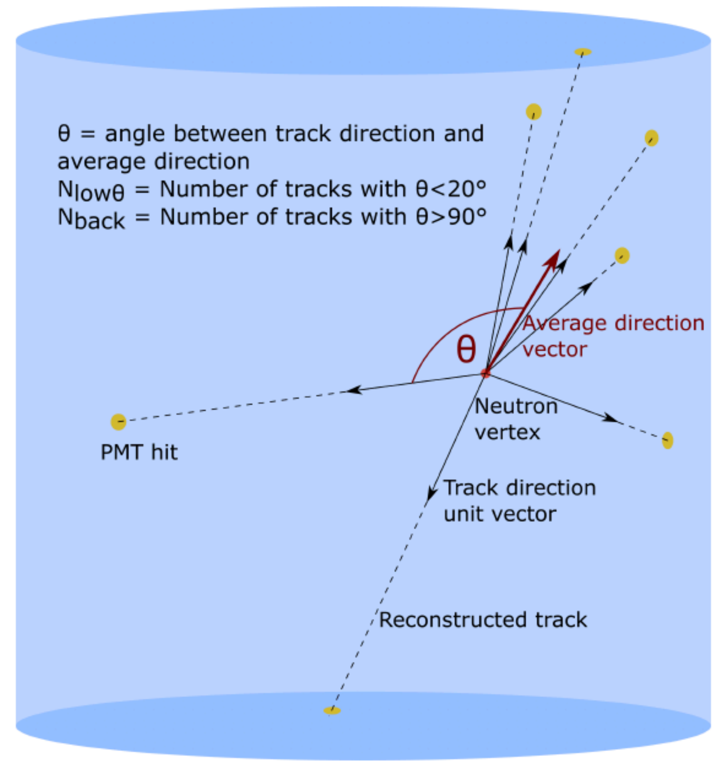

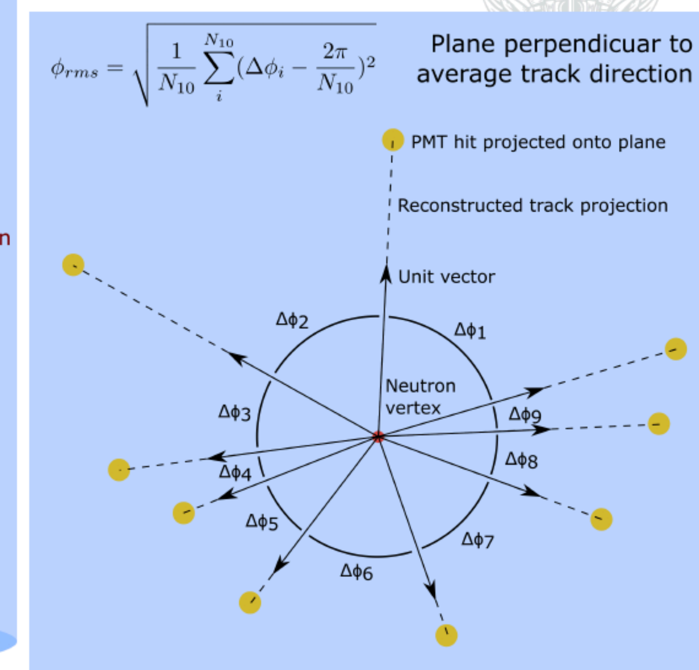

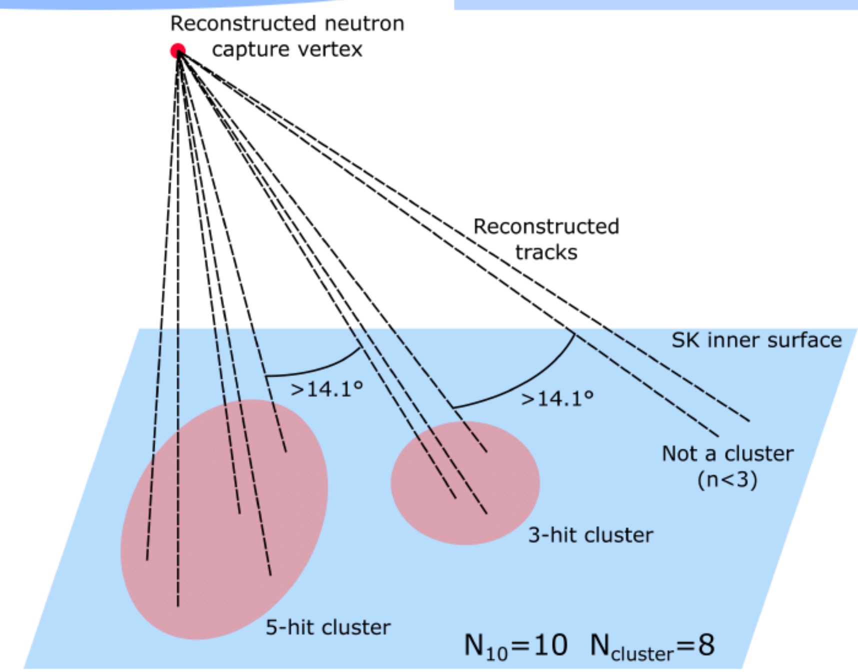

Neutron Tagging: The 22 Variables

from A. Gianpaolo (LLR)

DISCRIMINATING VARIABLES (2)

Additional variables to refine the zeroth-order vertex:

- Neut-Fit variables
  - NF_{wall}
  - δN_{10}
  - δT_{rms}
- BONSAI vertex fit Variables
  - BS_{wall}
  - BS_{energy}
- Fit agreement variables
  - BF_{dist}
  - FP_{dist}
- Combined-fit variables
  - $\mathcal{L}_{ratio} = \frac{\mathcal{L}_{combined}}{\mathcal{L}_{prompt} \times \mathcal{L}_{neutron}}$
  - $\mathcal{L}_{window}$

SK-I

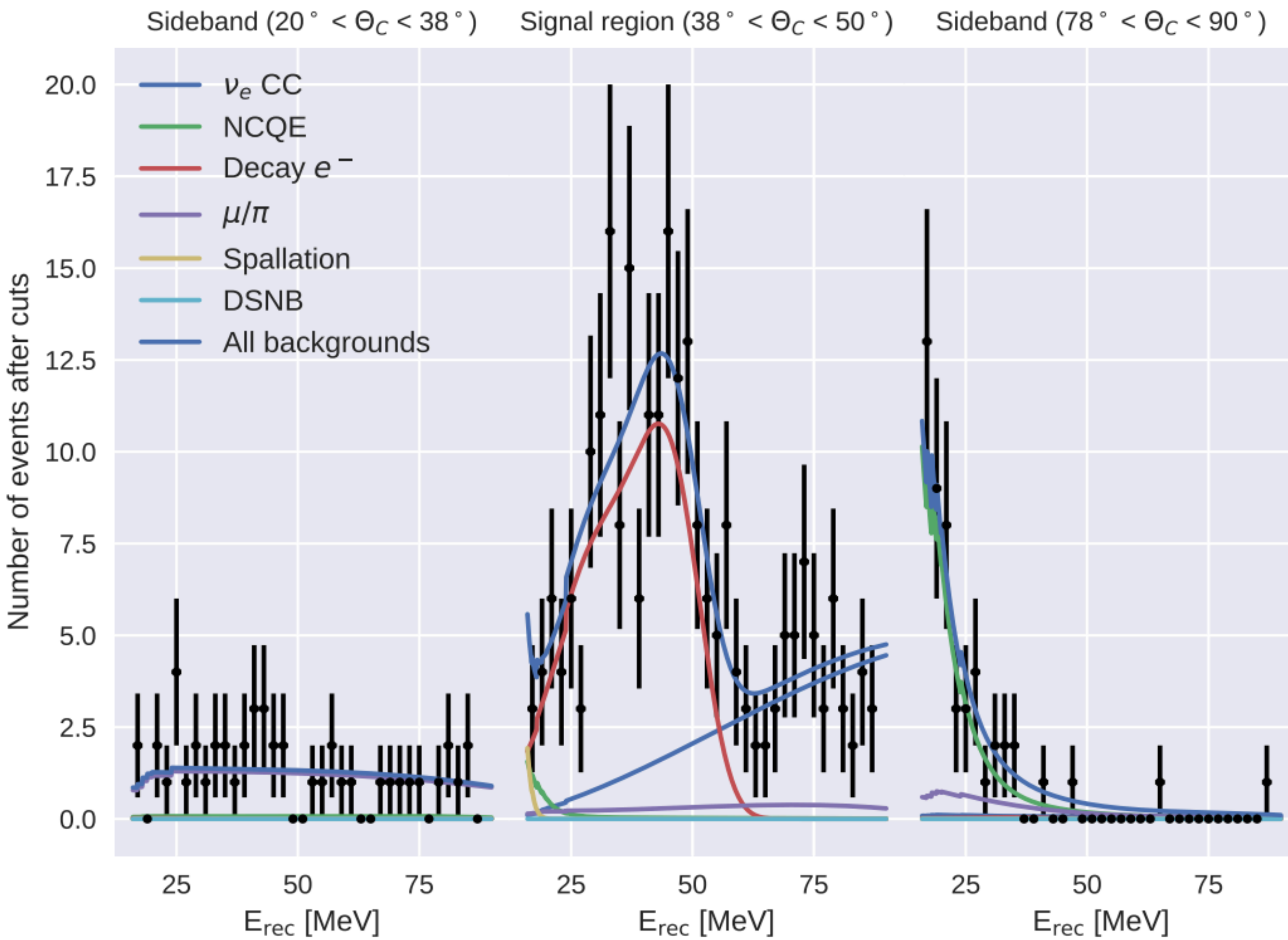
Sideband (20° < Θ_C < 38°)
Signal region (38° < Θ_C < 50°)
Sideband (78° < Θ_C < 90°)
ν_e CC
NCQE
Decay e⁻
μ/π
Spallation
DSNB
All backgrounds
Number of events after cuts
0.0
2.5
5.0
7.5
10.0
12.5
15.0
17.5
20.0
25
50
75
E_rec [MeV]

SK-II

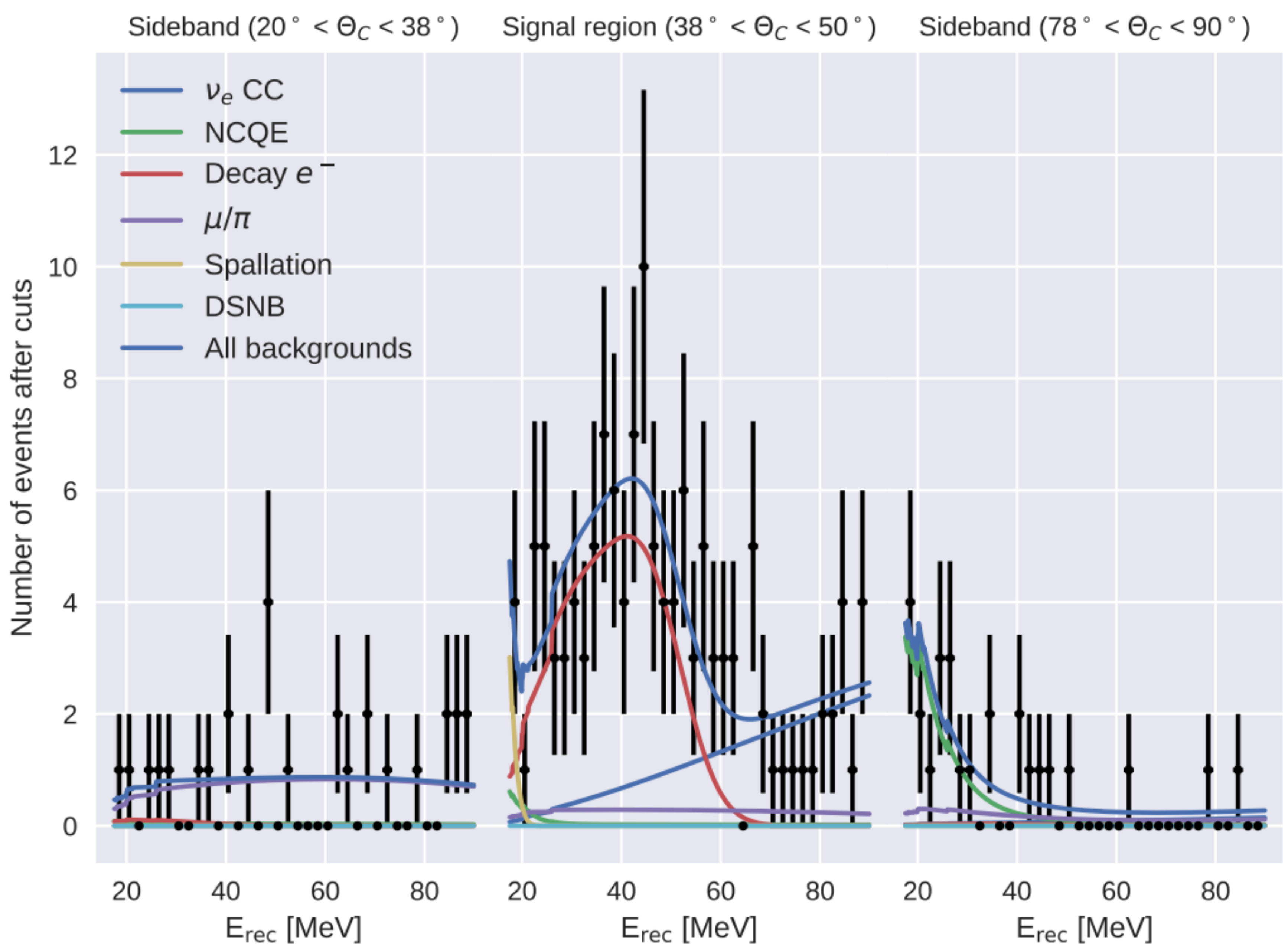

Sideband (20° < Θ_C < 38°)
Signal region (38° < Θ_C < 50°)
Sideband (78° < Θ_C < 90°)
ν_e CC
NCQE
Decay e⁻
μ/π
Spallation
DSNB
All backgrounds
Number of events after cuts
E_rec [MeV]
E_rec [MeV]
E_rec [MeV]

SK-III

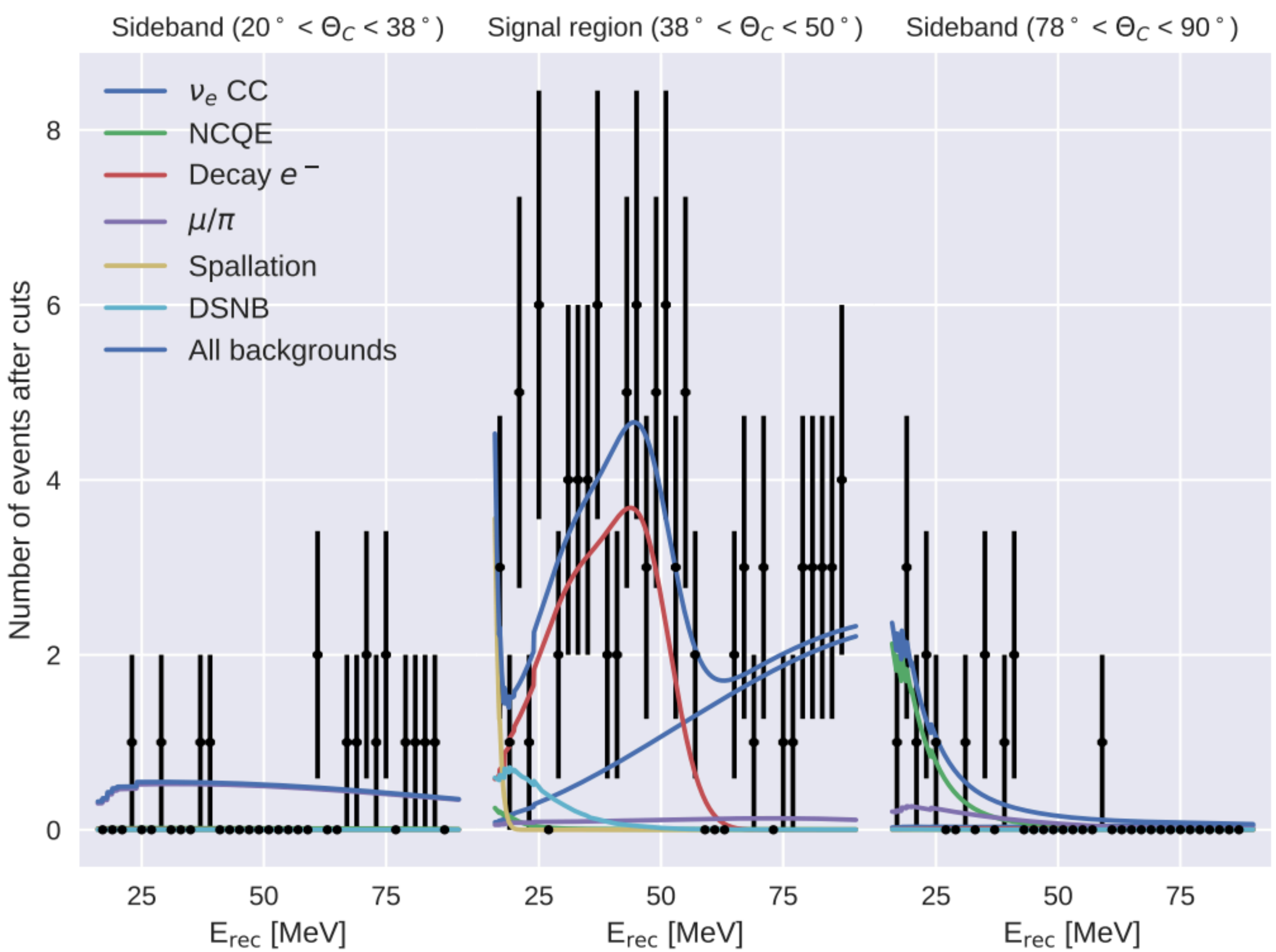

Sideband (20° < Θ_C < 38°)
Signal region (38° < Θ_C < 50°)
Sideband (78° < Θ_C < 90°)
ν_e CC
NCQE
Decay e^-
μ/π
Spallation
DSNB
All backgrounds
Number of events after cuts
0
2
4
6
8
25
50
75
E_{rec} [MeV]

SK-III

TABLE VIII. Best-fit values and the 90% C.L. upper limits on the DSNB fluxes (in $cm^{-2} \cdot sec^{-1}$) for the theoretical models for phases SK-I to IV as well as for the combined analysis. Here the upper limits are given for $E_\nu > 17.3$ MeV.

	Best fit		**90% CL limit**					**Pred.**
Model	**SK4**	**All**	**SK1**	**SK2**	**SK3**	**SK4**	**All**	
Totani+95 Constant	$2.5^{+1.4}_{-1.3}$	$1.3^{+0.9}_{-0.9}$	2.3	6.3	7.0	4.5	2.6	4.67
Kaplinghat+00 HMA (max)	$2.6^{+1.5}_{-1.3}$	$1.3^{+0.9}_{-0.9}$	2.3	6.7	7.1	4.7	2.6	3.00
Horiuchi+09 6 MeV, max	$2.6^{+1.4}_{-1.3}$	$1.3^{+0.9}_{-0.9}$	2.4	6.0	7.0	4.6	2.6	1.94
Ando+03 (updated 05)	$2.7^{+1.5}_{-1.4}$	$1.4^{+0.9}_{-0.9}$	2.3	6.6	7.2	4.7	2.7	1.74
Kresse+21 (High, NH)	$2.7^{+1.5}_{-1.3}$	$1.4^{+0.9}_{-0.9}$	2.3	6.7	7.2	4.7	2.7	1.57
Galais+09 (NH)	$2.5^{+1.4}_{-1.3}$	$1.3^{+0.9}_{-0.9}$	2.3	6.3	7.0	4.5	2.6	1.56
Galais+09 (IH)	$2.6^{+1.4}_{-1.3}$	$1.3^{+0.9}_{-0.9}$	2.3	6.4	7.0	4.5	2.6	1.50
Horiuchi+18 $\xi_{2.5} = 0.1$	$2.6^{+1.4}_{-1.3}$	$1.4^{+0.9}_{-0.9}$	2.4	6.1	7.1	4.6	2.7	1.23
Kresse+21 (High, IH)	$2.7^{+1.5}_{-1.3}$	$1.4^{+0.9}_{-0.9}$	2.3	6.7	7.1	4.7	2.7	1.21
Kresse+21 (Fid, NH)	$2.7^{+1.5}_{-1.3}$	$1.4^{+0.9}_{-0.9}$	2.3	6.8	7.2	4.7	2.7	1.20
Kresse+21 (Fid, IH)	$2.7^{+1.5}_{-1.3}$	$1.4^{+0.9}_{-0.9}$	2.3	6.8	7.2	4.7	2.7	1.02
Kresse+21 (Low, NH)	$2.7^{+1.5}_{-1.4}$	$1.4^{+0.9}_{-0.9}$	2.3	6.8	7.2	4.8	2.7	0.96
Tabrizi+21 (NH)	$2.7^{+1.5}_{-1.3}$	$1.4^{+0.9}_{-0.9}$	2.4	6.6	7.1	4.7	2.7	0.92
Kresse+21 (Low, IH)	$2.7^{+1.5}_{-1.4}$	$1.4^{+0.9}_{-0.9}$	2.3	6.8	7.2	4.8	2.7	0.84
Lunardini09 Failed SN	$2.8^{+1.5}_{-1.4}$	$1.4^{+0.9}_{-0.9}$	2.4	6.8	7.3	4.8	2.8	0.73
Hartmann+97 CE	$2.6^{+1.4}_{-1.3}$	$1.3^{+0.9}_{-0.9}$	2.3	6.5	7.1	4.6	2.6	0.63
Nakazato+15 (max, IH)	$2.7^{+1.5}_{-1.4}$	$1.4^{+1.0}_{-0.9}$	2.4	6.5	7.2	4.8	2.7	0.53
Horiuchi+18 $\xi_{2.5} = 0.5$	$2.7^{+1.5}_{-1.4}$	$1.3^{+0.9}_{-0.9}$	2.2	7.1	7.1	4.8	2.6	0.55
Horiuchi+21	$2.1^{+1.3}_{-1.2}$	$1.2^{+0.9}_{-0.9}$	3.4	4.3	5.9	3.9	2.5	0.28
Malaney97 CGI	$2.7^{+1.5}_{-1.3}$	$1.3^{+0.9}_{-0.9}$	2.3	6.8	7.1	4.7	2.6	0.26
Nakazato+15 (min, NH)	$2.8^{+1.5}_{-1.4}$	$1.4^{+1.0}_{-0.9}$	2.3	6.8	7.2	4.8	2.7	0.19